

Geochemical Studies in Alaska by the U.S. Geological Survey, 1989

Edited by RICHARD J. GOLDFARB, J. THOMAS NASH,
and J.W. STOESER

This volume is published as chapters A-F.
Chapter titles are listed in volume contents.
These chapters are not available separately

U.S. GEOLOGICAL SURVEY BULLETIN 1950

ERRATA

U.S. Geological Survey Bulletin 1950, Geochemical studies in Alaska by the U.S. Geological Survey, 1989.

The names "Windfall Creek" and "Windfall Creek area" are incorrect in the text of chapter A and in figure 4 and table 3 of chapter A. The correct names are "Ward Creek" and "Ward Creek area."

U.S. DEPARTMENT OF THE INTERIOR
MANUEL LUJAN, JR., Secretary



U.S. GEOLOGICAL SURVEY
Dallas L. Peck, Director

Any use of trade, product, or firm names in this publication is for descriptive purposes only and does not imply endorsement by the U.S. Government.

UNITED STATES GOVERNMENT PRINTING OFFICE: 1990

For sale by the
Books and Open-File Reports Section
U.S. Geological Survey
Federal Center
Box 25425
Denver, CO 80225

Library of Congress Cataloging-in-Publication Data

Geochemical studies in Alaska by the U.S. Geological Survey, 1989 / edited by Richard J. Goldfarb, J. Thomas Nash, and J.W. Stoeser.

p. cm. — (U.S. Geological Survey bulletin ; 1950)

Includes bibliographical references.

Supt. of Docs. no.: I 19.3:1950

1. Geochemistry—Alaska. 2. Ore deposits—Alaska. I. Goldfarb, R. J. II. Nash, J. Thomas (John Thomas), 1941— III. Stoeser, J. W. IV. Series.

QE75.B9 no. 1950

[QE515]

557.3 s—dc20

[551.9'09798]

90-14099

CIP

VOLUME CONTENTS

[Letters designate the chapters]

- (A) Interpretation of geochemical data from Admiralty Island, Alaska—Evidence for volcanogenic massive sulfide mineralization, by Karen Duttweiler Kelley.
- (B) Geochemical orientation study for identification of metallic mineral resources in the Sitka quadrangle, southeastern Alaska, by E. Lanier Rowan, Elizabeth A. Bailey, and Richard J. Goldfarb.
- (C) Geology and geochemistry of mineralization in the Bethel quadrangle, southwestern Alaska, by Thomas P. Frost.
- (D) Gold associated with cinnabar- and stibnite-bearing deposits and mineral occurrences in the Kuskokwim River region, southwestern Alaska, by John E. Gray, Thomas P. Frost, Richard J. Goldfarb, and David E. Detra.
- (E) Stable isotope systematics of epithermal mercury-antimony mineralization, southwestern Alaska, by Richard J. Goldfarb, John E. Gray, William J. Pickthorn, Carol A. Gent, and Barrett A. Cieutat.
- (F) Gold anomalies and newly identified gold occurrences in the Lime Hills quadrangle, Alaska, and their association with the Hartman sequence plutons, by Michael S. Allen.

Chapter A

Interpretation of Geochemical Data from Admiralty Island, Alaska—Evidence for Volcanogenic Massive Sulfide Mineralization

By KAREN DUTTWEILER KELLEY

U.S. GEOLOGICAL SURVEY BULLETIN 1950

GEOCHEMICAL STUDIES IN ALASKA BY THE U.S. GEOLOGICAL SURVEY, 1989

CONTENTS

Abstract	A1
Introduction	A1
Geology of Admiralty Island	A1
Mineral deposits	A3
Geochemical studies	A4
Methods and data evaluation	A4
Interpretation	A4
Conclusions	A8
References cited	A8

FIGURES

1-4. Maps showing:

1. Distribution of volcanogenic massive sulfide occurrences in the area of Admiralty Island A2
2. Geology of Admiralty Island A3
3. Distribution of Ag, Au, Sb, and W in sediment samples from Admiralty Island A6
4. Basin areas containing samples having anomalous scores for factors 3 and 5 A8

TABLES

1. Univariate statistical estimates for 380 sediment samples, Admiralty Island A5
2. Five-factor geochemical model for sediment samples, Admiralty Island A6
3. Concentrations of As, Au, Ba, Ni, Sb, and Zn in samples having anomalous scores for factor 3 (As-Ba-Ni-Zn), Admiralty Island A7

Interpretation of Geochemical Data from Admiralty Island, Alaska—Evidence for Volcanogenic Massive Sulfide Mineralization

By Karen Duttweiler Kelley

Abstract

Late Triassic sedimentary and intermediate to mafic volcanic rocks of the Alexander terrane on Admiralty Island host the Greens Creek and Pyrola Ag-Au-Pb-Zn syngenetic volcanogenic massive sulfide deposits. Other Au-Cu-Pb-Zn mineral occurrences and prospects are northeast of Greens Creek on the northernmost part of Admiralty Island.

Reconnaissance geochemical surveys conducted during the National Uranium Resource Evaluation (NURE) program included collection of 416 sediment samples from Admiralty Island. Results of factor analysis of the multi-element data include two geochemical associations—As-Ba-Ni-Zn and Pb-Zn-Cu—most likely indicative of volcanogenic massive sulfide mineralization. Three geographically distinct regions, underlain by Triassic volcanic and sedimentary rocks, are delineated as geochemically favorable areas for mineral occurrences: (1) the Greens Creek area surrounding the Greens Creek deposit and other nearby Au-Cu-Pb-Zn occurrences, (2) a large area southeast of the Pyrola deposit that includes most of the tributaries to Windfall Creek and adjacent drainage basins to the east and southeast, and (3) drainage basins north and south of Gambier Bay.

These three regions define a northwesterly trend from Gambier Bay in the southeast to the Greens Creek area in the northwest. This trend is consistent with a regional northwest-trending belt of syngenetic massive sulfide occurrences of Permian and Triassic age in southeastern Alaska.

INTRODUCTION

Admiralty Island is located 15 km south of Juneau in parts of the Sitka, Sumdum, and Juneau quadrangles (fig. 1). In 1982 the U.S. Department of Energy completed reconnaissance geochemical surveys of these quadrangles as part of the National Uranium Resource Evaluation (NURE) program. Stream- and lake-sediment samples and water samples were collected and analyzed for a variety of trace elements.

An initial evaluation of the data from the Sitka quadrangle was conducted by the U.S. Geological Survey during a preliminary mineral resource assessment. Data from the area of Admiralty Island within the Juneau and Sumdum quadrangles were subsequently added. This paper presents an evaluation and interpretation of the sediment geochemical data from Admiralty Island. The geochemical signature in sediment samples from streams draining the Greens Creek deposit is distinctive. Other possible mineralized areas are suggested based on similar geochemical anomalies and associations.

Acknowledgments.—I thank Rich Goldfarb, Bob Eppinger, and Tom Nash for their helpful reviews of this paper. Discussions with Sue Karl and Art Ford regarding the regional setting, stratigraphy, and structure of Admiralty Island greatly improved my understanding of the area. I also thank Karen Slaughter, who helped with the drafting.

GEOLOGY OF ADMIRALTY ISLAND

Admiralty Island is made up mostly of sedimentary, volcanic, and plutonic rocks (fig. 2) of the Alexander terrane of Silberling and Jones (1984). These rocks have been interpreted to represent intermittent volcanic arc activity along a convergent continental margin (Gehrels and Saleeby, 1987).

The oldest rocks on Admiralty Island are black radiolarian chert (Karl, 1989), argillite, graywacke, and minor altered volcanic rocks of the Ordovician Hood Bay Formation (Carter, 1977) and unnamed Silurian sedimentary rocks (Lathram and others, 1965). Thick carbonate sequences of Devonian age unconformably overlie the Silurian rocks. These are overlain by siliceous argillite, graywacke, and chert of the Permian Cannery Formation (Jones and others, 1981). Two different sequences of Late Triassic rocks have been recognized on Admiralty Island. The Hyd Group (Loney, 1964) consists of pillow lava flows, tuff, andesitic and basaltic breccia, and

Manuscript approved for publication, June 26, 1990.

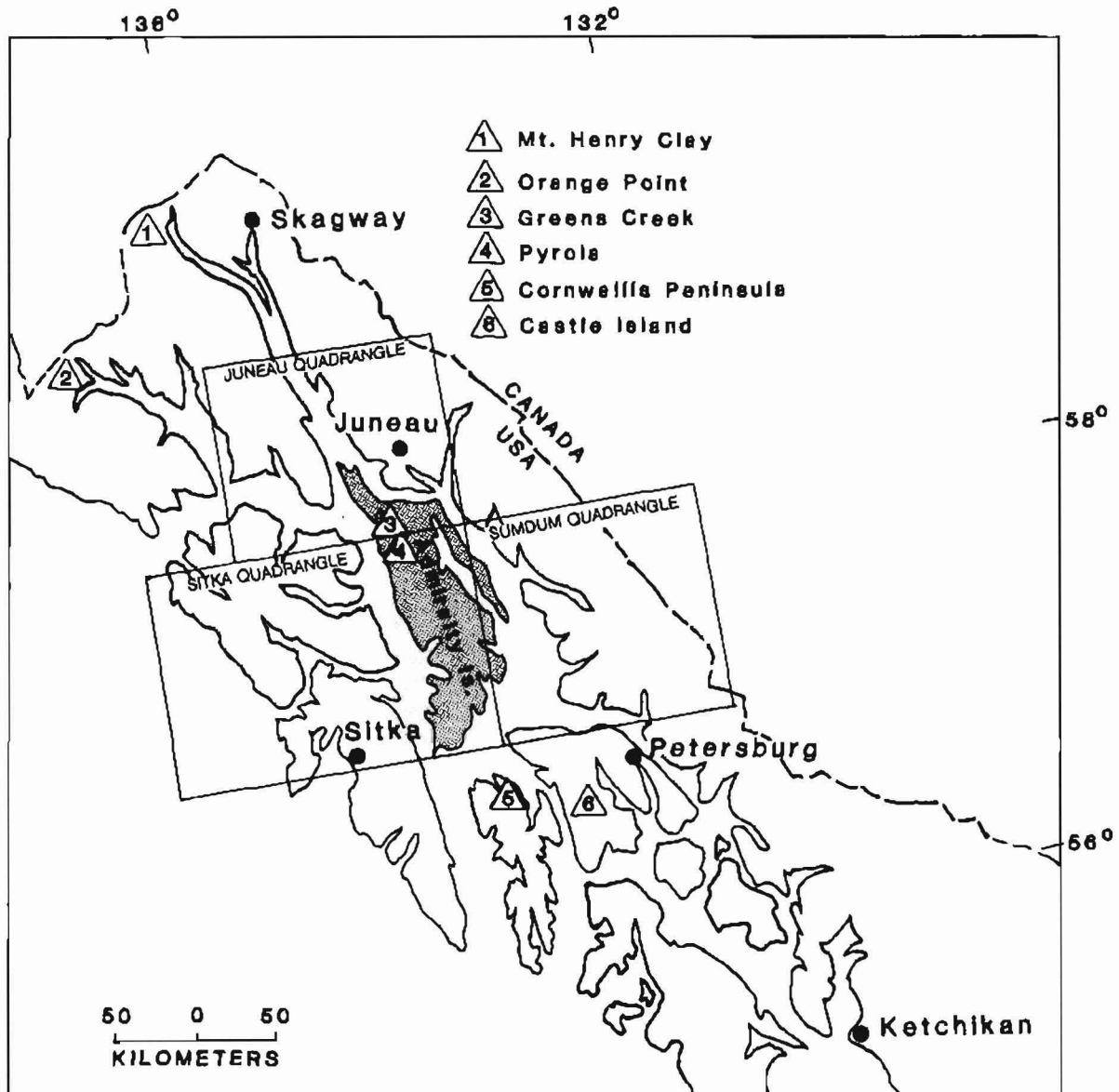


Figure 1. Distribution of volcanic massive sulfide occurrences of Permian and Triassic age within the Alexander terrane in the area of Admiralty Island. Modified from Goldfarb and others (1987).

fine-grained clastic and carbonate rocks, and the Retreat Group consists of deeper water volcanic and sedimentary rocks. The Retreat Group was originally considered to be Late Triassic (?) to Early Cretaceous (?) in age (Barker, 1957); its age was subsequently revised to Middle (?) Devonian (Lathram and others, 1965). Recent evidence, however, indicates that its age is Late Triassic (Ford and others, 1989). Chlorite-epidote-calcite phyllite and schist of the Gambier Bay Formation (Lathram and others, 1965) may be correlative with the Retreat Group on northern Admiralty Island (Ford and others, 1989).

Jurassic and Cretaceous graywacke turbidite and massive conglomerate of the Seymour Canal Formation and

basaltic (Ford and Brew, 1988) or andesitic flow breccia (Lathram and others, 1965) of the Douglas Island Volcanics comprise the Stephens Passage Group, which disconformably overlies Triassic rocks on northeastern Admiralty Island. The Paleozoic and Mesozoic rocks were intruded by Cretaceous plutonic rocks of intermediate, mafic, and ultramafic composition. The largest intrusive body in the central part of the island is a batholith composed dominantly of granodiorite and tonalite. Tertiary sedimentary and volcanic rocks include the Kootznahoo Formation and the Admiralty Island Volcanics (Lathram and others, 1965). The Kootznahoo Formation consists of pebble to cobble conglomerate, sandstone, carbonaceous shale, and sub-bituminous coal.

EXPLANATION

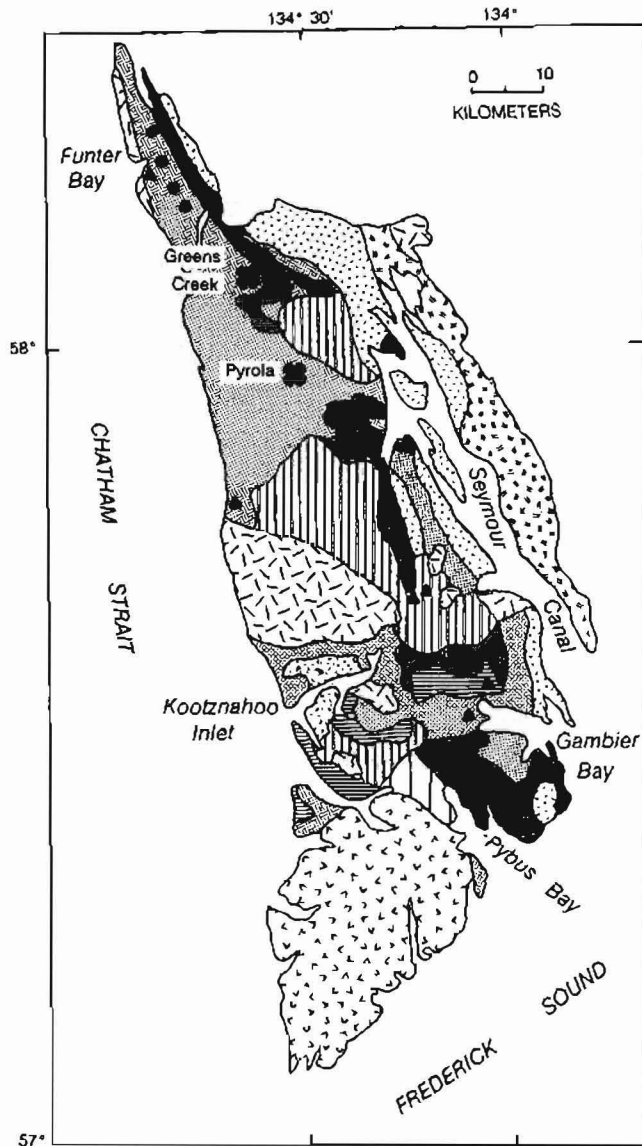


Figure 2. Geologic map of Admiralty Island. Generalized from Latham and others (1965) and Ford and others (1989).

The Admiralty Island Volcanics consist of massive porphyritic andesitic basalt flows that unconformably overlie pre-Tertiary rocks on the southern part of the island.

MINERAL DEPOSITS

The Greens Creek and Pyrola deposits are Ag-Au-Pb-Zn volcanogenic massive sulfide deposits hosted by Late Triassic volcanic and sedimentary rocks (fig. 2). Several other Au-Cu-Pb-Zn occurrences are northeast of the Greens Creek deposit (Latham and others, 1965), and syngenetic sulfide-barite mineral occurrences have been reported in the Pybus Bay area of southern Admiralty Island

- Tertiary rocks—Andesitic basalt flows, Admiralty Island Volcanics
- Tertiary rocks—Conglomerate, sandstone, shale, coal; Kootznahoo Formation
- Cretaceous rocks—Intermediate, mafic, and ultramafic plutonic rocks
- Cretaceous and Jurassic rocks—Argillite, conglomerate, and graywacke; Seymour Canal Formation
- Cretaceous and Jurassic rocks—Basaltic or andesitic flow breccia; Douglas Island Volcanics
- Triassic and Permian rocks—Volcanic and sedimentary rocks
- Triassic rocks—Chert, argillite, graywacke, carbonate rocks, and intermediate to mafic volcanic rocks. Consists of the Hyd Group, as mapped, and the Retreat Group and Gambier Bay Formation
- Mississippian and Devonian rocks—Argillite, graywacke, chert, and minor conglomerate, limestone, and volcanic rocks; Cannery Formation
- Devonian rocks—Marble enclosed tectonically within Gambier Bay Formation
- Silurian and Ordovician rocks—Argillite, chert, graywacke, and minor volcanic rocks; includes Ordovician Hood Bay Formation and sedimentary rocks
- Mesozoic or Paleozoic rocks—Metasedimentary and metigneous rocks
- Ag-Au-Pb-Zn deposit
- Au-Cu-Pb-Zn occurrence
- Au (±Cu) occurrence

(Van Nieuwenhuysse, 1984). Similar syngenetic massive sulfide occurrences in Permian- and Triassic-age rocks of the Alexander terrane to the north and south of Admiralty Island (Goldfarb and others, 1987) (fig. 1) form a belt almost 350 km long.

The Greens Creek stratiform massive sulfide deposit (Dressler and Dunbire, 1981) contains drill-indicated reserves of 3.5 million short tons of 23.8 oz/ton Ag, 0.18 oz/ton Au, 3.9 percent Pb, and 9.7 percent Zn. Mineralization is dominantly syngenetic, although remobilization and (or) additional mineralization is indicated by sulfide- and gold-bearing quartz veins (Crafford, 1989). The main orebody is situated between a structural hanging wall of altered mafic volcanic rocks and a footwall of black graphitic argillite. Recently discovered fossils in argillite fragments within the massive sulfide ore suggest a Late Triassic age for the mineralization (Crafford, 1989). The dominant ore minerals are sphalerite, galena, freibergite, and chalcopyrite; native gold and silver-sulfide and silver-sulfosalt minerals occur in lesser amounts. Quartz and barite are the primary gangue minerals (Crafford, 1989).

The Pyrola deposit, which lies at the contact between volcanic rocks and fine-grained clastic and carbonate rocks, consists of interbedded massive sulfide minerals and barite and an underlying siliceous stockwork zone containing auriferous pyrite. Sulfide minerals are pyrite, sphalerite, galena, and minor chalcopyrite; other minerals include the

lead-antimony sulfosalt minerals jamesonite and boulangerite (Van Nieuwenhuysse, 1984).

A nickel-copper deposit near Funter Bay (fig. 1) is hosted in a pipelike intrusive body of gabbroic and noritic composition. The ore minerals, chiefly pentlandite and chalcopyrite, are in veinlets or lenses and bands of sulfide ore (Reed, 1942; Lathram and others, 1965).

Six gold (\pm copper) prospects are reported on Admiralty Island (fig. 2). These are gold-bearing quartz veins in schistose rocks and disseminated gold in brecciated limestone and calcareous schist (Lathram and others, 1965; Cobb, 1972, 1978). In addition, dolomite breccia immediately north of Gambier Bay locally contains chalcopyrite and trace amounts of gold (Herbert and Race, 1965; Berg and Cobb, 1967).

GEOCHEMICAL STUDIES

Methods and Data Evaluation

*Concentration
on low water?*
During the course of the NURE program, 416 stream- and lake-sediment samples were collected from Admiralty Island. All samples were sieved to -100 mesh and analyzed for 44 elements using X-ray fluorescence and neutron activation methods (Los Alamos National Laboratories, 1982a, b, c).

Univariate statistics (table 1) and multivariate analysis were used to (1) evaluate the NURE geochemical data, (2) identify anomalous samples, and (3) relate anomalies to particular types of mineral deposits. Prior to data evaluation, 36 samples were eliminated due to the lack of analyses for As, Cu, Pb, and Zn. The remaining 380 sediment samples include 297 stream-sediment samples and 83 lake-sediment samples. Although stream- and lake-sediment samples may be considered two distinctly different sample media, data for the two media were combined prior to multi-element data analysis; initial evaluation of the two as separate data populations revealed that within each most elements show similar concentration ranges, geometric means, and interelement correlation.

Prior to multi-element data evaluation and interpretation, many elements were removed from the data set because of the large percentages of qualified values (concentrations below the lower determination limit). Although data for Au, Ag, Sb, and W were thereby removed, the few samples containing anomalous concentrations of one or more of these elements are noted on figure 3.

Correlation and R-mode factor analysis (Davis, 1986) were used to identify the major element associations in the sediment data set. R-mode factor analysis groups elements that tend to behave similarly into multi-element associations, or factors, based on their mutual linear

correlation coefficients. Different types of mineral deposits and rock types have distinct geochemical signatures that can be identified as factors.

The contribution of each variable to each factor is represented by a factor loading. The effect a particular factor may have on each sample site is represented by a factor score. When presented in map form, factor scores portray the areal variation of the interpreted geological and geochemical features or processes.

Interpretation

A five-factor model accounts for 71 percent of the total data variance and was selected as the geochemically most meaningful model to describe the major associations (table 2). Two of the factors reflect the dominant bedrock geochemistry. Factor 1 has high loadings for Mg, Sc, V, Cr, Fe, Al, Ca, Co, Ni, Na, Ti, Cu, and Mn. Samples having anomalous scores correlate with basaltic or andesitic flow breccias of the Douglas Island Volcanics or undivided Mesozoic or Paleozoic metamorphic rocks. Factor 2, which has high loadings for Hf, Zr, Ce, Lu, Eu, Th, Ti, Dy, Al, Na, U, and Fe, characterizes Cretaceous plutonic rocks of intermediate composition and andesitic basalt flows of the Admiralty Island Volcanics.

High positive loadings for Mn, Co, and Fe characterize factor 4. This factor association most likely represents an abundance of iron-manganese oxides in sediment samples produced during weathering and oxidation. Anomalous samples are widely scattered and are not associated with any particular rock unit.

Factors 3 (As, Ba, Ni, Zn) and 5 (Pb, Zn, Cu) are indicative of mineralization. Drainage basin areas characterized by samples having anomalous scores for these factors are shown on figure 4. Three relatively large regions are delineated: (1) the Greens Creek area surrounding the Greens Creek deposit and other nearby Au-Cu-Pb-Zn prospects, (2) the area southeast of the Pyrola deposit, which includes most of the tributaries to Windfall Creek and adjacent drainage basins to the east and southeast, and (3) drainage basins north and south of Gambier Bay. The concentrations of As, Ba, Ni, and Zn in samples having anomalous scores (≥ 1.31) for factor 3 from these areas are shown in table 3. Concentrations of Au and Sb are also shown. More than half of the samples have anomalous Ba concentrations ($\geq 1,200$ ppm); two samples from the Gambier Bay area have concentrations of 7,118 and 9,090 ppm, respectively. Many of the samples have anomalous concentrations of As (35–216 ppm), Ni (84–749 ppm), Sb (2–28 ppm), and (or) Zn (300–694 ppm). Barite, sphalerite, pyrite, sulfosalt minerals, or oxides derived from these minerals are the most likely sources for these highly anomalous concentrations.

Samples having scores greater than or equal to 1.25 for factor 5 are considered anomalous. Many of these

Table 1. Univariate statistical estimates for 380 sediment samples, Admiralty Island, Alaska

[Values in parts per million unless otherwise indicated. Analysis by neutron activation methods unless otherwise indicated. Leaders (-) indicate too many qualified values (below lower detection limit) to calculate accurate or meaningful statistics]

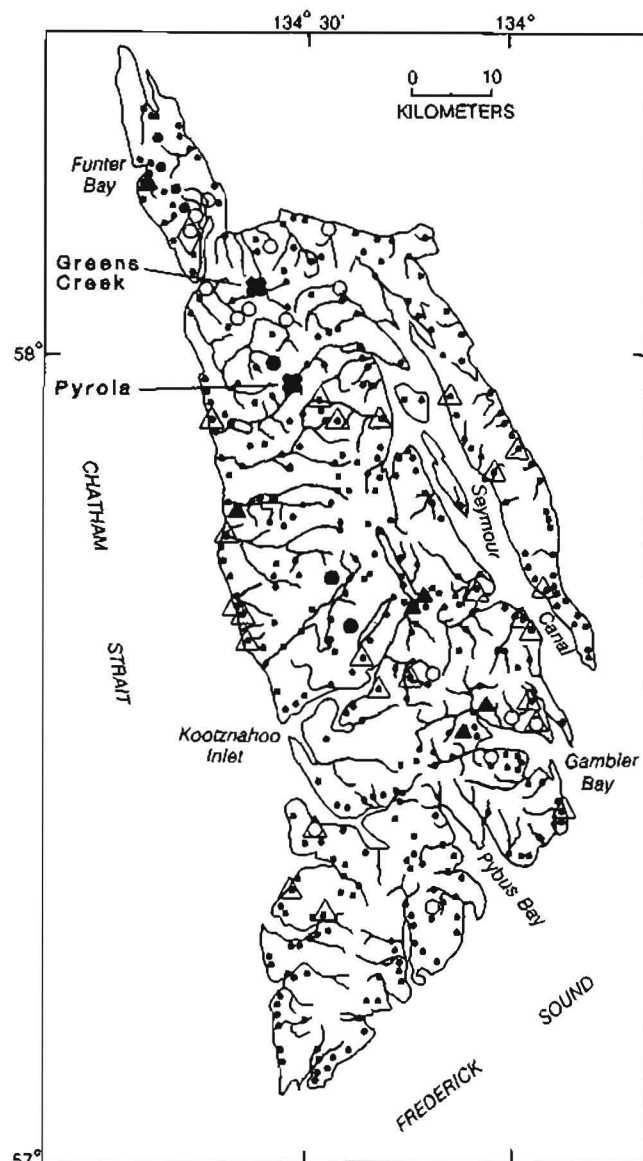
Element	Valid ²	NA ³	Minimum concentration	Geometric mean ⁴	90th percentile	99th percentile	Maximum concentration
Ag	3	116	5	-	--	--	7
Al%	378	0	0.6	6.0	8.3	9.1	9.5
As ¹	299	0	5	11	35	131	216
Au	1	0	1.07	--	--	--	1.07
Ba	243	0	271	435	1,115	3,101	9,090
Bi ¹	18	116	5	--	--	--	10
Ca%	357	0	0.3	1.7	4.7	7.5	16.8
Cd ¹	7	0	5	--	--	--	11
Ce	353	0	13	40	69	99	137
Cl	99	0	140	--	--	--	11,700
Co	362	0	3.3	20	43	61	106
Cr	352	0	23	109	277	440	1,772
Cs	47	0	2.1	--	--	--	18.7
Cu ¹	377	0	10	44	94	204	275
Dy	340	0	2	4	7	9	11
Eu	356	0	0.6	1.2	1.8	2.4	8.2
Fe%	376	0	0.3	4.7	7.6	9.6	13.0
Hf	307	0	1.5	3.3	6.2	10.1	12.8
K%	198	0	0.5	0.8	1.6	2.3	2.9
La	171	0	12	14.6	33	54	126
Lu	289	0	0.1	0.3	0.5	0.8	0.8
Mg%	344	0	0.4	1.3	2.7	4.1	6.1
Mn	380	0	40	1,288	2,836	6,340	13,370
Na%	380	0	0.07	1.5	2.3	32.9	3.5
Nb	0	116	--	--	--	--	--
Ni ¹	290	0	15	29	70	160	749
Pb ¹	138	0	5	5	10	52	132
Rb	3	0	54	--	--	--	81
Sb	17	0	2	--	--	--	28
Sc	379	0	0.9	18	31	46	54
Se	8	0	5	--	--	--	13
Sm	300	1	1.6	3.0	6.3	9.2	14.8
Sn ¹	1	116	10	--	--	--	10
Sr	12	5	357	--	--	--	1,055
Ta	4	0	2	--	--	--	3
Tb	17	8	1	--	--	--	3
Th	281	0	1.4	3	6	10	12.2
Ti%	350	0	0.12	0.45	0.8	1.2	1.4
U	380	0	0.26	2.5	5.1	18.0	129
V	372	0	17	286	286	383	530
W	26	0	15	--	--	--	40
Yb	134	0	1.7	2.4	4.9	7.3	9.1
Zn	164	0	49	84	227	470	857
Zr ¹	380	0	5	118	221	372	461

¹Analyzed by X-ray fluorescence spectrography.

²Number of samples that have concentrations above the lower determination limit (unqualified values).

³Number of samples not analyzed; sediment samples from the Juneau and Seward surveys (116 samples) were not analyzed for Ag, Bi, Nb, or Sn.

⁴Calculated on samples subsequent to log transformation of the data; values less than the detection limit were replaced with one-half the value of the lower limit of determination. Lower limit may vary for neutron activation analysis.



EXPLANATION

- Sb, 2–28 ppm
- △ W, 15–40 ppm
- Ag, 5–7 ppm
- ◇ Au, 1.07 ppm
- Sediment sample site
- ⊛ Au-Ag-Pb-Zn deposit
- Au-Cu-Pb-Zn occurrence
- ▲ Au (±Cu) occurrence

Figure 3. Distribution of anomalous concentrations of Ag, Au, Sb, and W in sediment samples from Admiralty Island.

Table 2. Five-factor geochemical model for sediment samples, Admiralty Island, Alaska

[Number of samples, 380. Total variance explained by the model is 71 percent; loadings greater than 0.4 shown in boldface type]

Element	VARIMAX FACTOR LOADINGS				
	Factor				
	1	2	3	4	5
Al	0.67	0.61	0.03	-0.03	-0.08
As	0.10	0.19	0.73	0.21	-0.06
Ba	0.15	0.15	0.71	-0.31	0.05
Ca	0.67	0.06	-0.32	0.22	-0.12
Ce	0.31	0.78	0.17	0.20	0.06
Co	0.63	0.24	0.11	0.60	0.04
Cr	0.81	0.01	0.33	-0.02	-0.01
Cu	0.49	-0.12	0.38	0.35	0.40
Dy	0.36	0.61	0.12	0.06	0.31
Eu	0.38	0.65	0.15	0.20	0.26
Fe	0.70	0.43	0.08	0.40	-0.04
Hf	-0.02	0.86	0.01	0.05	-0.09
Lu	0.03	0.65	0.03	0.22	0.32
Mg	0.90	0.13	0.10	0.12	0.08
Mn	0.41	0.25	0.08	0.71	-0.16
Na	0.62	0.56	-0.09	-0.16	-0.24
Ni	0.63	-0.18	0.49	0.16	0.14
Pb	-0.05	0.10	0.04	-0.16	0.80
Sc	0.87	0.31	0.02	0.18	0.05
Th	-0.03	0.63	0.38	-0.05	0.01
Ti	0.60	0.63	-0.07	-0.01	0.07
U	0.05	0.48	0.37	0.17	0.14
V	0.83	0.32	0.19	0.12	0.05
Zn	-0.04	0.09	0.48	0.22	0.41
Zr	0.32	0.86	-0.04	-0.05	-0.14
Percent of total variance	41	12	10	5	4

INTERPRETATION OF MODEL

Factor 1 (Mg-Sc-V-Cr-Fe-Al-Ca-Co-Ni-Na-Ti-Cu-Mn)—Jurassic and Cretaceous Douglas Island Volcanics; Mesozoic or Paleozoic metamorphic rocks.

Factor 2 (Hf-Zr-Ce-Lu-Eu-Th-Ti-Dy-Al-Na-U-Fe)—Cretaceous plutonic rocks; Tertiary Admiralty Island Volcanics.

Factor 3 (As-Ba-Ni-Zn)—Triassic volcanic and sedimentary rocks; base-metal sulfide and barite mineral occurrences.

Factor 4 (Mn-Co-Fe)—Iron and manganese oxide minerals; weathering and oxidation products.

Factor 5 (Pb-Zn-Cu)—Triassic volcanic and sedimentary rocks; base-metal sulfide mineral occurrences.

samples contain 200–385 ppm Zn and associated anomalous Cu (103–123 ppm) and Pb (20–132 ppm).

The anomalous concentrations and consistent association of these elements in samples from restricted geographic areas is good evidence that factors 3 and 5 are indicative of mineralization. Specifically, the data indicate

Table 3. Concentrations of As, Au, Ba, Ni, Sb, and Zn in samples having anomalous scores for factor 3 (As-Ba-Ni-Zn), Admiralty Island, Alaska

[In parts per million. Boldface type indicates anomalous concentrations (approximately 90th percentile or greater; table 1); L indicates value less than the lower determination limit]

Sample ¹	Score ²	As	Au	Ba	Ni	Sb	Zn
GREENS CREEK AREA							
3071535	2.16	47	L	2,712	222	L	L
3071536	2.15	47	L	1,612	89	L	250
3071537	1.40	26	L	1,450	84	5	238
3071541	1.55	39	L	1,556	55	L	299
3071543	2.03	47	L	2,944	66	L	183
3071544	2.64	101	1.07	2,628	48	7	368
3071545	2.56	51	L	4,217	61	7	267
3071547	1.44	26	L	2,623	46	2	L
3071548	1.70	27	L	1,119	58	L	153
3071640	2.72	42	L	3,259	66	5	694
3071836	2.40	81	L	1,041	67	28	176
3071840	1.46	11	L	542	749	L	L
3071841	1.78	72	L	1,216	50	L	359
Windfall CREEK AREA							
3080271	1.35	39	L	1,451	34	L	L
3080274	1.94	44	L	896	118	L	358
3080275	1.49	156	L	1,271	16	L	236
3080278	1.80	47	L	1,133	42	L	322
3080305	1.36	34	L	1,774	39	L	L
3080339	1.86	33	L	1,392	106	L	158
3080428	1.31	16	L	657	96	L	296
3080429	2.58	88	L	679	202	L	517
3080430	3.00	196	L	623	58	L	202
3080431	2.71	216	L	946	50	L	205
GAMBIER BAY AREA							
3080111	1.63	14	L	2,672	25	L	L
3080113	1.78	8	L	7,118	98	L	100
3080115	1.57	23	L	1,811	45	L	164
3080131	1.84	19	L	9,090	37	5	423
3080230	1.83	55	L	2,366	84	9	361
3080313	1.65	41	L	2,175	100	L	182
3080415	1.53	19	L	688	17	L	198

¹Location given in Los Alamos National Laboratory (1982a, b, c).

²Score greater than or equal to 1.31 considered anomalous.

favorability for volcanogenic massive sulfide mineralization based on the following observations:

1. Most samples from the drainage basin of the Greens Creek deposit and other small Au-Cu-Pb-Zn prospects are anomalous in As, Ba, and Zn and corresponding scores for factors 3 (As-Ba-Ni-Zn) and 5 (Pb-Zn-Cu). The Pyrola deposit is not delineated; however, the only samples collected along the creek that drains the deposit are 10 km downstream, below a lake (fig. 3).

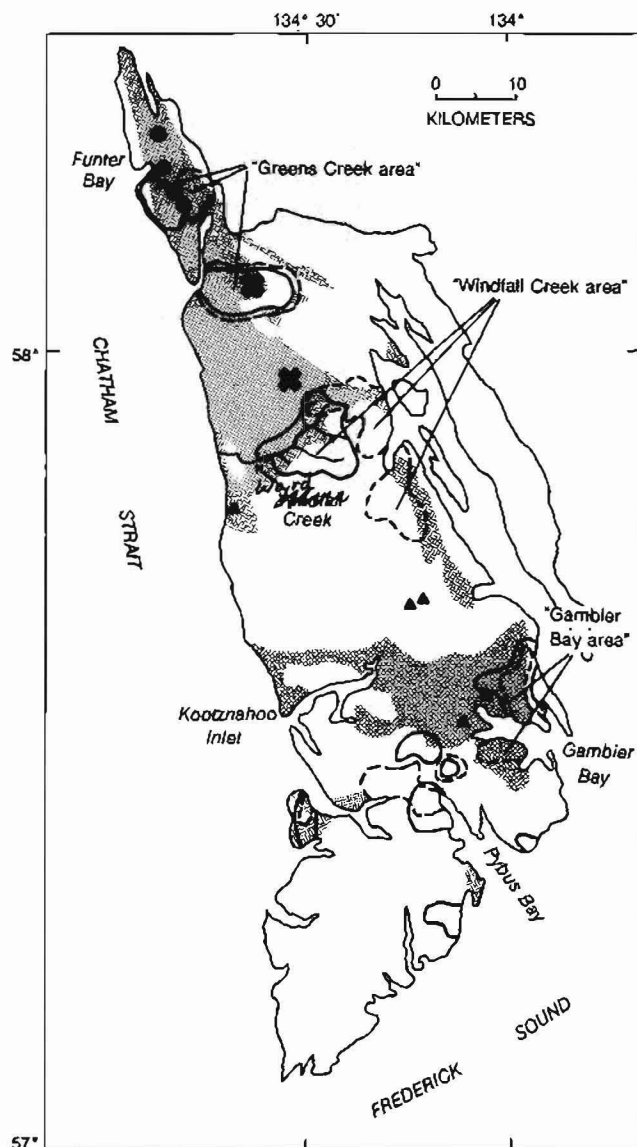
2. Barite, the most likely source of anomalous Ba in the sediment samples, is a common constituent in both the Greens Creek and Pyrola deposits (Van Nieuwenhuysse, 1984; Crafford, 1989).

3. Freibergite [(Ag, Cu)₁₂(Sb,As)₄S₁₃] is a common ore mineral at Greens Creek, and many of the samples in the Greens Creek area contain correspondingly anomalous Sb (fig. 3). Similar anomalous concentrations of Sb are in samples from the Gambier Bay area.

4. Except for the area north and southwest of Pybus Bay, samples having anomalous scores are associated with rocks of similar lithology and age as those that host the Greens Creek and Pyrola deposits.

The Greens Creek, Windfall Creek, and Gambier Bay areas form a northwest-trending belt (fig. 4). This trend is consistent with the regional northwest trend of syngenetic massive sulfide occurrences of Permian and Triassic age in southeastern Alaska (fig. 1) (Goldfarb and others, 1987).

Although the data are useful in targeting areas having high favorability for volcanogenic massive sulfide occurrences, evaluation of other types of deposits is not possible because of the lack of data for Au, Ag, Bi, Mo, Sn, and W. For instance, although six gold prospects are reported on Admiralty Island, they are not reflected by geochemical anomalies other than anomalous tungsten in one sediment sample (fig. 3).



EXPLANATION







-  Triassic and Permian volcanic and sedimentary rocks
-  Basin area containing samples having scores >90th percentile for factor 3 (As-Ba-Ni-Zn)
-  Basin area containing samples having scores >90th percentile for factor 5 (Pb-Zn-Cu)
-  Ag-Au-Pb-Zn deposit
-  Au-Cu-Pb-Zn occurrence
-  Au (±Cu) occurrence

Figure 4. Basin areas containing samples having anomalous scores for factors 3 and 5. Single-sample anomalies are not shown unless the sample was anomalous in both factor 3 and factor 5 scores. Areas labelled refer to text and table 3.

CONCLUSIONS

Factor analysis of the geochemical data from the NURE program is useful in determining the geochemical associations in sediment samples that are characteristic of the Late Triassic volcanogenic massive sulfide deposit at Greens Creek. These associations are reflected by factors 3 and 5 and consist of As-Ba-Ni-Zn and Pb-Zn-Cu, respectively. Based on these associations, two additional geochemically favorable areas underlain by Triassic volcanic and sedimentary rocks containing no known occurrences are outlined: the Windfall Creek and Gambier Bay areas. The Pyrola deposit could not be delineated because of insufficient sampling in the basin containing the deposit.

Sediment samples from the Greens Creek drainage have anomalous concentrations of Sb (5–28 ppm), As (35–101 ppm), Ba (1,200–4,217 ppm), Cu (106 ppm), Pb (as much as 132 ppm), and Zn (270–694 ppm). These are likely the result of concentrations of ore-related minerals such as barite, chalcopyrite, galena, sphalerite, and antimony- and arsenic-bearing sulfide and sulfosalt minerals. Sediments from Windfall Creek and Gambier Bay contain concentrations similar to or higher than those at Greens Creek. Concentrations of 7,118–9,090 ppm Ba are in sediment samples from near Gambier Bay. The Windfall Creek area is characterized by one or more samples containing as much as 216 ppm As and 123 ppm Cu.

The highly anomalous concentrations of ore-related elements in sediment samples from Windfall Creek and Gambier Bay indicate that these areas have been mineralized. Furthermore, the As-Ba-Ni-Zn and Pb-Zn-Cu geochemical associations that delineate these areas suggest that syngenetic volcanogenic massive sulfide mineralization similar to that at Greens Creek is most likely.

REFERENCES CITED

- Barker, Fred, 1957, Geology of the Juneau (B-3) quadrangle, Alaska: U.S. Geological Survey Map GQ-100, scale 1:63,360.
- Berg, H.C., and Cobb, E.H., 1967, Metalliferous lode deposits of Alaska: U.S. Geological Survey Bulletin 1246, 254 p.
- Carter, Claire, 1977, Age of the Hood Bay Formation, Alaska, in Sohl, N.F., and Wright, W.B., eds., Changes in stratigraphic nomenclature by the U.S. Geological Survey, 1976: U.S. Geological Survey Bulletin 1435-A, p. 117–118.
- Cobb, E.H., 1972, Metallic mineral resources map of the Sitka quadrangle, Alaska: U.S. Geological Survey Miscellaneous Field Studies Map MF-467, scale 1:250,000.

- _____. 1978, Summary of references to mineral occurrences (other than mineral fuels and construction materials) in the Sitka quadrangle, Alaska: U.S. Geological Survey Open-File Report 78-450, 124 p.
- Crafford, T.C., 1989, The Greens Creek Ag-Au-Pb-Zn massive sulfide deposit, Admiralty Island, southeast Alaska [abs.]: Alaska Miners Association Conference, Juneau, April, 1989, p. 27-29.
- Davis, J.C., 1986, *Statistics and data analysis in geology* (2nd ed.): New York, John Wiley and Sons, 646 p.
- Dressler, J.S., and Dunbire, J.C., 1981, The Greens Creek ore deposit, Admiralty Island, Alaska: Canadian Institute of Mining and Metallurgy Bulletin, v. 74, no. 833, p. 57.
- Ford, A.B., and Brew, D.A., 1988, The Douglas Island volcanics; basaltic-rift—not andesitic-arc—volcanism of the "Gravina-Nutzotin belt," northern southeastern Alaska: Geological Society of America Abstracts with Programs, v. 20, no. 7, p. 111.
- Ford, A.B., Karl, S.M., Duttweiler, K.A., Sutphin, D.M., Finn, C.A., and Brew, D.A., 1989, Sitka Quadrangle, Alaska—An AMRAP preassessment planning document: U.S. Geological Survey Administrative Report, 92 p.
- Gehrels, G.E., and Saleeby, J.B., 1987, Geologic framework, tectonic evolution, and displacement history of the Alexander terrane: *Tectonics*, v. 6, no. 2, p. 151-173.
- Goldfarb, R.J., Nelson, S.W., Berg, H.C., and Light, T.D., 1987, Distribution of mineral deposits in the Pacific Border Ranges and Coast Mountains of the Alaskan Cordillera, in Elliot, I.L., and Smee, B.W., eds., *Geoexpo/86—Exploration in the North American Cordillera*: Association of Exploration Geochemists, p. 19-41.
- Herbert, C.F., and Race, W.H., 1965, Geochemical investigations of selected areas in southeastern Alaska: Alaska Division of Mines and Minerals Geochemical Report 1, 45 p.
- Jones, D.L., Berg, H.C., Coney, P., and Harris, A., 1981, Structural and stratigraphic significance of Upper Devonian and Mississippian fossils from the Cannery Formation, Kupreanof Island, southeastern Alaska, in Albert, N.R.D., and Hudson, T., eds., *The United States Geological Survey in Alaska—Accomplishments during 1979*: U.S. Geological Survey Circular 823-B, p. 109-112.
- Karl, S.M., 1989, Paleoenvironment implications of Alaskan siliceous deposits, in Hein, J.R., and Obradovich, J.D., eds., *Siliceous deposits of the Tethys and Pacific regions*: New York, Springer-Verlag, p. 169-200.
- Lathram, E.H., Pomeroy, J.S., Berg, H.C., and Loney, R.A., 1965, Reconnaissance geology of Admiralty Island, Alaska: U.S. Geological Survey Bulletin 1181-R, 48 p.
- Loney, R.A., 1964, Stratigraphy and petrography of the Pybus-Gambier area, Admiralty Island, Alaska: U.S. Geological Survey Bulletin 1178, 103 p.
- Los Alamos National Laboratory, 1982a, Hydrogeochemical and stream sediment reconnaissance basic data for the Juneau quadrangle, Alaska: U.S. Department of Energy Report GJBX-90(82).
- _____. 1982b, Hydrogeochemical and stream sediment reconnaissance basic data for the Sitka quadrangle, Alaska: U.S. Department of Energy Report GJBX-128(82).
- _____. 1982c, Hydrogeochemical and stream sediment reconnaissance basic data for the Sumdum quadrangle, Alaska: U.S. Department of Energy Report GJBX-47(82).
- Reed, J.C., 1942, Nickel-copper deposit at Funter Bay, Admiralty Island, Alaska: U.S. Geological Survey Bulletin 936-O, p. 349-361.
- Silberfing, N.J., and Jones, D.L., eds., 1984, Lithotectonic terrane maps of the North American Cordillera: U.S. Geological Survey Open-File Report 84-523.
- Van Nieuwenhuysse, R.E., 1984, Geology and geochemistry of the Pyrola massive sulfide deposit, Admiralty Island, Alaska: Tucson, University of Arizona, M.S. thesis, 170 p.

Chapter B

Geochemical Orientation Study for Identification of Metallic Mineral Resources in the Sitka Quadrangle, Southeastern Alaska

By E. LANIER ROWAN, ELIZABETH A. BAILEY,
and RICHARD J. GOLDFARB

U.S. GEOLOGICAL SURVEY BULLETIN 1950

GEOCHEMICAL STUDIES IN ALASKA BY THE U.S. GEOLOGICAL SURVEY, 1989

CONTENTS

Abstract	B1
Introduction	B1
Tectonic-geologic setting	B3
Description of sampling and analytical methods	B3
Sample collection	B3
Sample preparation	B3
Analytical techniques	B3
Volcanogenic massive sulfide deposits	B4
Gold-quartz vein deposits	B7
Ultramafic-hosted nickel-copper sulfide deposits	B8
Chromite deposits	B10
Discussion and summary	B11
References cited	B11

FIGURES

- 1-2. Maps showing locations of:
 1. Sitka quadrangle, Alaska B1
 2. Mining districts and deposits and tectonostratigraphic terranes, Sitka quadrangle B2
- 3-6. Maps showing sample localities in vicinity of:
 3. Pyrola volcanogenic massive sulfide deposit, Admiralty Island B5
 4. Lucky Chance gold-quartz vein deposit, Baranof Island B7
 5. Bohemia Basin magmatic nickel-copper sulfide deposits, southern Yakobi Island B8
 6. Chromite occurrences, central Baranof Island B10

TABLES

- 1-3. Lower limits of determination for:
 1. Semiquantative emission spectrographic analysis of stream-sediment, heavy-mineral concentrate, and rock samples B4
 2. Analysis of stream-sediment and rock samples by ICP-10 B5
 3. ICP-40 analysis of stream-sediment and rock samples B5
- 4-5. Comparison of concentrations of selected elements in:
 4. Three stream-sediment size fractions and three magnetic fractions of the heavy-mineral concentrates from the Pyrola volcanogenic massive sulfide deposit B6
 5. Three stream-sediments size fractions from of the Lucky Chance gold-quartz vein deposit B8
6. Element concentrations determined by emission spectrography for rock samples from the Bohemia Basin nickel-copper sulfide deposits B9
7. Comparison of ore and pathfinder element concentrations in three stream-sediment size fractions from the Bohemia Basin nickel-copper sulfide district B9
8. Comparison of chromium concentrations in fine, medium, and coarse stream-sediment samples, and in magnetic, weakly magnetic, and nonmagnetic fractions of heavy-mineral concentrates from the chromite district of central Baranof Island B10

Geochemical Orientation Study for Identification of Metallic Mineral Resources in the Sitka Quadrangle, Southeastern Alaska

By E. Lanier Rowan, Elizabeth A. Bailey, and Richard J. Goldfarb

Abstract

Stream-sediment and rock samples were collected from the vicinity of four mineralized areas representative of the known principal ore deposit types in the Sitka region of southeastern Alaska. Results of chemical analyses of the samples provide information to guide future geochemical exploration programs in this region. Three size fractions of the stream-sediment samples were analyzed by semiquantitative emission spectrography (SQS), induction coupled plasma (ICP), and atomic absorption (AA) techniques. In addition, three magnetic fractions of heavy-mineral concentrates from stream-sediment samples were analyzed by SQS to determine the optimal sample media and analytical methods.

Four principal deposit types are known in the region of the Sitka quadrangle: (1) Kuroko-type volcanogenic massive sulfide deposits, (2) gold-quartz vein deposits, (3) chromite deposits hosted by ultramafic rocks, and (4) magmatic nickel-copper sulfide deposits in ultramafic rocks. Dispersion from the first three deposit types is readily identified through chemical analyses of the stream-sediment samples alone; however, the heavy-mineral concentrate samples provide additional mineralogical information and, at some localities, give better anomaly to background contrast.

Emission spectrography is adequate for recognition of dispersion trails from the volcanogenic massive sulfide and chromite deposit types. The more sensitive AA and ICP techniques, however, are required to detect arsenic, gold, cadmium, and antimony anomalies in stream-sediment samples downstream from gold-quartz vein deposits. The nickel-copper deposits were not detected at a distance greater than approximately 0.8 km downstream using any of the sample media or analytical methods tested. Identification of new nickel-copper occurrences will require detailed field investigation of ultramafic intrusive bodies that may be delineated by stream-sediment geochemistry.

INTRODUCTION

This study was undertaken to determine the stream-sediment sample types and analytical methods most effective in locating mineralized rocks in the Sitka quadrangle and in the surrounding region of southeastern Alaska (figs. 1, 2). Numerous operating or historic mines

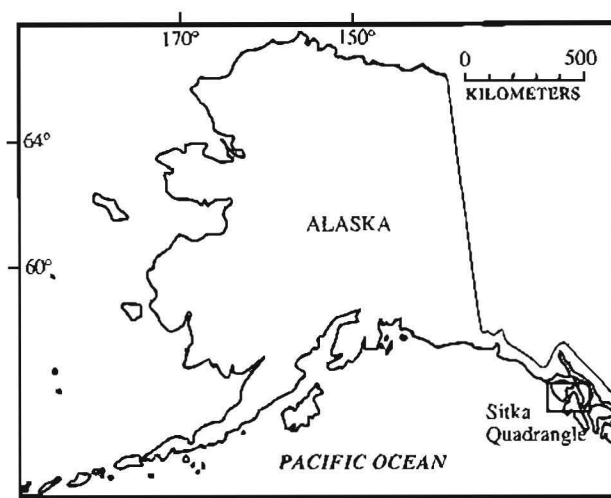


Figure 1. Location of the Sitka quadrangle, Alaska.

and prospects within or close to the Sitka quadrangle represent four different types of mineral deposits and present an unusual opportunity to conduct a pilot geochemical study. The results of this study provide guidelines for future geochemical exploration and assessment of metallic mineral resources in the Sitka quadrangle and in geologically similar regions in Alaska.

The principal mineral deposit types known in the Sitka quadrangle or just outside its boundaries are (fig. 2): (1) gold-quartz veins exemplified by the Chichagof and Apex-El Nido districts and the Lucky Chance deposit (Knopf, 1912; Reed and Coats, 1941; Rossmann, 1959), (2) Kuroko-type volcanogenic massive sulfide mineralized rocks at Pyrola (Van Nieuwenhuysse, 1984), (3) lenses of chromite hosted by serpentinized ultramafic rocks on central Baranof Island (Kennedy and Walton, 1946a; Loney and others, 1975), and (4) magmatic nickel-copper sulfide

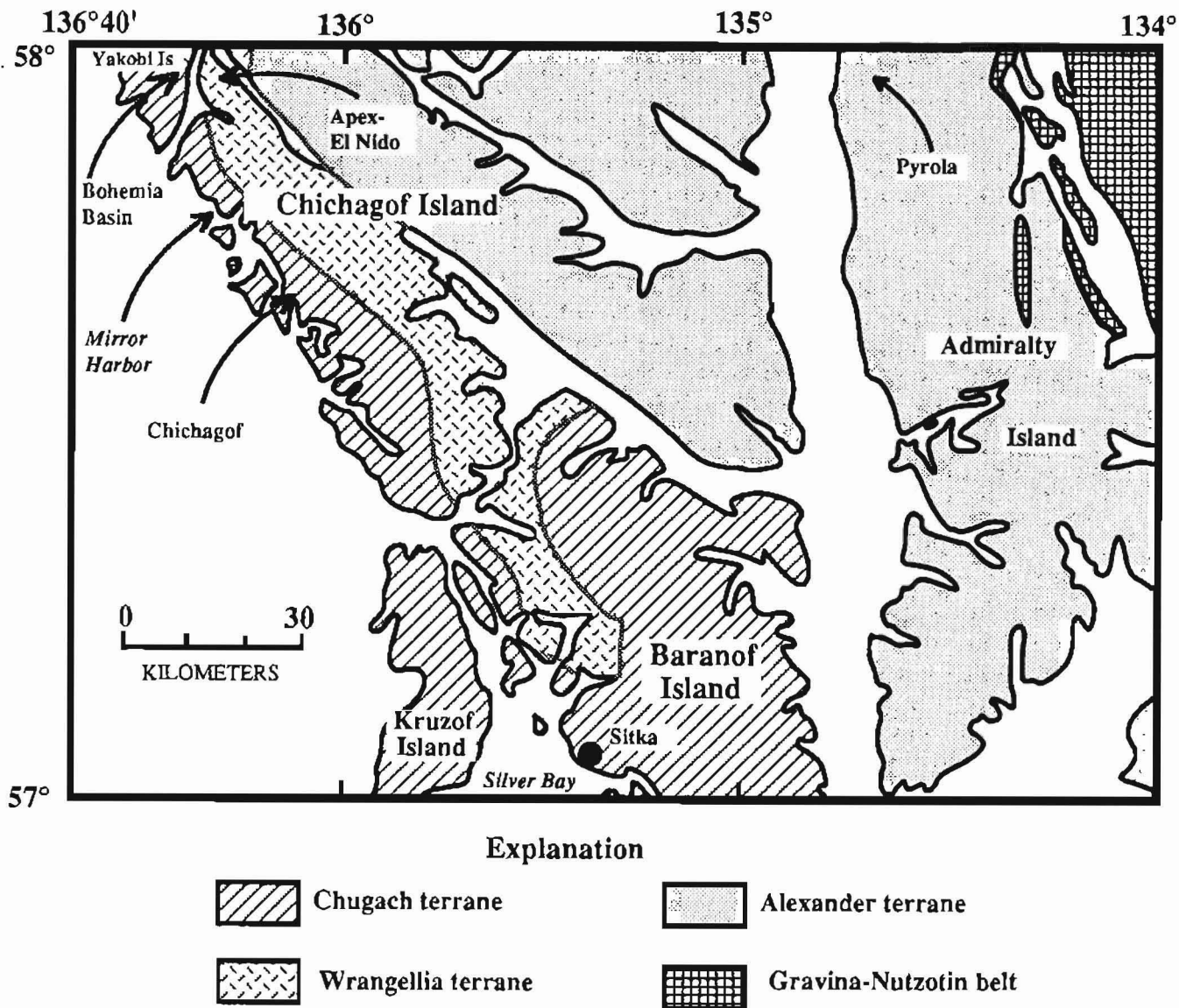


Figure 2. Mining districts and deposits (arrows) and tectonostratigraphic terranes in the Sitka quadrangle. Modified from Berg and others (1978) and Ford and others (1989).

segregations hosted by ultramafic rocks at Bohemia Basin and Mirror Harbor (Reed and Dorr, 1942; Kennedy and Walton, 1946b; Loney and others, 1975; Bundtzen and others, 1984; Still, 1988).

Thirty-one samples of stream sediments and heavy-mineral concentrates from stream sediments and seventeen rock samples were collected from localities believed to be typical of the four principal types of mineral deposits in the Sitka quadrangle. Coarse, medium, and fine fractions of each stream-sediment sample and the magnetic, weakly magnetic, and nonmagnetic fractions of heavy-mineral concentrates were analyzed by four techniques (emission

spectrography, atomic absorption, and inductively coupled plasma emission spectroscopy using two different digestion methods). Results were compared to determine optimal sampling media and analytical methods. For each deposit type except chromite, rock samples were used to define the characteristic suite of elements, including potential pathfinder elements.

Acknowledgments.—The authors gratefully acknowledge P.H. Briggs, J.R. Motooka, and R. O'Leary, who carried out some chemical analyses of the samples. We are also grateful to R.B. Tripp, who identified mineral grains in the heavy-mineral concentrates.

TECTONIC-GEOLOGIC SETTING

The rocks of the Sitka quadrangle constitute parts of three distinct tectonostratigraphic terranes—the Chugach, Wrangellia, and Alexander—and the Gravina-Nutzotin belt overlap assemblage (fig. 2) (Ford and others, 1989). The Chugach terrane consists of flysch and melange formed in a subduction complex; this terrane was accreted to and subducted below the Wrangellia and Alexander terranes in Late Cretaceous to early Tertiary time (Plafker and others, 1977). The Cretaceous Sitka Graywacke within the Chugach terrane hosts most of the gold-bearing quartz deposits. Mafic igneous rocks intruding metasedimentary units of the Chugach terrane are hosts for the nickel-copper and chromium occurrences.

Pre-Middle Pennsylvanian island-arc volcanic and sedimentary rocks overlain by Triassic rift-fill tholeiitic basalt and limestone make up the Wrangellia terrane (MacKevett, 1978; Nokleberg and others, 1985). The Alexander terrane is comprised of igneous, volcanic-arc, and sedimentary rocks of Precambrian (?) to Middle Jurassic age (Eberlein and others, 1983; Gehrels and Saleeby, 1987a, b). The Wrangellia and Alexander terranes were accreted to the craton by Late Cretaceous to early Tertiary time. The Gravina-Nutzotin overlap assemblage on the northwestern part of Admiralty Island consists of basaltic volcanic rocks (Ford and Brew, 1988), argillite, graywacke turbidite, and conglomerate (Loney, 1964) deposited in a basin formed between the amalgamated Alexander-Wrangellia terranes and previously accreted terranes to the east. The syngenetic Pyrola volcanogenic massive sulfide deposit is in argillite and volcanic rocks of the Triassic Retreat Group in the Alexander terrane (Van Nieuwenhuysse, 1984).

DESCRIPTION OF SAMPLING AND ANALYTICAL METHODS

Sample Collection

A total of 17 rock samples were collected from the vicinity of the four deposits or mining districts. In the Bohemia Basin, nickel-copper-rich samples were collected from mine waste piles. Mineralized float samples were collected from the stream channel approximately 200 m downstream from Pyrola. At the Lucky Chance deposit, samples were collected from ore or tailings piles within a few meters of the main mine portal. Most samples collected in these three areas contain visible sulfide minerals. No mineralized rock samples were collected from the chromite district.

At stream sample sites, sediment was collected from the active part of the stream channel and passed through a 10-mesh (2.0 mm) sieve to remove pebbles. In addition to a

stream-sediment sample, a heavy-mineral concentrate was obtained by panning additional sediment until most of the quartz, feldspar, organic material, and clay-size material was removed.

Sample Preparation

Rock samples were crushed and then pulverized to -0.15 mm using ceramic plates. Each rock was analyzed by all four methods of analysis (discussed below).

Stream sediments were air dried, then sieved to three fractions: -10 to $+60$ mesh (2.0–0.25 mm), -60 to $+200$ mesh (0.25–0.075 mm), and -200 mesh (0.075 mm). These three fractions correspond to coarse to medium sand, fine to very fine sand, and very fine sand to silt, respectively. All fractions were pulverized and then analyzed using all four analytical techniques.

Heavy-mineral concentrate samples were air dried then passed through a 30-mesh (0.59 mm) sieve. Any remaining quartz, feldspar, organic material, or clays less than 30 mesh were removed by allowing the heavy material in each sample to settle through bromoform (sp gr 2.85). The heavy fraction was then separated into magnetic, weakly magnetic, and nonmagnetic fractions using a Frantz Isodynamic Separator. The magnetic fraction (primarily magnetite), weakly magnetic fraction (mostly ferromagnesian silicate and oxide minerals), and nonmagnetic fractions (mostly ore minerals, rutile, zircon, sphene, and so on) were split again if enough sample was available. One split was saved for identification of mineral grains using a binocular microscope. The other split was handground for chemical analysis. The relatively small sample volumes restricted heavy-mineral concentrate analysis to the semi-quantitative emission spectrographic technique.

Analytical Techniques

The four methods of analysis used were atomic absorption spectrometry (AA) for gold, semiquantitative emission spectrography (SQS) for 35 elements (rock and stream-sediment samples) and 37 elements (heavy-mineral concentrates), and inductively coupled plasma atomic emission spectroscopy for 10 elements (ICP-10) and for 40 elements (ICP-40) using two different digestion methods.

The stream-sediment and rock samples were analyzed for gold by atomic absorption (AA) following a hydrobromic acid and bromine digestion and an MIBK extraction (Thompson and others, 1968). The lower limit of determination for gold is 0.05 ppm.

All sample media were analyzed for 35 or 37 elements using the six-step semiquantitative emission spectrographic (SQS) method of Grimes and Marranzino (1968). The elements and their lower limits of determination are

listed in table 1. Spectrographic results were obtained by visual comparison of spectra derived from the sample with spectra obtained from standards made from pure oxides and carbonates. The analytical values are geometrically spaced over any given order of magnitude of concentration (10, 7, 5, 3, 2, 1.5, and multiples of these numbers). The precision of this method is approximately plus or minus one reporting interval at the 83 percent confidence level and plus or minus two reporting intervals at the 96 percent confidence level (Motooka and Grimes, 1976).

The stream-sediment and rock samples were analyzed by two ICP methods. The first, ICP-10, employs the method of Motooka (1988). Silver, arsenic, gold, bismuth, cadmium, copper, molybdenum, lead, antimony, and zinc were extracted into the organic phase of 10 percent Aliquot 336 (tricaprylylmethylammonium chloride) DIBK (di-isobutyl ketone) in the presence of ascorbic acid and potassium iodide in 6N HCl. The organic phase was then separated for aspiration into the plasma, and the concentrations of the 10 elements were determined simultaneously. The lower limits of determination are listed in table 2.

The second method, ICP-40, employs a digestion without subsequent extraction into an organic phase. The samples were dissolved in HF, aqua regia, and HClO₄ and then dried (Crock and others, 1983; Lichte and others, 1987). The residues were redissolved in aqua regia and diluted to 10 mL with 1 percent HNO₃. The solution was then introduced into the plasma and the concentrations of 40 elements measured simultaneously. The 40 elements and their lower limits of determination are shown in table 3. The dissolution procedure described volatilizes silicon and boron and does not dissolve minerals such as zircon, tourmaline, cassiterite, rutile, and chromite.

VOLCANOGENIC MASSIVE SULFIDE DEPOSITS

The Pyrola deposit on Admiralty Island is the only known Kuroko-type volcanogenic massive sulfide deposit in the Sitka quadrangle, although the Greens Creek deposit to the north on Admiralty Island (in the Juneau quadrangle) is of the same type (Crafford, 1989). Similar mineralized rocks are associated with Triassic volcanic rocks throughout the length of southeastern Alaska (Goldfarb and others, 1987). The Pyrola deposit is at the contact between mafic volcanic rocks and fine-grained clastic and carbonate units of the Retreat Group. Massive pods of pyrite and sphalerite and adjacent lenses of silver-rich barite make up most of the deposit. Galena and lesser chalcopyrite, boulangerite, and jamesonite are additional sulfide phases. Chemical analyses of barite-rich float indicate significant arsenic and antimony concentrations associated with some of the ore (E.L. Rowan and others, unpub. data). Local sericite-pyrite-quartz alteration is superimposed on a broad chlorite-carbonate alteration halo (Van Nieuwenhuysse, 1984).

Table 1. Lower limits of determination for semiquantitative emission spectrographic (SQS) analysis of stream-sediment, heavy-mineral concentrate, and rock samples [Values for rock and stream-sediment samples are based on a 10-mg sample and for heavy-mineral concentrate samples on a 5-mg sample. Stream-sediment and rock samples were not analyzed for platinum and palladium]

Element	Stream-sediment and rock samples	Heavy-mineral concentrates
PERCENT		
Calcium (Ca).....	0.05	0.1
Iron (Fe).....	0.05	0.1
Magnesium (Mg).....	0.02	0.05
Sodium (Na).....	0.2	0.5
Phosphorus (P).....	0.2	0.5
Titanium (Ti).....	0.002	0.005
PARTS PER MILLION		
Manganese (Mn).....	10	20
Silver (Ag).....	0.5	1
Arsenic (As).....	200	500
Gold (Au).....	10	20
Barium (Ba).....	20	50
Boron (B).....	10	20
Beryllium (Be).....	1	2
Bismuth (Bi).....	10	20
Cadmium (Cd).....	20	50
Cobalt (Co).....	10	20
Chromium (Cr).....	10	20
Copper (Cu).....	5	10
Gallium (Ga).....	5	10
Germanium (Ge).....	10	20
Lanthanum (La).....	50	100
Molybdenum (Mo).....	5	10
Niobium (Nb).....	20	50
Nickel (Ni).....	5	10
Palladium (Pd).....	—	2
Platinum (Pt).....	—	10
Lead (Pb).....	10	20
Antimony (Sb).....	100	200
Scandium (Sc).....	5	10
Tin (Sn).....	10	20
Strontium (Sr).....	100	200
Vanadium (V).....	10	20
Tungsten (W).....	20	50
Yttrium (Y).....	10	20
Zinc (Zn).....	200	500
Zirconium (Zr).....	10	20
Thorium (Th).....	100	200

Stream-sediment and heavy-mineral concentrate samples were collected in a small, unmineralized watershed about 1.5 km east of Pyrola, on a small tributary approximately 0.3 km downstream from Pyrola, and on a major stream approximately 1.5, 5, and 8 km below the orebody (fig. 3). Emission spectrographic data for stream-

Table 2. Lower limits of determination for analysis of stream-sediment and rock samples by ICP-10 (and atomic absorption for gold)
[In parts per million]

Element	Lower limit	Element	Lower limit
Ag.....	0.045	Cu.....	0.05
As.....	0.60	Mo.....	0.09
Au.....	0.15	Pb.....	0.60
Au ¹	0.05	Sb.....	0.60
Bi.....	0.60	Zn.....	0.03
Cd.....	0.03		

¹Atomic absorption analysis.

Table 3. Lower limits of determination for ICP-40 analysis of stream-sediment and rock samples

Limit Element (percent)	Element	Limit (ppm)	Element	Limit (ppm)
Al.....0.05	Ag.....	2	Li.....	2
Ca.....0.05	As.....	10	Mn.....	10
Fe.....0.05	Au.....	8	Mo.....	2
K.....0.05	Ba.....	1	Nb.....	4
Mg.....0.005	Be.....	1	Nd.....	20
Na.....0.005	Bi.....	10	Ni.....	2
P.....0.005	Cd.....	2	Pb.....	4
Ti.....0.005	Ce.....	4	Sc.....	2
	Co.....	1	Sn.....	4
	Cr.....	1	Sr.....	2
	Cu.....	2	Th.....	4
	Eu.....	2	U.....	100
	Ge.....	20	V.....	2
	Ga.....	4	Y.....	2
	Ho.....	4	Yb.....	1
	La.....	2	Zn.....	4

sediment samples indicate dispersion trains for silver, barium, molybdenum, lead, and zinc in all three size fractions (table 4). Copper and iron distributions also show dispersion trains downstream from Pyrola, but only in the coarse sediment size fraction. Silver, barium, and lead show the broadest dispersion halos for the three stream-sediment size fractions. Anomalous values for these three elements persist to the sample site 8 km downstream from Pyrola. Anomaly to background contrast for the Pyrola area is strongest for silver and barium, especially in the fine (-200 mesh) size fraction. Silver values in the -200 mesh sediments range from not detected at a 0.5 ppm lower determination limit to 20 ppm, and barium values range from a 500 ppm background level at sites to the east of Pyrola, to greater than 5,000 ppm just below Pyrola, and 2,000 ppm 8 km downstream.

Semiquantitative emission spectrographic (SQS) analysis of stream-sediment samples is clearly adequate for use in regional exploration surveys in the Sitka area for massive sulfide deposits similar to Pyrola. It is possible, however, to determine a more complete suite of anomalous

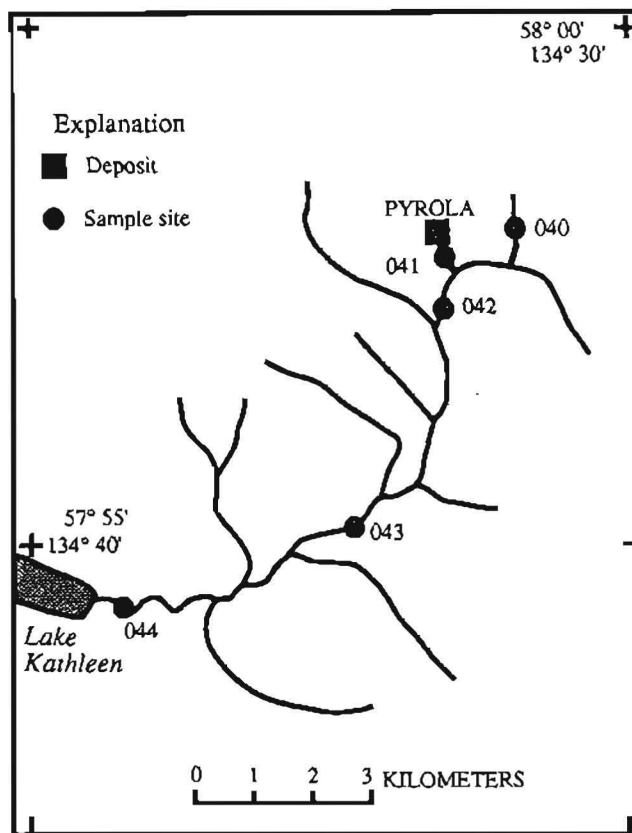


Figure 3. Sample localities in vicinity of Pyrola volcanogenic massive sulfide deposit, Admiralty Island.

metals, including arsenic, cadmium, and antimony, if SQS is combined with the more sensitive ICP-10 technique. ICP-10 data for all three elements from all three size fractions show enrichment relative to local background values at the site farthest below Pyrola; anomalies are strongest for antimony. Analytical values for antimony for all size fractions collected 8 km downstream from Pyrola are from 1.3 to 1.7 ppm, relative to background values of less than 0.6 ppm. Narrower dispersion halos also exist for potassium (determined by ICP-40) within all stream-sediment size fractions. The potassium enrichment most likely reflects sericitic alteration of the host rocks.

Background barium values for nonmagnetic heavy-mineral concentrate samples from streams underlain by rocks of the Retreat Group are approximately 2,000 ppm. All nonmagnetic heavy-mineral concentrate samples collected downstream from Pyrola contain more than 10,000 ppm Ba. Barite is, however, a common accessory mineral in unmineralized areas underlain by various facies of the Retreat Group; therefore, abundant barite in nonmagnetic concentrates, flagged by barium values above 10,000 ppm in the analytical data, does not necessarily signify terranes favorable for Kuroko-type massive sulfide

Table 4. Comparison of concentrations of selected elements in three stream-sediment size fractions and three magnetic fractions of the heavy-mineral concentrates from the Pyrola volcanogenic massive sulfide deposit

[Sample locations (fig. 3) in relation to mineralized rocks are as follows: 040 is from unmineralized rocks (background), 041 is immediately below Pyrola, 042 is 1.5 km downstream, 043 is 5 km downstream, and 044 is 8 km downstream. Potassium values are in percent, all other values are in parts per million. I indicates analysis by ICP; potassium obtained using ICP-40, other elements using ICP-10. S indicates analysis by emission spectrography. N, not detected; L, value less than lower limit of determination; G, value greater than upper limit of determination]

Sample	S-Fe	S-Ag	S-Ba	S-Mo	S-Cu	S-Pb	S-Zn	I-K	I-As	I-Cd	I-Sb
-10 TO +60 MESH											
040	1.5	N	300	N	20	10L	200N	1.3	8	0.1	0.6L
041	7	15	5,000	20	50	1,000	2,000	2.8	230	3.7	37
042	5	3	5,000	7	50	100	300	1.7	40	0.7	6
043	2	0.5	1,500	5L	30	20	200L	1.6	18	0.5	3
044	3	0.7	700	5N	20	30	200N	1.3	13	0.2	1.5
-60 TO +200 MESH											
040	5	N	500	N	50	L	N	1.3	13	0.1	0.6L
041	3	15	5,000G	10	50	500	2,000	2.6	200	6	34
042	7	3	5,000	L	70	100	500	2.0	51	1.4	8
043	5	0.5	5,000	N	30	20	200	1.5	20	0.5	3
044	5	L	1,500	N	20	20	N	1.4	13	0.1	1.3
-200 MESH											
040	7	N	500	N	70	10	N	1.4	18	0.5	0.6L
041	7	20	5,000G	20	70	700	3,000	2.2	180	8	28
042	7	7	5,000	7	70	100	500	1.9	54	2	8
043	5	1.5	2,000	N	20	30	200	1.7	17	0.8	3
044	5	0.5	2,000	N	30	20	N	1.5	18	0.3	1.7
NONMAGNETIC											
	S-Ag	S-Ba	S-Mo	S-Pb	S-Sr	S-Zn					
040	L	2,000	N	30	200	N					
041	50	10,000G	20	1,000	7,000	15,000					
042	15	10,000G	10	700	5,000	5,000					
043	5	10,000G	N	50	3,000	N					
044	N	10,000G	N	20	700	N					
WEAKLY MAGNETIC											
	S-Ag	S-Ba	S-Mo	S-Pb	S-Zn						
040	N	300	N	L	N						
041	100	10,000G	70	1,500	5,000	20	7,000	200	2,000		
042	15	5,000	20	200	1,000	5	5,000	100	1,000		
043	2	1,000	N	70	N	N	300	L	700		
044	N	700	N	50	N	N	300	L	700		
MAGNETIC											
	S-Ag	S-Ba	S-Pb	S-Zn							
040	N	300	L	N							
041	20	7,000	200	2,000							
042	5	5,000	100	1,000							
043	N	300	L	700							
044	N	300	L	700							

deposits. The absence of anomalous barium may help, however, to eliminate areas as potential massive sulfide targets.

For the nonmagnetic concentrate sample medium, emission spectrographic analyses for silver, molybdenum, lead, strontium, and zinc, in addition to barium, adequately identify upstream Kuroko-type occurrences. Below Pyrola, strong molybdenum, lead, and zinc anomalies extend at least as far as 1.5 km downstream, silver at least as far as 5 km, and strontium at least as far as 8 km. The anomalous strontium is most likely due to high concentrations of this element in barite. Excluding the anomalous barium and strontium, dispersion trains are generally narrower for nonmagnetic concentrates than for stream-sediment samples. This suggests that a significant amount of hydro-

morphic dispersion may characterize erosion of these Kuroko-type systems, and that geochemical surveys designed solely for massive sulfide exploration need not include nonmagnetic heavy-mineral concentrate samples.

The weakly magnetic and magnetic fractions of the heavy-mineral concentrate samples were also analyzed by emission spectrography. Silver, barium, molybdenum, lead, and zinc in the weakly magnetic samples and silver, barium, lead, and zinc in the magnetic samples are present in anomalous concentrations downstream from Pyrola (table 4). Barium and lead in the former medium and zinc in the latter are still significantly enriched in samples 8 km below Pyrola. Therefore, in some situations, the weakly magnetic and magnetic heavy-mineral concentrate fractions may prove useful in exploration.

GOLD-QUARTZ VEIN DEPOSITS

Several small gold mines and prospects are southeast of Silver Bay, within approximately 7 km of the southern boundary of the Sitka quadrangle (fig. 4). These gold-quartz lode occurrences, briefly described by Knopf (1912), are generally along slate-graywacke contacts within the Sitka Graywacke. Quartz veins are as wide as 2.5 m and contain free gold, pyrite, and (or) pyrrhotite (Knopf, 1912). Many rock samples that we collected from the vicinity of the Lucky Chance deposit (fig. 4) contain arsenopyrite. Chemical analyses of four vein samples indicate as much as 63 ppm Au, 16 ppm Ag, 1,600 ppm As, 0.47 ppm Cd, and 2.1 ppm Sb. No other elements are anomalous.

Two stream-sediment and two heavy-mineral concentrate samples were collected at sites about 0.5 and 7 km below the Lucky Chance deposit on Salmon Creek. An additional two stream-sediment and concentrate samples were collected nearby on an unnamed stream draining Pinta Lake. This drainage basin contains a number of other small gold occurrences (Knopf, 1912).

Stream-sediment data from the four sites indicate that arsenic and antimony are the most consistently anomalous pathfinder elements and that gold and cadmium are less useful ore indicators (table 5). Concentrations for all four elements at all sites are below the lower determination limits for emission spectrography and ICP-40 methods, but anomalous values are clearly defined using ICP-10 and AA

methods. Atomic absorption analysis is the only technique sensitive enough to detect gold, but ICP-10 is adequate for determination of arsenic, cadmium, and antimony in the stream-sediment samples.

The -200 mesh stream-sediment fraction was the most useful of the fractions; arsenic values are between 29 and 270 ppm, cadmium between 0.12 and 0.47 ppm, and antimony between 1.1 and 2.3 ppm. Gold was detected in two -200 mesh samples, one near the Lucky Chance deposit (008) and the other farthest downstream from Pinta Lake (026) (fig. 4). Silver was not detected.

The coarsest sediment fraction contains 83 ppm As at the site below the Lucky Chance deposit and 0.61–0.73 ppm Sb at the other three sites. Although not as obvious as in the finest sediment fraction, the coarse sediment fraction indicates that mineralized rocks are upstream. Two samples from the medium size fraction contain anomalous arsenic but no anomalous antimony. These data suggest preferential breakdown of many of the ore-related minerals into fine-grained stream sediment and perhaps some hydromorphic dispersion of antimony. The ~200 mesh stream-sediment fraction is therefore recommended for exploration for gold-quartz veins in the Sitka quadrangle.

Arsenopyrite, pyrite, and scheelite were observed during microscopic examination of the nonmagnetic heavy-mineral concentrate samples from two sites, 008 and 025 (fig. 4). Gold grains were also found in the concentrate from site 008 below the Lucky Chance mine. Samples from both sites contain highly anomalous arsenic concentrations that reflect the observed arsenopyrite; the sample downstream from the Lucky Chance deposit contains 10,000 ppm As and that closest to Pinta Lake contains 5,000 ppm As. The former also contains 700 ppm Pb and 2,000 ppm Sn, but these values are believed to reflect contamination from old mining activities.

The broadest dispersion halos were identified using ICP-10 and AA analytical methods on the fine-grained stream-sediment samples; however, collection of concentrate samples at each sample site is still recommended for gold exploration. Microscopic observation of the nonmagnetic concentrates provides information that is not available from the chemical analyses alone. Tripp and others (1985), in a study of the Valdez Group of south-central Alaska (stratigraphically equivalent to the Sitka Graywacke), noted that arsenopyrite is much more widespread than gold. Therefore, anomalous arsenic values in stream-sediment and concentrate samples may not always be indicative of upstream gold deposits. Also, because antimony-dominant sulfide mineral phases are not common in this type of gold-bearing system (Goldfarb and others, 1987), antimony may not be a consistently reliable pathfinder element. Therefore, both ICP-10 or AA analyses

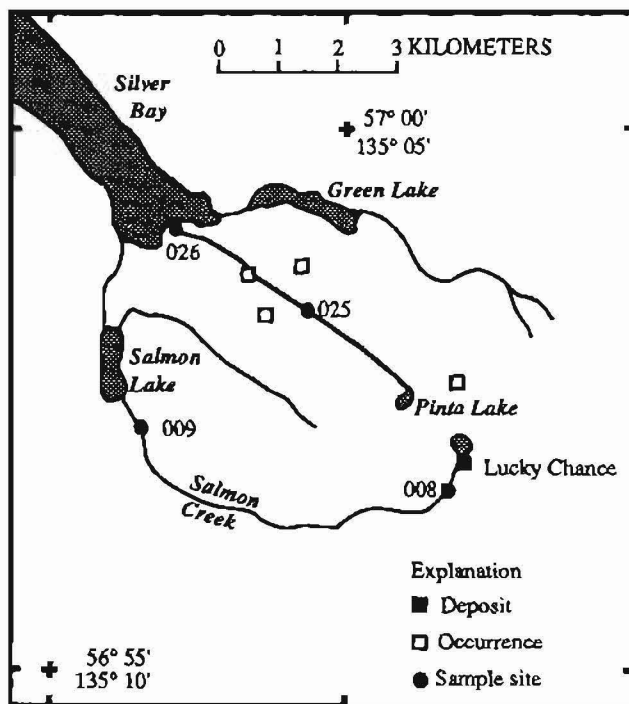


Figure 4. Sample localities in vicinity of Lucky Chance gold-quartz vein deposit, Baranof Island. Sample sites are within approximately 7 km of the southern boundary of the Sitka quadrangle.

Table 5. Comparison of concentrations of selected elements in three stream-sediment size fractions from the Lucky Chance gold-quartz vein deposit

[In parts per million. Observations made on the nonmagnetic fraction of the heavy-mineral concentrates are also shown. Sample locations in relation to mineralized rocks: 008 and 009 are 0.5 and 7 km below the Lucky Chance mine, respectively; 025 and 026 are in a basin draining several small gold prospects (fig. 4). N, not detected; L, value less than lower limit of determination]

Sample	Stream-sediment samples												Nonmagnetic concentrate samples
	-10 to +60 mesh				-60 to +200 mesh				-200 mesh				
	As	Cd	Sb	Au	As	Cd	Sb	Au	As	Cd	Sb	Au	
008	83	0.16	L	N	160	0.15	N	N	270	0.46	1.2	0.20	10,000 ppm As; pyrite, gold, scheelite.
009	13	0.09	0.73	N	12	0.07	N	N	29	0.31	1.1	N	---
025	21	0.08	0.65	N	42	0.11	N	N	140	0.47	2.3	*	5,000 ppm As; pyrite, scheelite, arsenopyrite, malachite.
026	12	0.04	0.61	N	17	0.03	N	N	49	0.12	1.2	1	---

*Insufficient sample for analysis.

of stream-sediment samples for gold and microscopic examination of concentrate samples for coarser gold grains are recommended for targeting areas that may contain vein gold deposits.

ULTRAMAFIC-HOSTED NICKEL-COPPER SULFIDE DEPOSITS

Two nickel-copper sulfide deposits have been recognized in the Sitka quadrangle: Bohemia Basin (sampled in this study), on Yakobi Island, and Mirror Harbor, on the west coast of Chichagof Island (fig. 2). These deposits formed as segregations of sulfide minerals, primarily pyrrhotite, pentlandite, and chalcopyrite, from a norite magma (Kennedy and Walton, 1946b). They are hosted by Tertiary (?) norite plutons that generally have intruded Mesozoic sedimentary rocks (Loney and others, 1975).

Several small, abandoned mine workings, trenches, and prospect pits are on the north and south sides of Bohemia Basin. Six rock samples were collected from the mine dumps. A total of nine stream-sediment samples was collected from the immediate vicinity of the mine workings and from approximately 0.8, 1.6, 2.8, and 4 km downstream of the mines (fig. 5).

All but one rock sample contains visible sulfide minerals, and all are characterized by high levels of nickel, copper, silver, cobalt, and chromium (table 6). Comparison of the concentrations of these elements with background levels for mafic and ultramafic rocks (Rose and others, 1979) indicates that metal concentrations are anomalous for nickel, copper, silver, and cobalt. High levels of chromium in various media may only indicate the presence of mafic or ultramafic rocks, and thus chromium probably is not useful as an ore pathfinder element. Silver was detected by SQS in four of the rock samples but was not detected by ICP-40 in any of the samples. Silver values were confirmed by ICP-10, which has the lowest detection limit of the three methods, although the SQS detection limits are adequate.

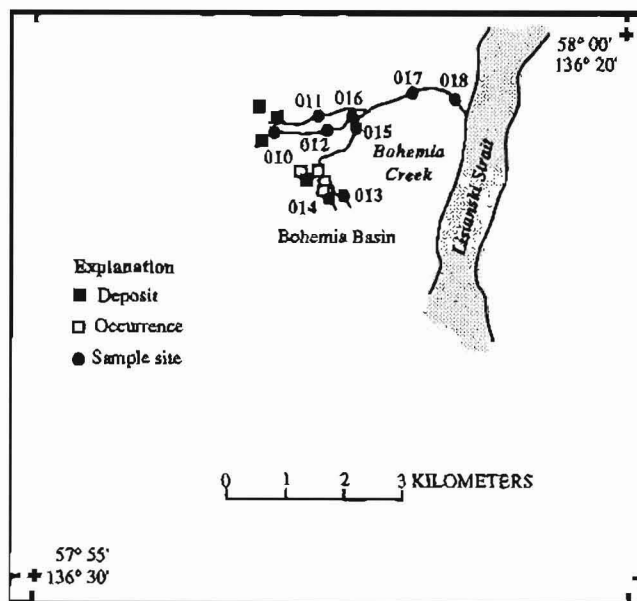


Figure 5. Sample localities in vicinity of Bohemia Basin magmatic nickel-copper sulfide deposits, southern Yakobi Island.

Stream-sediment samples were examined with particular attention to the four elements anomalous in rock samples (nickel, copper, silver, and cobalt). Concentrations of silver and copper are slightly higher in the -200 mesh stream-sediment fraction, whereas concentrations of nickel and cobalt are higher in the two coarser fractions (table 7). Sample 010, collected in the immediate vicinity of a mine, contains anomalous concentrations of silver and copper in the fine fraction (0.5 ppm and 1,500 ppm, respectively) and of cobalt and nickel in the coarser size fractions (100 ppm and 1,000 ppm, respectively) relative to the other stream-sediment samples. In a sample collected only 0.8 km downstream, however, concentrations are at background levels (<0.5, ≤100, ≤70, and ≤100 ppm for silver, copper, cobalt, and nickel, respectively) in all stream-sediment size fractions, and they remain unchanged with increasing distance downstream from the mine (fig. 5).

Table 6. Element concentrations determined by emission spectrography for rock samples from the Bohemia Basin nickel-copper sulfide deposits

[In parts per million. Sulfide minerals were visible in each sample except 6A. Background values for ultramafic and mafic rocks are given in the last two columns. Data from Rose and others (1979). N, not detected]

Element	Sample						Ultramafic	Mafic
	5A	5B	5C	6A	6B	6C		
Ag.....	0.7	N	1	N	1	0.7	0.06	0.1
Co.....	700	150	200	50	300	150	110	48
Cr.....	1,000	700	1,000	200	2,000	2,000	2,980	170
Cu.....	1,500	1,000	1,500	20	2,000	100	42	72
Ni.....	5,000	2,000	>5,000	100	>5,000	5,000	2,000	130

Table 7. Comparison of ore and pathfinder element concentrations in three stream-sediment size fractions from the Bohemia Basin nickel-copper sulfide district

[In parts per million. N, not detected; L, value less than lower limit of determination]

Sample	Ag	Co	Cu	Ni
-200 MESH				
010	0.5	50	1,500	500
011	N	70	50	50
012	N	70	100	100
013	N	30	70	30
014	N	100	100	50
015	N	70	70	70
016	N	70	70	70
017	N	50	100	50
018	N	100	70	100
-60 TO +200 MESH				
010	L	100	1,000	1,000
011	N	70	50	70
012	N	70	100	100
013	N	20	50	20
014	N	50	70	50
015	N	30	50	100
016	N	70	50	50
017	N	50	70	50
018	N	50	30	70
-10 TO +60 MESH				
010	L	100	1,000	1,000
011	N	50	50	50
012	N	30	50	100
013	N	20	50	20
014	N	30	50	50
015	N	50	50	100
016	N	50	20	50
017	N	30	30	30
018	N	30	50	50

Heavy-mineral concentrates were equally unsatisfactory for defining any significant dispersion train. Concentrations of copper and nickel are higher in the sample collected nearest the mine but are at background levels just 0.8 km downstream. Silver was detected only in the magnetic fraction of sample 010, at a level below the quantifiable detection limit of 1.0 ppm.

Difficulty in exploring for nickel-copper deposits such as those at Bohemia Basin and Mirror Harbor was discussed by Ford and others (1989). They reported that a regional reconnaissance stream-sediment survey failed in both districts to identify either the ultramafic rocks hosting mineralized rocks or the deposits themselves because copper and nickel concentrations do not significantly exceed background in the unmineralized, surrounding mafic rocks. The mafic rocks of the Goon Dip Greenstone on Yakobi Island, for example, have background nickel and copper values of 100–150 ppm and 100–200 ppm, respectively (Johnson and Elliot, 1984). These values exceed the stream-sediment values determined in this study for all Bohemia Basin samples, except for sample 010 collected adjacent to a mine (fig. 5). Ford and others (1989) found that the element association Cr-Ni-Mg-Cu-Co-V-Sc-Ca-Mn-Fe generally coincides with mafic rock types but is not reliable in identifying magmatic nickel-copper deposits. The stream-sediment sample density for the reconnaissance surveys discussed by Ford and others (1989) is approximately one per two square kilometers. Our more detailed orientation survey, which includes one sample site in a drainage only meters below a mine, permits unambiguous conclusions to be drawn on the difficulties detecting this deposit type using stream-sediment samples.

Given that groups of existing mines (whose ore and tailings dumps expose large quantities of sulfide minerals to surface weathering) are not detectable more than approximately 0.8 km downstream, we conclude that conventional exploration geochemistry using stream-sediment samples or heavy-mineral concentrates will be ineffective in locating new, undeveloped deposits of this type. In nonmafic rocks that have relatively low Fe-Mg-Cr-Ni-Cu background, stream-sediment geochemistry should be useful in delineating previously unrecognized mafic intrusive bodies. Detailed followup mapping, field examination, and geochemical sampling of these bodies might lead to further discoveries of ultramafic intrusive bodies of the type that host nickel-copper sulfide deposits.

CHROMITE DEPOSITS

Chromite lenses hosted by small, sheared, lenticular serpentinite bodies occur on central Baranof Island in a belt trending southeast from Silver Bay (fig. 6). These serpentinite bodies were emplaced in Mesozoic and Tertiary metasedimentary rocks (Loney and others, 1975). Thirteen stream-sediment samples were collected from within and near this belt of mineralized serpentinites, within approximately 10 km of the southern boundary of the Sitka quadrangle (fig. 6). No mineralized rock samples were collected.

Two samples (001 and 002) were collected from first-order streams within drainage basins that do not contain known chromite occurrences (fig. 6). These two samples are assumed to contain background concentrations of possible pathfinder elements for chromite occurrences. Drainage basins for the remaining 11 samples contain small chromite occurrences (Kennedy and Walton, 1946a).

In this study, chromium was found to be the best pathfinder element in exploration for chromite occurrences. In the stream-sediment samples, chromium is anomalously high relative to background samples (001 and 002) in all three stream-sediment size fractions for each of the other 11 samples (table 8). The highest chromium concentration is in sample 003, the sample closest to a chromite occurrence. The intensity of the chromium anomaly is strongest in the medium size fraction (-60 mesh) and weakest in the fine (-200 mesh) fraction (table 8).

The heavy-mineral concentrates show a similar chromium enrichment pattern in that the weakly magnetic fraction provides the clearest distinction between the anomalous and background samples. Chromium values are 150–300 ppm in the background samples and 1,500–10,000 ppm in the remaining samples (table 8). Relatively high iron

Table 8. Comparison of chromium concentrations in fine, medium, and coarse stream-sediment samples, and in magnetic, weakly magnetic, and nonmagnetic fractions of heavy-mineral concentrates from the chromite district of central Baranof Island
[In parts per million]

STREAM-SEDIMENT SAMPLES			
Sample	-200 mesh	-60 to +200 mesh	-10 to +60 mesh
001	70	100	70
002	100	100	70
003	700	2,000	1,000
004	700	1,500	200
005	700	500	200
006	200	700	150
007	200	1,000	300
019	100	700	150
020	100	200	100
021	200	500	200
022	100	150	100
023	150	200	200
024	150	300	300

HEAVY-MINERAL CONCENTRATES			
Sample	Magnetic	Weakly magnetic	Nonmagnetic
001	100	150	70
002	150	300	150
003	5,000	10,000	2,000
004	2,000	10,000	500
005	3,000	10,000	2,000
006	2,000	10,000	100
007	5,000	7,000	150
019	5,000	5,000	1,000
020	3,000	1,500	200
021	2,000	2,000	500
022	5,000	2,000	3,000
023	3,000	7,000	1,500
024	5,000	2,000	2,000

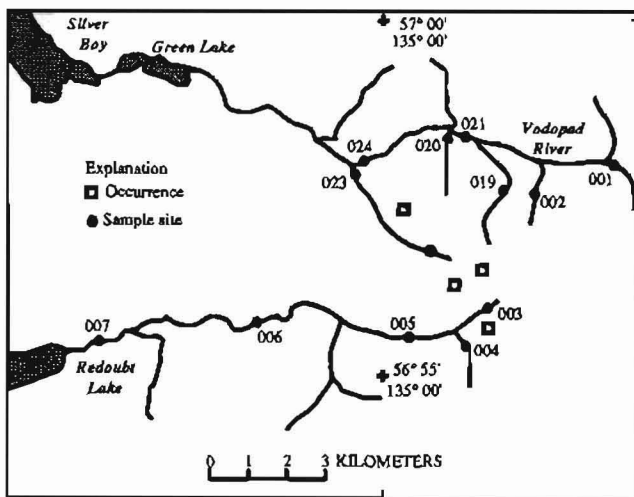


Figure 6. Sample localities in vicinity of chromite occurrences, central Baranof Island. Sample sites are within approximately 10 km of the southern boundary of the Sitka quadrangle.

content in the chromite (Guild and Balsley, 1942) is responsible for the magnetic properties of the chromite and the concentration of chromite in the weakly magnetic fraction. Concentrate samples do not show a consistent dispersion pattern downstream.

The anomaly to background ratio is smaller for stream-sediment samples than for heavy-mineral concentrates. The concentrates thus provide a slightly more distinct dispersion halo than do the stream sediments (table 8). Of the two sample media, the concentrates should be more useful in identifying chromium mineralization. In the weakly magnetic and magnetic concentrates, chromium enrichment of as much as 50 times background persists as far as 11 km downstream from known chromite occurrences, whereas chromium values in stream-sediment samples were only 3–10 times background. Concentrations of chromium in both stream-sediments and heavy-mineral concentrates are high enough for easy detection by emission spectrography, even in the background samples. Therefore, more sensitive analytical techniques are not required in the exploration for this mineral deposit type.

Anomalous concentrations of nickel, arsenic, antimony, silver, and gold in the stream-sediment samples and heavy-mineral concentrates collected in this region are not believed to be related to chromite occurrences. Silver, arsenic, gold, and antimony likely reflect gold-quartz vein deposits similar to those at the Lucky Chance deposit, 5–8 km to the east. The mineral phase contributing as much as 2,000 ppm Ni in magnetic heavy-mineral concentrates is unknown, but serpentine, pyroxene, magnetite, and other minerals derived from the serpentinized peridotite bodies and identified in the heavy-mineral concentrates likely contribute to a high nickel background (see table 6). Nickel-bearing minerals have not been described in association with the chromite occurrences (Kennedy and Walton, 1946a).

DISCUSSION AND SUMMARY

The origins and host rock types of ore deposits in the Sitka quadrangle are diverse. An efficient stream-sediment geochemical exploration program aimed at identifying all deposit types described herein must make compromises. Of the gold-quartz vein, massive sulfide, chromite, and magmatic nickel-copper deposits examined in this study, all except nickel-copper deposits show clearly recognizable geochemical signatures dispersed over distances of several kilometers downstream in stream-sediment samples and heavy-mineral concentrates. The difficulty in identifying nickel-copper sulfide deposits, noted by Ford and others (1989) based on a large-scale reconnaissance survey, has not been resolved by our more detailed survey. The nickel-copper occurrences were not detected more than about 0.8 km downstream using any of the sample media. Apparently, the rapid breakdown of nickel and copper sulfide minerals produces a small anomaly close to the deposit that drops to background levels less than a kilometer downstream.

The -200 mesh fraction of the stream-sediment samples generally yields the highest concentrations and the highest anomaly to background ratios for ore and pathfinder elements. For chromite deposits, however, analyses of the fine fraction did not identify several sites where anomalous chromium was detected in the medium size fraction (-60 to +200 mesh); the medium size fraction was significantly more sensitive than either the coarse or the fine stream-sediment fraction. Emission spectrography adequately identified ore and pathfinder elements for the chromite and massive sulfide deposits; however, the gold-quartz lodes require more sensitive techniques to detect ore and pathfinder elements. Atomic absorption analysis was necessary for gold analyses and ICP-10 was required for adequate sensitivity to detect the pathfinder elements arsenic, cadmium, and antimony.

Emission spectrographic analyses of the heavy-mineral concentrates adequately detected dispersion halos downstream of mineralized rocks. The nonmagnetic

fraction of heavy-mineral concentrates best revealed ore and pathfinder anomalies for massive sulfide deposits, although analyses from the magnetic and weakly magnetic fractions also revealed anomalies for many of the same elements. Analyses from stream sediments provided a broader dispersion halo and should therefore be more useful in exploration for massive sulfide deposits. For the chromite deposits, the weakly magnetic fraction provided the strongest anomalies, but the stream-sediment samples alone would have sufficiently identified the mineralized region. For the gold-quartz vein deposits, -200 mesh stream-sediment samples were useful in delineating a dispersion halo, but heavy-mineral concentrates generally were not as consistently anomalous in ore or pathfinder elements.

In summary, the stream-sediment samples were adequate to identify dispersion from three major deposit types in the Sitka quadrangle: volcanogenic massive sulfide, chromite, and gold-quartz vein deposits. Although not required to identify these types of deposit, heavy-mineral concentrates may provide higher anomaly to background contrasts than stream sediments (as for the chromite deposits). Of the analytical techniques tested, emission spectrography was adequate for recognition of the massive sulfide and chromite deposits, but atomic absorption and ICP-10 techniques were necessary to identify gold-quartz vein deposits. Atomic absorption, the most sensitive of the techniques available, was required to detect gold in stream sediments below gold-quartz vein deposits, and ICP-10 techniques were required to detect the pathfinder elements arsenic, antimony, and cadmium.

REFERENCES CITED

- Berg, H.C., Jones, D.L., and Coney, P.J., 1978, Map showing pre-Cenozoic tectonostratigraphic terranes of southeastern Alaska and adjacent areas: U.S. Geological Survey Open-File Report 78-1085, scale 1:1,000,000, 2 sheets.
- Bundtzen, T.K., Eakins, G.R., Clough, J.G., Lueck, L.L., Green, C.B., Robinson, M.S., and Coleman, D.A., 1984, Alaska's mineral industry 1983: Alaska Division of Geological and Geophysical Surveys Special Report 33, 56 p.
- Crafford, T.C., 1989, The Greens Creek Ag-Au-Pb-Zn massive sulfide deposit, Admiralty Island, southeast Alaska: Alaska Miners Association, Symposium on Metallogeny and Mineral Development in Southeast Alaska, the Yukon, and British Columbia, Abstracts of Professional Papers, p. 27-29.
- Crock, J.G., Lichte, F.E., and Briggs, P.H., 1983, Determination of elements in National Bureau of Standards geological reference materials SRM 278 obsidian and SRM 688 basalt by inductively coupled argon plasma-atomic emission spectroscopy: *Geostandards Newsletter*, v. 7, no. 2, p. 335-340.
- Eberlein, G.D., Churkin, M., Carter, C., Berg, H.C., and Ovenshine, A.T., 1983, Geology of the Craig Quadrangle, Alaska: U.S. Geological Survey Open-File Report 83-91, 28 p.

Anomalous concentrations of nickel, arsenic, antimony, silver, and gold in the stream-sediment samples and heavy-mineral concentrates collected in this region are not believed to be related to chromite occurrences. Silver, arsenic, gold, and antimony likely reflect gold-quartz vein deposits similar to those at the Lucky Chance deposit, 5–8 km to the east. The mineral phase contributing as much as 2,000 ppm Ni in magnetic heavy-mineral concentrates is unknown, but serpentine, pyroxene, magnetite, and other minerals derived from the serpentinized peridotite bodies and identified in the heavy-mineral concentrates likely contribute to a high nickel background (see table 6). Nickel-bearing minerals have not been described in association with the chromite occurrences (Kennedy and Walton, 1946a).

DISCUSSION AND SUMMARY

The origins and host rock types of ore deposits in the Sitka quadrangle are diverse. An efficient stream-sediment geochemical exploration program aimed at identifying all deposit types described herein must make compromises. Of the gold-quartz vein, massive sulfide, chromite, and magmatic nickel-copper deposits examined in this study, all except nickel-copper deposits show clearly recognizable geochemical signatures dispersed over distances of several kilometers downstream in stream-sediment samples and heavy-mineral concentrates. The difficulty in identifying nickel-copper sulfide deposits, noted by Ford and others (1989) based on a large-scale reconnaissance survey, has not been resolved by our more detailed survey. The nickel-copper occurrences were not detected more than about 0.8 km downstream using any of the sample media. Apparently, the rapid breakdown of nickel and copper sulfide minerals produces a small anomaly close to the deposit that drops to background levels less than a kilometer downstream.

The -200 mesh fraction of the stream-sediment samples generally yields the highest concentrations and the highest anomaly to background ratios for ore and pathfinder elements. For chromite deposits, however, analyses of the fine fraction did not identify several sites where anomalous chromium was detected in the medium size fraction (-60 to +200 mesh); the medium size fraction was significantly more sensitive than either the coarse or the fine stream-sediment fraction. Emission spectrography adequately identified ore and pathfinder elements for the chromite and massive sulfide deposits; however, the gold-quartz lodes require more sensitive techniques to detect ore and pathfinder elements. Atomic absorption analysis was necessary for gold analyses and ICP-10 was required for adequate sensitivity to detect the pathfinder elements arsenic, cadmium, and antimony.

Emission spectrographic analyses of the heavy-mineral concentrates adequately detected dispersion halos downstream of mineralized rocks. The nonmagnetic

fraction of heavy-mineral concentrates best revealed ore and pathfinder anomalies for massive sulfide deposits, although analyses from the magnetic and weakly magnetic fractions also revealed anomalies for many of the same elements. Analyses from stream sediments provided a broader dispersion halo and should therefore be more useful in exploration for massive sulfide deposits. For the chromite deposits, the weakly magnetic fraction provided the strongest anomalies, but the stream-sediment samples alone would have sufficiently identified the mineralized region. For the gold-quartz vein deposits, -200 mesh stream-sediment samples were useful in delineating a dispersion halo, but heavy-mineral concentrates generally were not as consistently anomalous in ore or pathfinder elements.

In summary, the stream-sediment samples were adequate to identify dispersion from three major deposit types in the Sitka quadrangle: volcanogenic massive sulfide, chromite, and gold-quartz vein deposits. Although not required to identify these types of deposit, heavy-mineral concentrates may provide higher anomaly to background contrasts than stream sediments (as for the chromite deposits). Of the analytical techniques tested, emission spectrography was adequate for recognition of the massive sulfide and chromite deposits, but atomic absorption and ICP-10 techniques were necessary to identify gold-quartz vein deposits. Atomic absorption, the most sensitive of the techniques available, was required to detect gold in stream sediments below gold-quartz vein deposits, and ICP-10 techniques were required to detect the pathfinder elements arsenic, antimony, and cadmium.

REFERENCES CITED

- Berg, H.C., Jones, D.L., and Coney, P.J., 1978, Map showing pre-Cenozoic tectonostratigraphic terranes of southeastern Alaska and adjacent areas: U.S. Geological Survey Open-File Report 78-1085, scale 1:1,000,000, 2 sheets.
- Bundtzen, T.K., Eakins, G.R., Clough, J.G., Lueck, L.L., Green, C.B., Robinson, M.S., and Coleman, D.A., 1984, Alaska's mineral industry 1983: Alaska Division of Geological and Geophysical Surveys Special Report 33, 56 p.
- Crafford, T.C., 1989, The Greens Creek Ag-Au-Pb-Zn massive sulfide deposit, Admiralty Island, southeast Alaska: Alaska Miners Association, Symposium on Metallogeny and Mineral Development in Southeast Alaska, the Yukon, and British Columbia, Abstracts of Professional Papers, p. 27-29.
- Crock, J.G., Lichte, F.E., and Briggs, P.H., 1983, Determination of elements in National Bureau of Standards geological reference materials SRM 278 obsidian and SRM 688 basalt by inductively coupled argon plasma-atomic emission spectroscopy: *Geostandards Newsletter*, v. 7, no. 2, p. 335-340.
- Eberlein, G.D., Churkin, M., Carter, C., Berg, H.C., and Ovenshine, A.T., 1983, Geology of the Craig Quadrangle, Alaska: U.S. Geological Survey Open-File Report 83-91, 28 p.

- Ford, A.B., and Brew, D.A., 1988, Major-element geochemistry of metabasalts of the Juneau-Haines region, southeastern Alaska, in Galloway, J.P., and Hamilton, T.D., eds., *Geologic studies in Alaska during 1987*: U.S. Geological Survey Circular 1016, p. 150-155.
- Ford, A.B., Karl, S.M., Dittweiler, K.A., Sutphin, D.M., Finn, C.A., and Brew, D.A., 1989, Sitka Quadrangle, Alaska—An AMRAP preassessment planning document: U.S. Geological Survey Administrative Report, 92 p.
- Gehrels, G.E., and Saleeby, J.B., 1987a, Geology of southern Prince of Wales Island, southeastern Alaska: *Geological Society of America Bulletin*, v. 98, p. 123-137.
- 1987b, Geologic framework, tectonic evolution, and displacement history of the Alexander terrane: *Tectonics*, v. 6, no. 2, p. 151-173.
- Goldfarb, R.J., Nelson, S.W., Berg, H.C., and Light, T.V., 1987, Distribution of mineral deposits in the Pacific Border Ranges and Coast Mountains of the Alaskan Cordillera, in Elliot, I.L., and Snee, B.W., eds., *Geoexpo/86—Exploration of the North American Cordillera*: Association of Exploration Geochemists, p. 19-41.
- Grimes, D.J., and Marranzino, A.P., 1968, Direct-current arc and alternating-current spark emission spectrographic field methods for the semiquantitative analysis of geologic materials: U.S. Geological Survey Circular 591, 6 p.
- Guild, P.W., and Balsley, J.R., 1942, Chromite deposits of Red Bluff Bay and vicinity, Baranof Island, Alaska: U.S. Geological Survey Bulletin 936-G, p. G171-G187.
- Johnson, B.R., and Elliot, G.S., 1984, Map showing the distribution and abundance of copper in bedrock samples, Western Chichagof-Yakobi Islands Wilderness Study Area, southeastern Alaska: U.S. Geological Survey Open-File Report 81-27-D, scale 1:125,000.
- Kennedy, G.C., and Walton, M.S., 1946a, Geology and associated mineral deposits of some ultrabasic rock bodies in southeastern Alaska: U.S. Geological Survey Bulletin 947-D, p. 65-84.
- 1946b, Nickel investigations in southeast Alaska: U.S. Geological Survey Bulletin 947-C, p. 39-64.
- Knopf, A., 1912, The Sitka mining district, Alaska: U.S. Geological Survey Bulletin 904, 32 p.
- Lichte, F.E., Golightly, D.W., and Lamothe, P.J., 1987, Inductively coupled plasma-atomic emission spectrometry, in Baedeker, P.A., ed., *Methods for geochemical analysis*: U.S. Geological Survey Bulletin 1770, p. B1-B10.
- Loney, R.A., 1964, Stratigraphy and petrography of the Pybus-Gambier area, Admiralty Island, Alaska: U.S. Geological Survey Bulletin 1178, 103 p.
- Loney, R.A., Brew, D.A., Muffler, L.J.P., and Pomeroy, J.S., 1975, Reconnaissance geology of Chichagof, Baranof, and Kruzof Islands, southeastern Alaska: U.S. Geological Survey Professional Paper 792, 105 p.
- MacKevett, E.M., 1978, Geologic map of the McCarthy quadrangle, Alaska: U.S. Geological Survey Miscellaneous Investigations Series Map I-1032, scale 1:250,000.
- Motooka, J.R., 1988, An exploration geochemical technique for the determination of preconcentrated organometallic halides by ICP-AES: *Applied Spectroscopy*, v. 42, no. 7, p. 1293-1296.
- Motooka, J.R., and Grimes, D.J., 1976, Analytical precision of one-sixth order semiquantitative spectrographic analyses: U.S. Geological Survey Circular 738, 25 p.
- Nokleberg, W.J., Jones, D.L., and Silberling, N.J., 1985, Origin and tectonic evolution of the Maclaren and Wrangellia terranes, eastern Alaska Range, Alaska: *Geological Society of America Bulletin*, v. 96, p. 1251-1270.
- Plafker, G., Jones, D.L., and Pessagno, E.A., 1977, A Cretaceous accretionary flysch and melange terrane along the Gulf of Alaska margin, in Blean, K.M., ed., *The U.S. Geological Survey in Alaska—Accomplishments during 1976*: U.S. Geological Survey Circular 751-B, p. B41-B43.
- Reed, J.C., and Coats, R.R., 1941, Geology and ore deposits of the Chichagof mining district, Alaska: U.S. Geological Survey Bulletin 929, 148 p.
- Reed, J.C., and Dorr, J.V.N., 1942, Nickel deposits of Bohemia Basin and vicinity, Yakobi Island, Alaska: U.S. Geological Survey Bulletin 931-F, p. 105-138.
- Rose, A.W., Hawkes, H.E., and Webb, J.S., 1979, *Geochemistry in mineral exploration*: New York, Academic Press, 657 p.
- Rossmann, D.L., 1959, Geology and ore deposits of northwestern Chichagof Island, Alaska: U.S. Geological Survey Bulletin 1058-E, p. E139-E216.
- Still, J.C., 1988, Distribution of gold, platinum, palladium, and silver in selected portions of the Bohemia Basin deposits, southeast Alaska (with an appendix on Mirror Harbor): U.S. Bureau of Mines Open-File Report 10-88, 10 sheets, 42 p.
- Tripp, R.B., Goldfarb, R.J., and Pickthorn, W.J., 1985, Geochemical map showing distribution of gold within Chugach National Forest, Alaska: U.S. Geological Survey Miscellaneous Field Studies Map MF-1645-D, scale 1:250,000.
- Thompson, C.E., Nakagawa, H.M., and Van Sickle, G.H., 1968, Rapid analysis for gold in geologic materials, in *Geological Survey Research 1968*: U.S. Geological Survey Professional Paper 600-B, p. B130-B132.
- Van Nieuwenhuysse, R.E., 1984, Geology and geochemistry of the Pyrola massive sulfide deposit, Admiralty Island, Alaska: Tucson, University of Arizona, M.S. thesis, 170 p.

Chapter C

Geology and Geochemistry of Mineralization in the Bethel Quadrangle, Southwestern Alaska

By THOMAS P. FROST

U.S. GEOLOGICAL SURVEY BULLETIN 1950

GEOCHEMICAL STUDIES IN ALASKA BY THE U.S. GEOLOGICAL SURVEY, 1989

CONTENTS

Abstract	C1
Introduction	C1
Mineral deposits and occurrences	C3
Gold veins in the Nyac terrane	C3
Silica-carbonate and serpentinite zones	C4
Tourmaline-quartz replacement zones	C4
Mercury-antimony deposits	C5
Gold Lake "red spots"	C5
Other gold occurrences	C8
Summary	C9
References cited	C9

FIGURE

1. Map showing regional geology and mineral occurrences in the Bethel quadrangle and parts of the Russian Mission and Goodnews quadrangles, southwestern Alaska C2

TABLE

1. Analytical results for selected samples from the Bethel quadrangle and surrounding areas C6

Geology and Geochemistry of Mineralization in the Bethel Quadrangle, Southwestern Alaska

By Thomas P. Frost

Abstract

Geologic and geochemical data indicate the presence of several types of lode deposits in the Bethel 1°x2° quadrangle in southwestern Alaska. Hydrothermally mineralized rocks include gold-bearing quartz veins apparently associated with Early Cretaceous plutonism west of the Golden Gate fault; mercury- and antimony-rich veins that may have anomalous gold and silver and are present for the most part in areas underlain by sedimentary rocks of the Kuskokwim Group or in rhyolite domes; and quartz veins that have anomalous Ag, As, Au, and Pb in clastic rocks and chert in the older terranes of the southeastern part of the quadrangle. Quartz veins containing gold are also associated with several 60- to 70-million-year-old granitoid plutons that cut Cretaceous sedimentary rocks of the Kuskokwim Group. Localized boron metasomatism in Upper Cretaceous volcanic and volcanoclastic rocks in the northeastern part of the quadrangle has resulted in quartz-tourmaline replacement zones that are anomalous in Ag, Au, Hg, Pb, Sn, and Zn.

INTRODUCTION

The Bethel 1°x2° quadrangle in southwestern Alaska contains numerous gold placer deposits and occurrences and lode occurrences that contain anomalous Au, Ag, Hg, and Sb. Several anomalies identified from stream-sediment and panned-concentrate samples suggest additional areas favorable for these mineral deposit types. This report describes the geology and geochemistry of these new areas and offers interpretations for the source of the metal anomalies.

The western third of the Bethel quadrangle is covered by thick, unconsolidated Quaternary deposits of the Yukon-Kuskokwim delta. The remainder of the quadrangle is underlain by at least five distinct accreted tectono-stratigraphic terranes (Box and Murphy, 1987; Jones and others, 1987) that are made up of rocks of Precambrian through Early Cretaceous age (fig. 1). Deposited unconformably on most of the older terranes is a thick sequence of highly deformed, predominantly turbiditic sedimentary rocks of the Lower and Upper Cretaceous Kuskokwim Group (Hoare and Coonrad, 1959a, b). Cretaceous and Tertiary high-level granitoid plutons, basaltic through

dacitic volcanic fields, and hypabyssal rhyolite intrusions and extrusive (?) domes were intruded through and (or) deposited on all older rock units.

Rocks of the Tikchik terrane crop out in the southeastern corner of the quadrangle (fig. 1) and consist of a structurally complex assemblage of Paleozoic and Mesozoic chert and Permian limestone, basalt, and clastic rocks (Mertie, 1938; Hoare and Coonrad, 1959a, 1978; Hoare and Jones, 1981). The original nature of the boundary between the Tikchik terrane and the Togiak terrane to the west is uncertain but is presently marked in part by the active right-lateral Togiak fault (Box and Murphy, 1987).

The Togiak terrane is composed of complexly deformed andesitic volcanic and volcanoclastic rocks that have yielded Late Triassic through Early Cretaceous fossils from the Goodnews quadrangle to the south (Hoare and Coonrad, 1978). The boundary between the rocks of the Togiak terrane and the Goodnews terrane to the west is covered by the Lower and Upper Cretaceous sedimentary rocks of the Kuskokwim Group in the Bethel quadrangle (Box and Murphy, 1987). It is uncertain whether the Kuskokwim Group depositionally overlies or is faulted against the rocks of the Togiak terrane.

Rocks of the Goodnews terrane are exposed in erosional windows through the overlying Kuskokwim Group. The Goodnews terrane consists of a structurally complex assemblage of variably foliated metabasalt, low-grade schist, marble, chert, graywacke, and slate (Hoare and Coonrad, 1959a, 1978; Box and Murphy, 1987). Box and Murphy (1987) reported a K-Ar metamorphic age of 146 Ma from an actinolite-bearing schist. Fossils are Permian to Early Cretaceous in age (Murphy, 1987). The structural relationship between the rocks of the Goodnews terrane and Precambrian rocks to the west is uncertain, although both groups of rocks are overlain by basal conglomerate of the Kuskokwim Group that contains clasts derived in part from both terranes (Box and Murphy, 1987).

Precambrian orthogneiss, amphibolite, and quartz-mica schist of the Kilbuck terrane crop out in a narrow tectonic sliver in the southern part of the Bethel quadrangle

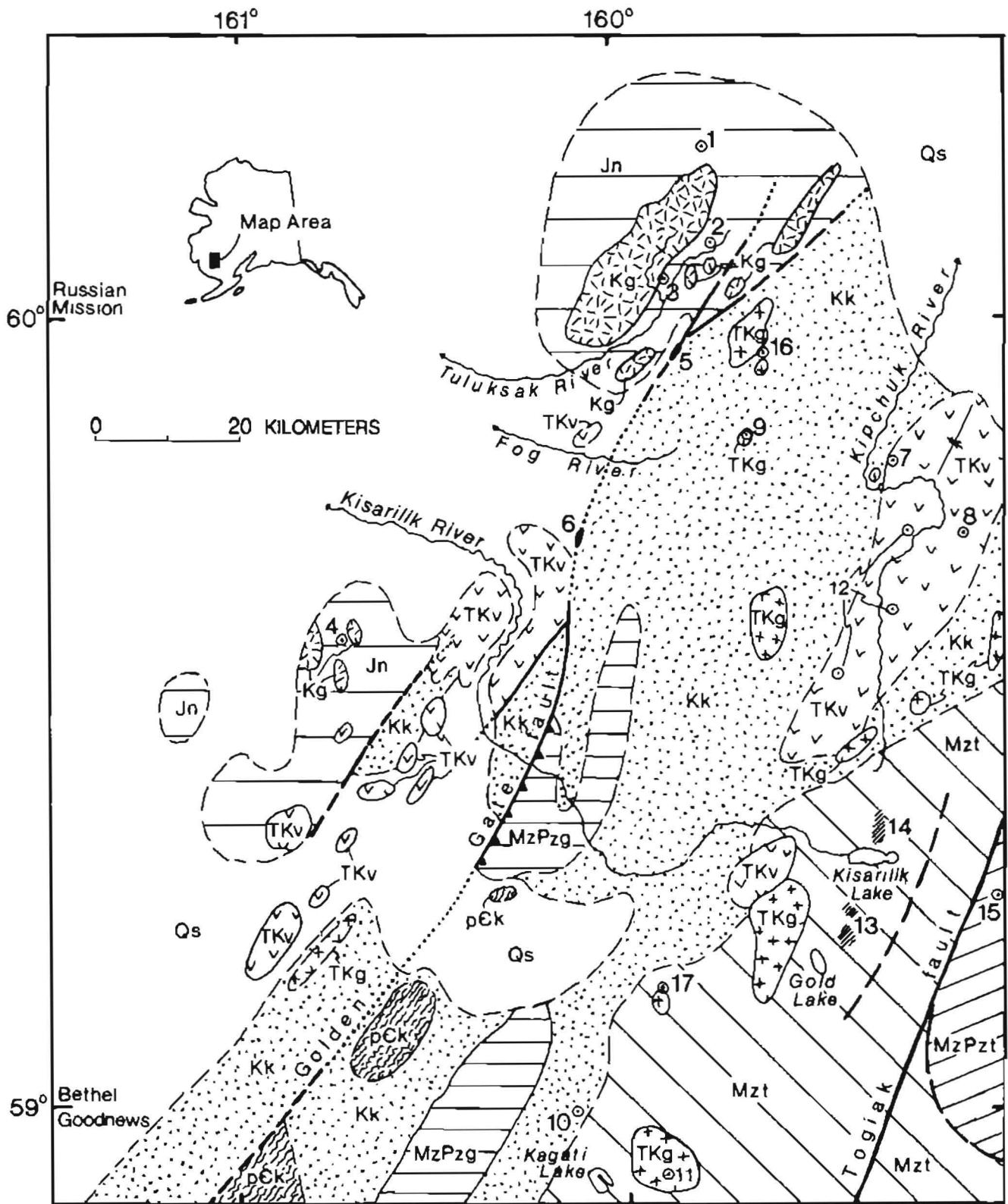
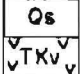



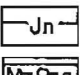
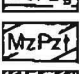

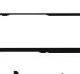
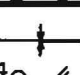





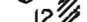


Figure 1 (above and facing page). Regional geology and mineral occurrences in the Bethel quadrangle and parts of the Russian Mission and Goodnews quadrangles, southwestern Alaska. Geology adapted from Hoare and Coonrad (1959a, b, 1978) and Box and Murphy (1987).

EXPLANATION

Overlap sequences

	Surficial deposits (Quaternary)
	Volcanic rocks (early Tertiary and Late Cretaceous)—Basalt to rhyolite flows and domes, includes some hypabyssal rocks.
	Granitic to granodioritic plutonic rocks (early Tertiary to Late Cretaceous)
	Granitic to granodioritic plutonic rocks (Early Cretaceous)
	Kuskokwim Group (Late and Early Cretaceous)
Pre-mid-Cretaceous terranes	
	Togiak terrane (Early Cretaceous to Late Triassic)—Andesitic volcanic rocks, volcanoclastic rocks, and tuffaceous argillite
	Nyac terrane (Middle Jurassic)—Andesitic volcanic rocks and minor volcanoclastic sedimentary rocks
	Goodnews terrane (Mesozoic and Paleozoic)—Tuffaceous argillite, chert, basalt, metabasite, metachert, and marble
	Tikchik terrane (Mesozoic and Paleozoic)—Metavolcanic rocks, metachert, graywacke, and limestone
	Kitluc terrane (Precambrian)—Amphibolite facies orthogneiss and minor amphibolite and quartz-mica schist
	Contact—Dashed where inferred
	Fault—Dashed where approximate, dotted where inferred
	Thrust fault—Teeth on upper plate
	Syncline axis
	Locality or area described in text: number refers to text and table 1

and in the Goodnews quadrangle west of the Goodnews terrane (Turner and others, 1983; S.E. Box, U.S. Geological Survey, written commun., 1989).

Middle Jurassic andesitic volcanic rocks and volcanoclastic sandstones of the Nyac terrane are the westernmost basement rocks exposed in the Bethel quadrangle (Box and Murphy, 1987). The contact between the Nyac terrane and rocks to the east is not exposed but probably is marked in part by the Golden Gate fault or its equivalent in the northern part of the Bethel quadrangle (Hoare and Coonrad, 1959a).

The Kuskokwim Group is represented by a thick sequence of shale, siltstone, sandstone, and minor basal conglomerate that was deposited unconformably on all older rocks except those of the Nyac terrane (Box and Murphy, 1987). The Kuskokwim Group is composed predominantly of marine turbidite, with the exception of shallow marine and nonmarine sedimentary rocks in the southwestern part of the quadrangle (Box and Murphy, 1987). Albian to Coniacian fossils have been recovered from the Kuskokwim Group in different parts of the quadrangle (Hoare and Coonrad, 1959a, 1978; Box and Murphy, 1987; Murphy, 1987), but regional age control is

poor. The Kuskokwim sedimentary rocks host a wide variety of granitoid intrusions, volcanic fields, and intermediate to silicic dikes, which are common in many parts of the quadrangle.

Early Cretaceous (125–120 Ma) granitoid plutons are restricted to the Nyac terrane west of the Golden Gate fault; granitoid plutons and volcanic fields in other terranes and the Kuskokwim Group are Late Cretaceous to early Tertiary (72–65 Ma) in age (Shew and Wilson, 1981; Robinson and Decker, 1986; Frost and others, 1988). Most plutons are elliptical in outline and surrounded by a biotite-bearing hornfels zone as wide as a kilometer. The plutons are porphyritic or coarse grained; many have small miarolytic cavities. The most common plutonic rock types are hornblende-biotite granodiorite through granite, although augite-biotite diorite and gabbro are present in some plutons (Robinson and Decker, 1986; Frost and others, 1988).

Late Cretaceous to early Tertiary volcanic rocks crop out in the northeastern corner of the quadrangle on both sides of the Kipchuk River and in an elongate northeast-trending belt in the lowlands west of the Golden Gate fault (fig. 1). These rocks consist mainly of bedded basaltic to dacitic flows and tuffs, and some volcanoclastic sedimentary rocks. Platy to massive felsic domes, at least some of which are intrusive along their upper contacts, are scattered through all the volcanic fields. The felsic domes are composed, for the most part, of biotite rhyolite containing partially resorbed quartz phenocrysts. Some rocks have a glassy groundmass, but in most rocks the glass has devitrified. Intermediate to felsic dikes cut all older rock types in many parts of the quadrangle.

Acknowledgments.—This manuscript profited from reviews by Stephen E. Box, Richard J. Goldfarb, and John Galloway. Analytical work was provided by Richard M. O'Leary, David E. Detra, Leon A. Bradley, Betty Bailey, Floyd Brown, Zoe A. Brown, D. Fey, P. Hageman, J. Motooka, K. Romine, and E.P. Welsch.

MINERAL DEPOSITS AND OCCURRENCES

Placer gold has been the major mineral commodity produced in southwestern Alaska, and mercury has been produced predominantly from small scattered lode deposits (Sainsbury and MacKevett, 1965; Hoare and Cobb, 1977). Field work and petrographic interpretation, supported by geochemical data, have identified several previously unknown, or at least undocumented, mineral occurrences and additional drainage basins favorable for the discovery of new occurrences. This report also provides new, detailed information on known mineral occurrences.

Gold Veins in the Nyac Terrane

Placer gold has been produced from the headwaters of the Tuluksak River since the 1910's (Hoare and Coonrad,

1959a). No data on lode gold in the Bethel quadrangle has been published to date. Anomalous gold concentrations have been identified by atomic absorption spectroscopy of samples of pyrite- and iron-oxide-bearing quartz and calcite veins from several old prospect pits in the Russian Mission and the Bethel quadrangles (fig. 1, locs. 1-4, table 1). Most of the gold-bearing veins cut hornfelsed and sericitized pyroxene andesite or volcanoclastic rocks of the Nyac terrane, although one gold-bearing vein (fig. 1, loc. 4) cuts sericitized quartz porphyry that may be part of the Early Cretaceous plutonic system. The veins are characterized by euhedral quartz prisms that have abundant open space between crystals; quartz, calcite, and chlorite are the most common gangue minerals. Several generations of quartz veins may be present at any locality, and they all may contain gold.

At one locality (fig. 1, loc. 3) the oldest veins occupy en echelon fractures and contain as much as 20 ppm Au. Later quartz veins are coarsely brecciated and contain as much as 4.5 ppm Au. Gold-bearing quartz vein samples from the Nyac terrane contain 0.6-2.3 ppm Hg; one sample contains 500 ppm As and 10 ppm Ag (table 1). Stream-sediment samples from several drainages in the Nyac terrane that contain as much as 180 ppm As (T.P. Frost, unpub. data) suggest additional undiscovered lode occurrences in the Nyac terrane. The known lode gold occurrences are located near Early Cretaceous granitoid plutons that cut the Jurassic volcanic and volcanoclastic rocks of the Nyac terrane. The spatial association between veins and plutons suggests that the plutons provided at least a heat source to circulate hydrothermal fluids that deposited the gold. The field relations, petrography, and geochemistry indicate that the gold-bearing quartz veins in the Nyac terrane are epithermal or mesothermal.

Silica-Carbonate and Serpentinite Zones

Small areas of bright-red-orange-weathering and unvegetated silica-carbonate rock are scattered through the tundra along the topographic break at the foot of the Kuskokwim Mountains in the Bethel and the Goodnews quadrangles (fig. 1, table 1, locs. 5, 6). North of the Kisarilik River, these areas are along what is probably the trace of the Golden Gate fault or its equivalent (Hoare and Coonrad, 1959a, b, 1978). Silica-carbonate rock, sheared and unshaped serpentinite, and lesser gabbro, dunite, and pyroxenite blocks are in the rubble outcrops. Silica-carbonate rock is the most common rock type and consists of quartz and several crosscutting generations of carbonate veins, in many cases containing relicts of serpentinite. Chromium and nickel contents as high as 0.5 percent and 1,500 ppm, respectively, reflect the original mafic to ultramafic compositions of the protoliths. Several silica-carbonate samples contain as much as 1,500 ppm Zn and 1,500 ppm As. Silica-carbonate rock at Slate Creek (fig. 1,

table 1, loc. 5) is anomalous in mercury, one sample contains more than 36 ppm Hg. Football-sized dunite and gabbro blocks in sheared serpentinite from south of the Fog River (fig. 1, table 1, loc. 6) have gold contents of 0.05 and 0.10 ppm. Geology, geochemistry, and tectonic setting suggest that the ultramafic and mafic rocks and their altered equivalents along the Golden Gate fault may be similar in origin to the rocks of the ultramafic complex 70 km south of the southern edge of the Bethel quadrangle at Goodnews Bay (Mertie, 1976; Southworth, 1986). The ultramafic complex at Goodnews Bay is an important source for platinum group elements (PGE), and therefore the ultramafic rocks along the Golden Gate fault may have PGE resource potential. The silica-carbonate alteration is similar to hydrothermal alteration common to many epithermal lodes in southwestern Alaska (Sainsbury and MacKevett, 1965).

Tourmaline-Quartz Replacement Zones

Tourmaline-quartz replacement of volcanic rocks and waterlain tuffs occurred at two localities near the base of the Kipchuk volcanic field flanking the Kipchuk River in the northeastern corner of the Bethel quadrangle (fig. 1, locs. 7, 8). The altered rocks are brownish red to black; weathered surfaces commonly are bright red. Vegetation in the altered areas is restricted for the most part to sparse lichens and mosses.

At the northern tourmaline-quartz replacement zone (fig. 1, loc. 7), a small pluton of biotite-orthopyroxene quartz diorite cuts Kuskokwim sedimentary rocks stratigraphically below the altered volcanoclastic rocks. The pluton is itself mostly unaltered; samples from the pluton and surrounding metasedimentary hornfels lack anomalous geochemical values. The northern tourmaline-quartz replacement zone is restricted to a waterlain tuff unit at the local base of the overlying volcanic field.

At the southern tourmaline-quartz replacement zone, no plutons or dikes have been identified (fig. 1, loc. 8). The southern tourmaline-quartz replacement zone is at least 100 m above the base of the volcanic section. Tourmaline-quartz replacement of plagioclase porphyry is gradational over several hundred meters along the eastern contact, although the southern contact is no greater than 20 m wide. In incipiently altered rocks, tourmaline replaces phenocrysts in the rock, whereas quartz replaces groundmass. With increasing alteration, the original texture is completely obscured and the rock consists of a granular aggregate of fine-grained quartz and clumps of prismatic tourmaline. Some rocks are distinctly layered or "orbicular" and are made up of alternating layers rich in quartz and tourmaline. Many orbs have a coarse-grained vuggy core of prismatic tourmaline, quartz, and iron oxide minerals. Very small cassiterite (?) crystals line some vugs.

In addition to boron, the tourmaline-quartz rocks are high in Ag, As, Ba, Pb, Sb, and Sn, and less consistently in

Bi, Cu, and Zn. One sample contains 0.10 ppm Au, and the mercury content in most samples is 0.10–3 ppm; one sample contains greater than 36 ppm Hg. Little or no correlation between anomalous elements from sample to sample suggests that mineralization occurred erratically in the altered zones. Gold, cinnabar, scheelite, tourmaline, barite, arsenopyrite, pyrite, and an unidentified brown mineral (probably cassiterite) are present in heavy-mineral concentrates downstream from the northern tourmalinized area and in streams draining the entire volcanic field north and east of the Kipchuk River (R. Tripp, U.S. Geological Survey, written commun., 1988). The quartz-tourmaline occurrences result from hydrothermal replacement. Available data suggests that these occurrences may have affinities to syngenetic, exhalative or skarn deposits.

Mercury-Antimony Deposits

Mercury and (or) antimony deposits and occurrences are widely scattered through southwestern Alaska (Sainsbury and MacKevett, 1965). Occurrences in the Bethel region include simple quartz-stibnite veins, quartz-cinnabar-stibnite veins, realgar-quartz veins, composite tourmaline-quartz-cinnabar-stibnite-realgar veins, and rhyolite domes and dikes having anomalous mercury contents. In the Bethel quadrangle, veins, fault zones, felsic intrusive bodies cut by veins, and altered rhyolite containing anomalous mercury for the most part are restricted to areas underlain by or adjacent to sedimentary rocks of the Kuskokwim Group.

At Fisher Dome (fig. 1, loc. 9) in the north-central part of the Bethel quadrangle, quartz-stibnite veins as wide as 10 cm cut a mildly peraluminous hypabyssal biotite quartz porphyry (Hoare and Coonrad, 1959a; Frost and others, 1988; T.P. Frost, unpub. data). Known stibnite-bearing veins are restricted to an area of less than 100 m². Stibnite is present as coarse blades as long as 5 cm and may comprise 50 percent of a given vein. Mercury content in the veins is less than 10 ppm, but as much as 1.0 ppm Au is present (table 1).

Mercury and antimony are present in two types of distinctly textured veins at Rainy Creek (Rutledge, 1948; Hoare and Coonrad, 1959a; Sainsbury and MacKevett, 1965) (fig. 1, loc. 10) at the southern boundary of the Bethel quadrangle. The first type consists of irregular mineralized breccias that cut and locally silicify Kuskokwim shale. The breccia matrix is composed of granular aggregates of realgar and lesser amounts of euhedral quartz, orpiment, cinnabar, and stibnite and clasts of country rock. Individual breccia zones are as wide as 1 m, but few can be traced more than a few meters. As much as 0.05 ppm Au is present in some samples of this type. The second type is near vertical, N. 20° E. striking, massive quartz veins that contain less than 5 percent cinnabar and stibnite. Some vein surfaces have two sets of slickensides, plunging 45° N. and 80° S.

The order of emplacement and relationship between the two textural types of veins is not clear.

East of Kagai Lake in the Goodnews quadrangle (fig. 1, loc. 11), composite quartz-calcite-cinnabar-stibnite-tourmaline veins cut a hornblende-biotite granite and granodiorite pluton (Sainsbury and MacKevett, 1965). The veins are vertical and strike N. 20° W. Individual veins are as wide as 15 cm; most are gently anastomosing or en echelon. The veins are zoned and have a margin of blue-green to brown tourmaline needles growing into a core of coarse quartz and calcite. Faceted cinnabar crystals and bladed stibnite as large as 2 mm and minor realgar and orpiment are scattered through the quartz at the cores of the veins. The textures of the veins suggest that tourmaline and quartz were the earliest minerals to crystallize and that additional quartz, calcite, stibnite, cinnabar, realgar, and orpiment were deposited later, probably in a different hydrothermal event. Gold content of individual vein samples is as high as 2.9 ppm (table 1). Hornblende and biotite in the host granite are partially replaced by chlorite and calcite, and plagioclase is partially altered to sericite within 5 cm of the veins.

Numerous silicic volcanic rocks emplaced through the sedimentary rocks of the Kuskokwim Group have anomalous mercury and (or) gold contents. Samples from prominent white to pinkish-white rhyolite and rhyodacite domes and dikes in the Kipchuk-Tulip area (fig. 1, loc. 12) have mercury contents as high as 14.4 ppm, gold contents as high as 0.30 ppm, and arsenic contents as high as 140 ppm (table 1). Quartz and (or) plagioclase rhyolite and rhyodacite porphyries have been extensively altered to assemblages of quartz, fine-grained white mica or clays, and hematite and limonite. Hematite-bearing quartz veins are also present in many of the rhyolites. The available data do not conclusively indicate whether mercury and (or) gold are disseminated in the altered rhyolite, in quartz veins, or in both. Stream-sediment samples from streams draining volcanic rocks of the Kipchuk-Tulip area have as much as 5.2 ppm Hg, 238 ppm As, and 17 ppm Sb (T.P. Frost, unpub. data). The widely scattered anomalies suggest that the Kipchuk-Tulip volcanic field has potential for epithermal mercury-gold mineralization.

Gold Lake "Red Spots"

Many prominent "red spots" scattered through the rugged higher elevations in the southeastern part of the Bethel quadrangle are areas of oxidized pyrite-bearing rhyolite dikes and sulfide-bearing quartz veins that cut argillite, sandstone, and volcanic and volcanoclastic rocks of the Tikchik and Togiak terranes (fig. 1). Most of the rhyolite dike-quartz vein zones are exposed over areas of less than a few tens of square meters, but some larger zones extend erratically over several square kilometers. The dike-vein

Table 1. Analytical results for selected samples from the Bethel quadrangle and surrounding areas

[Location shown by number in figure 1. Latitude and Longitude in degrees, minutes, and seconds, north and west, respectively. Abbreviations for sample types: ss, sandstone; qtz, quartz; carb, carbonate; tour, tourmaline; cin, cinnabar; alt'd, altered; orp, orpiment. Most analyses by semiquantitative spark-source emission spectrography, except Au (flame atomic absorption), Hg (cold-vapor atomic absorption), and As, Bi, Cd, Sb, and Zn (inductively coupled plasma emission spectroscopy; where results of the last two methods are not yet available, semiquantitative spectroscopy data is shown in parentheses. All values in parts per million. N, not detected at level shown; L, detected but not quantifiable; G, greater than value shown; H, no data due to interference from other elements: ND, no data]

Map location and sample no.	Sample type	Latitude	Longitude	Ag	As	Au	B	Ba	Bi	Cr
NYAC TERRANE QUARTZ VEINS										
1.	9TF042B...Qtz vein	61 13 27	159 47 47	10.0	(500)	12.00	15	300	(N10)	L10
2.	8TF034A...Qtz vein	61 06 01	159 46 32	N0.5	2.1	20.00	30	30	N1	L10
	8TF034C...Qtz vein	61 06 01	159 46 32	N0.5	N10	4.50	30	30	N1	10
	8TF034D...Qtz vein	61 06 01	159 46 32	N0.5	2.4	0.25	N10	N20	N1	20
3.	7SB20...Qtz vein	61 03 20	159 55 40	N0.5	N10	4.90	20	700	21	15
4.	7YB14A...Ss w/ qtz vein	60 37 15	160 41 54	N0.5	N10	0.40	20	150	N1	30
GOLDEN GATE FAULT ZONE										
5.	9TF073A...Silica-carb rk	60 57 00	159 55 15	N0.5	(200)	N0.05	N10	N20	(N10)	1,000
	9TF073E...Silica-carb rk	60 57 00	159 55 15	N0.5	(N200)	N0.05	N10	30	(N10)	700
	9TF073E...Breccia	60 57 00	159 55 15	N0.5	(1,500)	N0.05	10	50	(N10)	1,500
	9TF116B...Silica-carb rk	61 03 36	159 44 33	0.7	(1,500)	N0.05	20	150	(N10)	150
6.	7SB102H...Pyroxenite	60 47 08	160 07 47	N0.5	N10	N0.05	30	L20	N1	700
	7SB102I...Dunite	60 47 08	160 07 47	N0.5	N10	0.05	L10	70	N1	G5,000
	7SB102L...Gabbro	60 47 08	160 07 47	N0.5	N10	0.10	10	L20	N1	5,000
KIPCHUK AREA										
7.	89ML227...Altered tuff(?)	60 50 10	159 17 00	70.0	(1,500)	L0.05	500	300	(300)	700
	89TF32B...Qtz-tour rock	60 49 51	159 16 45	1.5	(200)	N0.05G2,000		150	(10)	150
	89TF32C...Qtz-tour rock	60 49 51	159 16 45	7.0	(200)	N0.05G2,000		300	(30)	100
8.	9TF67C...Qtz-tour rock	60 44 59	159 07 10	30.0	(1,000)	N0.05G2,000		500	(30)	70
	9TF67D...Qtz-tour rock	60 44 59	159 07 10	5.0	(1,500)	0.10G2,000		150	(N10)	200
	9TF67J...Qtz-tour rock	60 44 59	159 07 10	70.0	(2,000)	N0.05G2,000		100	(30)	200
FISHER DOME STIBNITE VEINS										
9.	8TF058...Stibnite-qtz	60 50 01	159 44 15	7.0	(1,500)	1.00	300	100	(N10)	N10
	FD-4...Stibnite-qtz	60 50 01	159 44 15	N0.5	(300)	0.20	30	30	(N10)	L10
RAINY CREEK VEINS										
10.	7B031R1...Realgar-orp	60 00 08	160 12 46	N0.5	17,000	0.05	50	70	N1	15
	7B034R1...Qtz-cin	60 01 37	160 07 59	N0.5G20,000		N0.05	70	150	N1	30
KAGATI LAKE VEINS										
11.	8TF071...Qtz-cin-tour	59 54 50	159 54 54	3.0	(2,000)	2.90	300	100	(N10)	N10
RHYOLITE DIKES AND DOMES—KIPCHUK/TULIP AREA										
12.	9SB137A...Rhyolite	60 44 52	159 15 05	N0.5	(N200)	N0.05	700	150	(N10)	70
	8-238...Rhyolite	60 37 24	159 17 10	N0.5	140	0.30	200	1,500	6	L0.6
	7CZ001...Rhyolite	60 33 22	159 26 35	N0.5	10	N0.05	70	700	N1	L10
GOLD LAKE AREA										
13.	7SB143A...Qtz vein	60 13 25	159 23 18	7.0	7,000	1.10	50	150	30	L10
	7SB143B...Rhyolite	60 13 25	159 23 18	7.0	1,500	L0.05	500	300	15	L10
	7SB143D...Breccia	60 13 25	159 23 18	5.0G10,000		0.15	10	70	15	L10
	9TF080L...Breccia	60 13 25	159 23 18	7.0G10,000		2.00	N10	700	(70)	L10
KISARILIK LAKE AREA										
14.	8CZ039D...Qtz vein	60 21 10	159 18 00	1.5	(7,000)	0.41	300	200	N1	70
	8CZ039E...Rhyolite	60 21 10	159 18 00	1.5	(3,000)	0.23	200	300	N1	N10
15.	9TF107B...Rhyolite	60 17 10	159 01 26	3.0	(N200)	(N10)	15	G5,000	(L10)	L10
OTHER GOLD REPORTS										
16.	7TF003...Alt'd ss	60 57 28	159 39 00	0.5	8.00	0.10	15	70	L2	300
17.	7JM36B...Qtz vein	60 09 08	159 56 11	N0.5	20.00	0.35	30	700	31	150

networks have anomalous concentrations of various combinations of Ag, As, Au, Cu, Hg, Mo, Pb, Sb, and W (table 1). The highest anomalous values for Au, Ag, and As are from red spots where both rhyolite dikes and quartz veins are present, although anomalies are also present in

spots in which only one or the other rock type has been identified.

The largest and best exposed of the dike-vein networks crops out in ridges and valleys east of Gold Lake in the northeastern corner of the Bethel A-2 quadrangle (fig.

Table 1. Continued

Sample no.	Cu	Mn	Mo	Ni	Pb	Sb	Sn	W	Zn	Hg
NYAC TERRANE QUARTZ VEINS										
9TF042B.....	7	200	15	5	30	(N100)	N10	N20	(N200)	N0.02
8TF034A.....	70	700	5	7	N10	1.6	N10	N20	N0.05	0.84
8TF034C.....	70	700	30	10	N10	N1	N10	N20	5.8	0.60
8TF034D.....	30	1,500	N5	10	N10	1.7	N10	N20	42.0	2.28
7SB20.....	L5	1,000	N5	7	L10	N2	N10	N20	20.0	0.08
7YB14A.....	15	1,500	10	30	20	N2	N10	70	40.0	0.02
GOLDEN GATE FAULT ZONE										
9TF073A.....	10	700	N5	700	N10	(N100)	N10	N20	(N200)	4.20
9TF073E.....	30	700	N5	500	N10	(N100)	N10	N20	(N200)	1.90
9TF073E.....	50	700	N5	1,500	15	(N100)	N10	N20	(N200)	G36
9TF116B.....	20	300	N5	700	50	(N100)	20	N20	(1500)	4.00
7SB102H.....	100	1,000	N5	70	N10	N2	N10	N20	10.0	0.12
7SB102I.....	7	500	N5	1,000	N10	N2	N10	N20	25.0	0.04
7SB102L.....	150	1,500	N5	700	N10	N2	N10	N20	10.0	0.52
KIPCHUK AREA										
89ML227....	1,000	300	N5	200	2,000	(1,500)	100	N20	(G10,000)	G36
89TF32B.....	15	150	N5	30	70	(L100)	15	N20	(N200)	1.20
89TF32C.....	10	150	N5	30	100	(N100)	30	N20	(N200)	2.40
9TF67C.....	500	300	7	30	7,000	(5,000)	30	N20	(N200)	1.80
9TF67D.....	15	300	5	50	50	(500)	20	N20	(1,000)	0.60
9TF67J.....	70	300	5	30	5,000	(7,000)	30	N20	(N200)	4.40
FISHER DOME STIBNITE VEINS										
8TF058.....	30	500	N5	7	50	(G10,000)	N10	N20	(N200)	ND
FD-4.....	L5	70	L5	L5	70	(G10,000)	N10	N50	(N200)	4.80
RAINY CREEK VEINS										
7B031R1.....	15	70	N5	5	10	11,000	N10	N20	50.0	ND
7B034R1.....	70	700	N5	20	L10	8,200	N10	L20	85.0	160
KAGATI LAKE VEINS										
8TF071.....	30	500	N5	7	50	(G20,000)	N10	N20	(N200)	ND
RHYOLITE DIKES AND DOMES—KIPCHUK/TULIP AREA										
9SB137A.....	30	300	N5	30	30	(N100)	N10	N20	(N200)	14.40
8-238.....	20	700	7	N5	30	3.8	N10	N20	65.0	3.24
7CZ001.....	5	30	N5	L5	15	2.0	N10	N50	100.0	11.00
GOLD LAKE AREA										
7SB143A.....	100	2,000	20	L5	300	150.0	N10	N20	20.0	0.14
7SB143B.....	70	50	30	N5	100	24.0	N10	N20	15.0	0.04
7SB143D.....	15	100	N5	L5	30	10.0	15	N20	15.0	0.02
9TF080L.....	70	30	N5	L5	10	(L100)	10	N20	(N200)	0.06
KISARILIK LAKE AREA										
8CZ039D.....	N5	500	7	7	N10	20.0	15	70	15.0	H
8CZ039E.....	200	70	15	N5	10	100.0	15	30	20.0	0.40
9TF107B.....	30	70	100	5	50	(N100)	N10	N20	(N200)	0.08
OTHER GOLD REPORTS										
7TF003.....	200	1,500	N5	50	N10	L2	70	N20	6.0	0.32
7JM36B.....	70	700	10	70	15	8.0	N10	N20	30.0	0.32

1, loc. 13). The Gold Lake occurrence was first visited by U.S. Geological Survey geologists in 1987; it also was found by Cominco geologists and staked by them in

September of 1988. The ridges on the north side of Kisarilik Lake (fig. 1, loc. 14) also host a prominent Au-Ag-As-Sb-bearing dike-vein network. Pyrite-bearing rhyolite

dikes and quartz veins east of the Togiak fault in volcanic rocks of the Tikchik terrane (fig. 1, loc. 15) contain anomalous amounts of Ag, Pb, and Mo. Other red spots scattered through the Tikchik and Togiak terranes yield anomalies in some or all the metals of the Gold Lake-type veins but are not shown on figure 1 (T.P. Frost, unpub. data).

Altered rhyolite dikes containing partially resorbed quartz phenocrysts and pyrite cubes as large as 2 mm are prominent at the Gold and Kisarilik Lake occurrences and at most other red spots. The rhyolite is white to pale yellowish white on unweathered surfaces; oxidation of pyrite on weathered surfaces produces the bright-red color of most spots. The dikes are as wide as 3 m and are relatively resistant to erosion; in many areas they hold up ridges. The groundmass of most rhyolite is replaced by sericite or illite and quartz. Relict plagioclase phenocrysts are present and are partially replaced by albite and sericite. Samples of rhyolite contain as much as 7 ppm Ag, 3,000 ppm As, 0.23 ppm Au, 100 ppm Mo, and 100 ppm Sb. It is uncertain whether the metals are disseminated in the rhyolite or are present in quartz veins.

At the Gold Lake locality, several generations of zoned quartz veins containing as much as 20 percent galena cut all rock types. Common vein assemblages are quartz, quartz+calcite, quartz+(chlorite), quartz+iron (?) oxides, quartz+pyrite, and quartz+galena. Argillite and sandstone wall rocks and rhyolite dikes are incipiently to extensively altered to quartz, sericite, calcite, and iron oxide minerals near quartz veins. Most veins are less than 2 cm wide, although some may be as wide as 12 cm. Quartz is present as euhedral prisms as long as 1 cm. The prisms have clear cores, but the outer third of most crystals contains very fine grained fluid and mineral inclusions in concentric layers. The quartz in the layered rims has irregular extinction. Two generations of carbonate are present in the veins, both of which postdate crystallization of most of the quartz. The earliest carbonate is a brown, fine-grained aggregate that is intergrown with fine-grained quartz and galena. A later generation of coarse-grained, clear calcite fills in remaining space. Quartz veins contain as much as 7 ppm Ag, 7,000 ppm As, 1.1 ppm Au, 30 ppm Bi, 300 ppm Pb, 150 ppm Sb, and 70 ppm W (table 1). Hydrothermal breccia dikes or veins composed of pale-greenish-gray clays, quartz clasts, and oxide minerals have gold contents as high as 2.0 ppm (table 1). Coarse calcite veins at the Gold Lake locality have black alteration halos and contain as much as 0.05 ppm Au (T.P. Frost, unpub. data).

The rhyolite dike-quartz vein association at Gold Lake is dominated by anomalous arsenic and antimony concentrations and less consistent, but locally significant, enrichments in Ag, Au, Ba, and Pb. The veins are probably best classified as deep epithermal or shallow mesothermal polymetallic veins. Similar dike-vein associations are scattered through the southeastern corner of the Bethel

quadrangle in rocks of the Togiak and Tikchik terranes, but most that were located in this study have small surface expressions. Analytical values for arsenic and antimony as high as 180 ppm and 28 ppm, respectively, for stream-sediment samples in many drainages in the Togiak terrane and to a lesser extent the Tikchik terrane (T.P. Frost, unpub. data) suggest that there may be other rhyolite-quartz vein occurrences in the southeastern part of the Bethel quadrangle. Heavy-mineral concentrate samples from the same areas also yield anomalous As (to 5,000 ppm) and Sb (to 15,000 ppm), as well as locally anomalous Pb (to 200 ppm), W (to 5,000 ppm), and Zn (to 2,000 ppm) (T.P. Frost, unpub. data). Anomalous As, Au, Ag, Hg, and Pb contents in rock and stream-sediment samples in areas underlain by the Togiak and Tikchik terranes in the Goodnews, Taylor Mountains, and Dillingham quadrangles (Coonrad and others, 1978; Hessin and others, 1978a, b) suggest that mineralized rocks similar to those at Gold Lake may be present throughout these terranes.

Other Gold Occurrences

Gold was detected in red-weathering quartz veins in hornfelsed volcanoclastic sandstone in the vicinity of the Marvel Dome and Mt. Plummer plutons (fig. 1, loc. 16), just upstream from the Marvel Creek gold placer east of the Golden Gate fault (Hoare and Coonrad, 1959a; Hoare and Cobb, 1977). The sandstone contains amoeboid opaque minerals that probably grew in place. The sample also contains anomalous tin (table 1). The gold is probably in the quartz veins, although the source of the tin is less certain. The Mt. Plummer and Marvel Dome plutons probably are continuous below the present level of exposure. The plutons intrude sedimentary rocks of the Kuskokwim Group and have yielded a biotite K-Ar age of 70 Ma (S.E. Box, written commun., 1988).

Quartz veins cut hornfelsed argillite and fine-grained sandstone of the Togiak terrane in the vicinity of the Canyon Creek pluton (fig. 1, loc. 17) and contain as much as 0.35 ppm Au. Placers downstream from the pluton have produced significant gold (Hoare and Coonrad, 1959a; Hoare and Cobb, 1977). Stream-sediment and heavy-mineral concentrate samples downstream from the pluton contain anomalous As, Au, Cu, Hg, Pb, Sb, and W (T.P. Frost, unpub. data).

Gold was observed in pan concentrate samples or detected analytically (T.P. Frost, unpub. data) in at least one first- or second-order stream draining every pluton in the Bethel quadrangle. The granitoid plutons in the Bethel quadrangle provide favorable targets for additional undiscovered gold-bearing veins or related placer occurrences.

SUMMARY

The Bethel quadrangle contains several types of lode mineralization having potential for gold and mercury and lesser potential for silver and lead as byproducts. Gold-bearing quartz veins spatially associated with Early Cretaceous felsic granitic plutons are in Jurassic andesitic and volcanoclastic rocks of the Nyaq terrane. Gold placers east of the the Nyaq terrane in the the Bethel quadrangle and in the southern part of the Russian Mission quadrangle apparently are derived from quartz veins and hornfels surrounding 60- to 72-million-year-old granitic plutons. Mercury- and antimony-bearing quartz veins predominantly in Kuskowkim sedimentary rocks contain gold at significant levels. Base- and precious-metal-bearing rhyolite and quartz veins are scattered through the Paleozoic and Mesozoic volcanic and sedimentary rocks of the Togiak and Tikchik terrane in the southeastern part of the quadrangle. Small areas of quartz-tourmaline replacement in Upper Cretaceous volcanic and volcanoclastic rocks near the Kipchuk River contain variable but anomalous amounts of silver, gold, lead, and zinc.

REFERENCES CITED.

- Box, S.E., and Murphy, J.M., 1987, Late Mesozoic structural and stratigraphic framework, eastern Bethel quadrangle, southwestern Alaska, in Hamilton, T.D., and Galloway, J.P., eds., *Geologic studies in Alaska by the U.S. Geological Survey during 1986*: U.S. Geological Survey Circular 998, p. 78-82.
- Coonrad, W.L., Hoare, J.M., Taufen, P.M., and Hessin, T.D., 1978, Geochemical analyses of rock samples in the Goodnews and Hagemeister Island quadrangles region, southwestern Alaska: U.S. Geological Survey Open-File Report 78-9-H, 1 sheet, scale 1:250,000.
- Frost, T.P., Calzia, J.P., Kistler, R.W., and Vivit, D.V., 1988, Petrogenesis of the Crooked Mountains pluton, Bethel quadrangle—A preliminary report, in Galloway, J.P., and Hamilton, T.D., eds., *Geologic studies in Alaska by the U.S. Geological Survey during 1987*: U.S. Geological Survey Circular 1016, p. 126-131.
- Hessin, T.D., Taufen, P.M., Seward, J.C., Quintana, S.J., Clark, A.L., Grybeck, Donald, Hoare, J.M., and Coonrad, W.L., 1978a, Geochemical and generalized geological map showing distribution and abundance of lead in the Goodnews and Hagemeister Island quadrangles region, southwestern Alaska: U.S. Geological Survey Open-File Report 78-7-N, scale 1:250,000.
- _____, 1978b, Geochemical and generalized geological map showing distribution and abundance of arsenic, gold, silver, and platinum in the Goodnews and Hagemeister Island quadrangles region, southwestern Alaska: U.S. Geological Survey Open-File Report 78-7-R, scale 1:250,000.
- Hoare, J.M., and Cobb, E.H., 1977, Mineral occurrences (other than mineral fuels and construction materials) in the Bethel, Goodnews, and Russian Mission quadrangles, Alaska: U.S. Geological Survey Open-File Report 77-156, 98 p.
- Hoare, J.M., and Coonrad, W.L., 1959a, Geology of the Bethel quadrangle, Alaska: U.S. Geological Survey Miscellaneous Investigations Map I-285, scale 1:250,000.
- _____, 1959b, Geology of the Russian Mission Quadrangle, Alaska: U.S. Geological Survey Miscellaneous Investigations Map I-292, scale 1:250,000.
- _____, 1978, Geologic map of the Goodnews and Hagemeister Island quadrangles, Alaska: U.S. Geological Survey Open-File Report 78-9-B, scale 1:250,000.
- Hoare, J.M., and Jones, D.L., 1981, Lower Paleozoic radiolarian chert and associated rocks in the Tikchik Lakes area, southwestern Alaska, in Albert, N.R.D., and Hudson, Travis, eds., *The United States Geological Survey in Alaska—Accomplishments during 1979*: U.S. Geological Survey Circular 823-B, p. B44-B45.
- Jones, D.L., Silberling, N.J., Concy, P.J., and Plafker, George, 1987, Lithotectonic terrane map of Alaska (west of the 141st meridian): U.S. Geological Survey Miscellaneous Field Studies Map MF-1874-A, scale 1:2,500,000.
- Mertie, J.B., Jr., 1938, The Nushagak district, Alaska: U.S. Geological Survey Bulletin 903, 96 p.
- _____, 1976, Platinum deposits of the Goodnews Bay District, Alaska: U.S. Geological Survey Professional Paper 938, 42 p.
- Murphy, J.M., 1987, Early Cretaceous cessation of terrane accretion, northern Eek Mountains, southwestern Alaska, in Hamilton, T.D., and Galloway, J.P., eds., *Geologic studies in Alaska by the U.S. Geological Survey during 1986*: U.S. Geological Survey Circular 998, p. 83-85.
- Robinson, M.S., and Decker, John, 1986, Preliminary age data and analytical data for selected igneous rocks from the Sleetmute, Russian Mission, Taylor Mountain, and Bethel quadrangles, southwestern Alaska: Alaska Division of Mining and Geological and Geophysical Surveys Public-Data File 86-98, 9 p.
- Rutledge, F.A., 1948, Investigation of the Rainy Creek mercury prospect, Bethel district, Kuskokwim region, southwestern Alaska: U.S. Bureau of Mines Report of Investigations 4361, 7 p.
- Sainsbury, C.L., and MacKevett, E.M., Jr., 1965, Quicksilver deposits of southwestern Alaska: U.S. Geological Survey Bulletin 1187, 89 p.
- Shew, Nora, and Wilson, F.H., 1981, Map and table showing radiometric ages of rocks in southwestern Alaska: U.S. Geological Survey Open-File Report 81-866, 26 p.
- Southworth, D.D., 1986, Geology of the Goodnews Bay ultramafic complexes: Fairbanks, University of Alaska, M.S. thesis, 114 p.
- Turner, D.L., Forbes, R.B., Aleinikoff, J.N., Hedge, C.E., and McDougall, Ian, 1983, Geochronology of the Kilbuck terrane of southwestern Alaska: Geological Society of America Abstracts with Programs, v. 15, p. 407.

Chapter D

Gold Associated with Cinnabar- and Stibnite-Bearing Deposits and Mineral Occurrences in the Kuskokwim River Region, Southwestern Alaska

By JOHN E. GRAY, THOMAS P. FROST,
RICHARD J. GOLDFARB, and DAVID E. DETRA

U.S. GEOLOGICAL SURVEY BULLETIN 1950

GEOCHEMICAL STUDIES IN ALASKA BY THE U.S. GEOLOGICAL SURVEY, 1989

CONTENTS

Abstract	D1
Introduction	D1
Geology	D1
Geochemical results for mineralized vein samples	D2
Significance of gold associated with mercury-antimony deposits	D4
Summary	D5
References cited	D5

FIGURE

1. Map showing cinnabar- and stibnite-bearing deposits and mineral occurrences in the Kuskokwim River region, southwestern Alaska D2

TABLES

1. Geochemical results of ores from cinnabar-stibnite deposits, southwestern Alaska D3
2. Geochemical results of cinnabar and stibnite separates from deposits and mineral occurrences, southwestern Alaska D4

Gold Associated with Cinnabar- and Stibnite-Bearing Deposits and Mineral Occurrences in the Kuskokwim River Region, Southwestern Alaska

By John E. Gray, Thomas P. Frost, Richard J. Goldfarb, and David E. Detra

Abstract

Several epithermal mercury-antimony vein deposits in the Kuskokwim River region of southwestern Alaska contain anomalous gold concentrations. Gold contents in vein samples containing cinnabar and stibnite are 0.05–6.9 ppm; samples are from the Red Devil, Mountain Top, White Mountain, Cinnabar Creek, Fisher Dome, Kagali Lake, and Snow Gulch deposits. In addition, analyses of cinnabar separates from Red Devil and stibnite separates from Fisher Dome and Snow Gulch contain as much as 10 ppm Au.

Gold concentrations in the ores exposed at the surface of these deposits are significant. These concentrations suggest that gold may be a byproduct of some of these epithermal systems, which previously were recognized only as mercury and antimony bearing. Gold-rich veins and stockworks may have also formed below these epithermal mercury-antimony deposits. These gold-rich zones may be found in deeper, hotter parts of the systems in southwestern Alaska by processes analogous to those operating in vertically zoned deposits in other parts of the world. The gold anomalies indicate that analytical methods for gold that are sensitive to parts per billion should be part of regional exploration programs in Alaska in order to target precious-metal occurrences.

INTRODUCTION

Epithermal cinnabar and stibnite lodes are scattered over several hundred thousand square kilometers in the Kuskokwim River region of southwestern Alaska (fig. 1). Cinnabar and stibnite are the dominant ore minerals; lesser amounts of realgar, orpiment, native mercury, pyrite, limonite, and hematite are present (Sainsbury and MacKevett, 1965). Dickite is a common alteration mineral at many of these deposits. Ore minerals are typically in quartz-carbonate veins hosted within and adjacent to mafic dikes, carbonate rock, graywacke, rhyolite, or monzonite to granodiorite bodies. Commonly, mineralized veins are localized where bedding-plane faults in the surrounding sedimentary rocks intersect these more competent units (Sainsbury and MacKevett, 1960). Approximately 41,000 flasks of mercury have been produced from the region, mostly from mines in

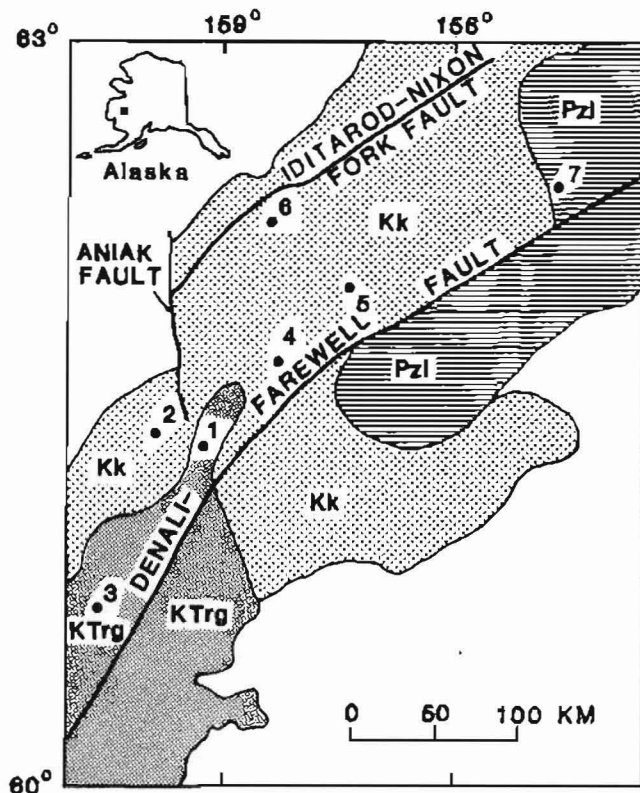
the Red Devil area where about 35,000 flasks were recovered (Miller and others, 1989).

Although geological evaluations have been conducted on many of these mercury-antimony deposits (for example, Webber and others, 1947; Rutledge, 1950; Sainsbury and MacKevett, 1965), few studies report the presence of gold. The lack of reported gold is due in part to the relatively high limit of determination for gold in analytical techniques utilized in these studies. For example, in the most comprehensive study of the mercury-antimony systems in southwestern Alaska, Sainsbury and MacKevett (1965) reported that ores from several cinnabar-stibnite deposits in southwestern Alaska were below the emission spectrography lower limit of determination of 20 ppm for gold. In this paper, we present gold analyses of mineralized vein samples determined by atomic absorption (AA) or inductively coupled plasma-atomic emission spectroscopy (ICP-AES), techniques that have lower limits of determination of 0.05 ppm and 0.15 ppm, respectively. We also report emission spectrographic results of Au, Ag, Sb, and As of cinnabar and stibnite separates from the deposits.

Acknowledgments.—The authors would like to thank Bruce Roushey, Randy Hill, Phil Hageman, and Jerry Motooka for chemical analyses of samples. Assistance with field work was provided by Robert Eppinger and James Kilburn. We also recognize the assistance of Karen E. Slaughter with drafting. We gratefully acknowledge Bruce Hickock of the Calista Corporation for helpful discussions and permission to visit several deposits and mineral occurrences during this study. The manuscript was strengthened by technical reviews by Robert Eppinger, Cliff Taylor, Tom Nash, Jim Dover, and John Galloway.

GEOLOGY

Rocks of the Cambrian to Devonian Holitna Group are the oldest known to host mercury-antimony deposits in the Kuskokwim River region. Strata of the Holitna Group



- EXPLANATION**
- GEOLOGY**
- Kk Cretaceous Kuskokwim Group
 - KTrg Triassic and Lower Cretaceous Gemuk Group
 - Pzl Cambrian to Devonian Holitna Group
- DEPOSITS AND MINERAL OCCURRENCES**
- 1 Cinnabar Creek
 - 2 Fisher Dome
 - 3 Kagati Lake
 - 4 Mountain Top
 - 5 Red Devil
 - 6 Snow Gulch
 - 7 White Mountain

Figure 1. Cinnabar- and stibnite-bearing deposits and mineral occurrences in the Kuskokwim River region, southwestern Alaska. Geology modified from Decker and others (Alaska Division of Geological and Geophysical Surveys, written commun., 1989).

consist of massive to thinly bedded limestone and dolomite and minor, local conglomerate (Cady and others, 1955). Mineral occurrences in the White Mountain area are found in rocks of the Holitna Group.

Cinnabar- and stibnite-bearing deposits are also found in rocks of the Triassic and Lower Cretaceous Gemuk Group. The Gemuk Group is composed of massive siltstone interbedded with lesser amounts of chert, volcanic rock (tuffs and lavas), limestone, and graywacke (Cady and others, 1955). The Cinnabar Creek area, the type locality for the Gemuk Group, hosts a number of epithermal cinnabar and stibnite mineral occurrences. Mercury- and antimony-bearing quartz veins are also found in Cretaceous-Tertiary quartz monzonite and granodiorite bodies that intrude rocks of the Gemuk Group; for example, at the Kagati Lake mineral occurrence (Sainsbury and MacKevett, 1965).

Many of the cinnabar and stibnite deposits are hosted in rocks of the Cretaceous Kuskokwim Group. The Kuskokwim Group consists primarily of marine turbidites composed of interbedded graywacke, siltstone, shale, minor conglomerate, and occasional thin coal seams (Miller and others, 1989). These rocks unconformably overly other rock units in the region including those of the Gemuk and Holitna Groups. Cretaceous to Tertiary dikes of intermediate to mafic composition intrude rocks of the Kuskokwim Group and commonly host quartz-carbonate veins containing cinnabar and stibnite. At Red Devil and Mountain Top, mineralized veins are found in mafic dikes, in graywacke and shale of the Kuskokwim Group, and at contacts between the dikes and sedimentary rocks. Similarly, at Fisher Dome, quartz-stibnite veins are present in a Cretaceous-Tertiary granite pluton that intrudes rocks of the Kuskokwim Group (Hoare and Coonrad, 1959). At the Snow Gulch deposit in the Donlin Creek area, cinnabar and stibnite are present in rhyolite where hypabyssal rhyolite dikes intrude graywacke and shale of the Kuskokwim Group.

GEOCHEMICAL RESULTS FOR MINERALIZED VEIN SAMPLES

Utilizing the AA and ICP-AES methods we were able to identify the presence of significant gold in several cinnabar- and stibnite-bearing deposits in the Kuskokwim River region (table 1). Our results indicate anomalous concentrations of gold in mineralized samples from the Red Devil, Cinnabar Creek, Mountain Top, and White Mountain deposits. In addition, McGimsey and others (1988) reported anomalous gold in ore samples from the Snow Gulch deposit (table 1). Mineralized vein samples from the Fisher Dome and Kagati Lake mineral occurrences are also anomalous in gold (Frost, this volume). Geochemical studies of rocks that host cinnabar and stibnite deposits throughout the Kuskokwim River region indicate that background gold concentrations are less than 0.05 ppm (McGimsey and others, 1988; J.E. Gray, unpub. data). Therefore, it is noteworthy that many of the deposits in the Kuskokwim River region contain anomalous amounts of gold of greater than 0.05 ppm.

Table 1. Geochemical results of ores from cinnabar-stibnite deposits and mineral occurrences, southwestern Alaska
 [All values are in parts per million. Leaders (-), not determined; N, not detected at the value shown; L, detected but not quantifiable; G, greater than the value shown]

Location	Sample	Au	Ag	Hg	Sb	As
Red Devil ¹	RD1C ^a	4.4	0.26	36G	8,000G	4,463
Red Devil ¹	RD1D ^b	1.1	0.45	36G	8,000G	387
Red Devil ²	88ATF043A ^a	0.10	0.5L	--	100L	1,500
Red Devil ²	88ATF043B ^a	0.4	0.5L	--	10,000G	7,000
Red Devil ²	88ATF043C ^b	1.3	0.5	--	10,000G	7,000
Red Devil ²	88ATF043D ^b	0.05N	0.5N	--	300	2,000
Mountain Top ¹	MT1C ^a	0.32	0.12	36G	3.8	7.3
White Mountain ¹	WM1A ^a	0.37	0.09	36G	18	20
White Mountain ²	88ATF047 ^a	0.05	0.5N	--	150	200N
Cinnabar Creek ²	88ATF049 ^c	0.10	0.5N	--	5,000	1,500
Cinnabar Creek ²	88ATF050 ^d	0.40	0.5N	--	10,000G	7,000
Cinnabar Creek ²	88ATF051 ^d	0.20	0.5N	--	500	2,000
Fisher Dome ²	88ATF058 ^b	1.0	7	--	10,000G	1,500
Fisher Dome ²	FD-4 ^b	0.70	0.5N	4.8	10,000G	300
Kagati Lake ²	88ATF071A ^c	2.9	3	--	10,000G	2,000
Kagati Lake ²	88ATF071B ^c	1.7	2	--	10,000G	2,000
Snow Gulch ³	I0337RA ^b	6.9	38	10G	1,000G	1,600
Snow Gulch ³	I0337RB ^b	4.1	13	10G	1,000G	2,000G

¹Concentrations of Au, Ag, Sb, and As were determined by inductively coupled plasma atomic emission spectrometry; Hg by cold-vapor atomic absorption.

²Concentrations for Au were determined by atomic absorption; Ag, Sb, and As by semiquantitative emission spectrography; Hg (when listed) by cold-vapor atomic absorption.

³Results from McGimsey and others (1988). Concentrations of Au, Ag, Sb, and As were determined by atomic absorption; Hg by cold-vapor atomic absorption.

^aOre sample containing predominantly cinnabar.

^bOre sample containing predominantly stibnite.

^cOre sample containing cinnabar and stibnite.

^dOre sample containing abundant cinnabar and native mercury, abundant cinnabar and native mercury, and minor stibnite.

At the Red Devil mine, both vein samples containing abundant cinnabar and those containing predominantly stibnite are anomalous in gold (table 1). Quartz-carbonate veins hosted in graywacke of the Kuskokwim Group at Red Devil contain cinnabar and minor stibnite and 0.40–4.4 ppm Au. Other mineralized vein and breccia samples from Red Devil that are hosted in altered mafic dikes and Kuskokwim graywacke, but contain vug fillings of abundant stibnite, have as much as 1.3 ppm Au. At the Mountain Top deposit, high-grade mercury ore having anomalous gold concentrations is found in brecciated mafic dikes that cut graywacke and shale of the Kuskokwim Group. A sample of quartz-carbonate vein from Mountain Top contains abundant cinnabar open-space filling and 0.32 ppm Au (table 1).

Two samples of high-grade mercury ore from the White Mountain deposit contain 0.05 and 0.37 ppm Au. These vein samples contain vug fillings of cinnabar that cut brecciated and silicified dolomite of the Holitna Group. In the Cinnabar Creek area, two samples of silicified and brecciated siltstone and graywacke of the Gemuk Group are cut by numerous stockworks containing cinnabar, stibnite, and abundant free mercury. These samples contain 0.20 and

0.40 ppm Au. Another sample of brecciated siltstone from the Gemuk Group in the Cinnabar Creek area contains cinnabar and stibnite in quartz stockworks and 0.10 ppm Au.

Two quartz-stibnite vein samples that cut a hypabyssal biotite quartz porphyry at the Fisher Dome mineral occurrence contain 0.20 and 1.0 ppm Au (Frost, this volume) (table 1). Frost also reports as much as 2.9 ppm Au in quartz-calcite-cinnabar-stibnite veins in a hornblende-biotite granite stock from the Kagati Lake locality. Anomalous gold is present in two samples of quartz vein with abundant stibnite cutting rhyolite at Snow Gulch (McGimsey and others, 1988) (table 1). These samples contain 4.1 and 6.9 ppm Au, some of the highest concentrations yet determined for any of the mercury-antimony lodes in the region.

Native gold was recognized in a heavy-mineral separate of Red Devil ore. Semiquantitative spectrographic analysis indicates that cinnabar and stibnite separates from Red Devil, Fisher Dome, and Snow Gulch contain 10 ppm Au (table 2). In addition, heavy-mineral-concentrate samples collected downstream from the Fisher Dome, White Mountain, and Mountain Top deposits contain finely

Table 2. Geochemical results of cinnabar and stibnite separates from deposits and mineral occurrences, southwestern Alaska

[All determinations were made by semiquantitative emission spectrography. Values are in parts per million. N, not detected at the value shown; L, detected at the value shown, but not quantifiable; G, greater than the value shown]

Location	Sample	Au	Ag	Sb	As
Red Devil	RD1C ^a	10	2	1,000	10,000G
Mountain Top	MT1C ^a	10N	1	100N	1,000
White Mountain	WM1A ^a	10N	.5N	300	200
White Mountain	WM2 ^a	10N	.5N	100	200N
Cinnabar Creek	CCA ^a	10N	.5N	300	200N
Fisher Dome	FD1 ^b	10L	50	10,000G	200N
Fisher Dome	FD2 ^b	10	50	10,000G	200L
Snow Gulch	SG1 ^b	10	200	10,000G	10,000
Snow Gulch	SG2 ^b	10	150	10,000G	10,000G

^aCinnabar mineral separate, 95-99 percent pure.

^bStibnite mineral separate, 95-99 percent pure.

particulate free gold (Gray and others, 1990; T.P. Frost, unpub. data). These results suggest that the gold in the cinnabar-stibnite deposits is native gold.

Placer gold deposits below stibnite lodes in the Donlin Creek area (which includes Snow Gulch) also provide evidence that gold is derived from upstream mercury-antimony lodes. Cady and others (1955) reported cinnabar and stibnite, as well as gold, in placer concentrates in the Donlin Creek area. Gold in cinnabar nuggets from placers in the Donlin Creek area (Cady and others, 1955) is evidence that some gold is associated with mercury-antimony lodes. These findings led Cady and others (1955) to suggest that cinnabar and stibnite lodes were the source of placer gold in the Donlin Creek area.

In addition to the gold anomalies discussed previously, many cinnabar- and stibnite-bearing veins in the Kuskokwim River region contain appreciable Hg, Sb, As, and Ag (table 1). Anomalous Hg, Sb, and As reflect the presence of cinnabar, stibnite, and realgar, which are common in these mineral systems. The presence of "a small amount of silver" was previously reported in the Donlin Creek area by Cady and others (1955); however, silver has not been previously reported from the other mercury-antimony deposits in this study. Appreciable silver was found in mineralized vein samples from Snow Gulch (13-38 ppm), Fisher Dome (7 ppm), and Kagati Lake (2-3 ppm) (table 1). Silver concentrations of 50-200 ppm were also found in stibnite separates from Fisher Dome and Snow Gulch (table 2). The association of anomalous Au, Ag, and Sb in mineralized samples from these deposits is suggestive of silver association with gold in electrum, or silver enrichment in stibnite.

SIGNIFICANCE OF GOLD ASSOCIATED WITH MERCURY-ANTIMONY DEPOSITS

Our results are important because they are the first gold anomalies reported for many of the cinnabar and stibnite deposits in the Kuskokwim River region. The

discovery of these anomalies indicates that regional exploration programs should include parts per billion level determinations for gold, such as those obtained using AA or ICP-AES techniques. The low-level gold determinations should be useful for identifying epithermal mercury-antimony systems that are also favorable for precious-metal resources.

These findings indicate that gold may be a significant, yet unrecognized, byproduct in these mercury-antimony deposits. The data shown in table 1 indicate that gold was deposited along with the other trace metals. However, the geochemical studies presented here were conducted on grab samples of high-grade mercury and antimony ore, and additional studies are needed to more precisely determine gold ore grades and the lateral and vertical extent of gold. Although the gold content in samples of some of these deposits is high, mineralized veins are commonly small and discontinuous, and thus ore tonnages are generally low.

Perhaps more importantly, our results suggest that more gold may be found in deeper environments below these deposits. The presence of such concealed gold deposits is dependent on a number of factors including the thermal gradient of the hydrothermal systems and the lateral and vertical extent of veining.

The light stable isotope (Goldfarb and others, this volume) and fluid inclusion (Roedder, 1963; Miller and others, 1989) compositions of the ore fluids from these epithermal mercury-antimony deposits are compatible with an origin from dehydration of surrounding sedimentary rocks by igneous activity or burial metamorphism. Fluid inclusion data from the Red Devil deposit indicate that the Kuskokwim deposits formed at temperatures of approximately 150-210 °C (Miller and others, 1989). Such low ore-fluid temperatures commonly hinder the mobilization of gold because the solubility of gold bisulfide decreases sharply between 300 and 200 °C (Seward, 1984). Therefore, assuming that the Kuskokwim ore fluids were hot enough at some depth to have carried significant gold

and the gold was transported as bisulfide complex, much of the gold would have been precipitated from the fluids before they reached the low-temperature, near-surface environment.

The presence of dickite and hematite at many of the Kuskokwim deposits indicates acidification and oxidation of ore fluids near the surface. Acidic and oxidizing conditions further limit gold bisulfide complex stability (Seward, 1984). Significant gold deposition is more probable under more reducing and neutral pH fluid conditions. Such physicochemical conditions are more common below the near-surface environment.

Higher gold concentrations are more likely at deeper levels of these hydrothermal systems, where fluid temperatures were 250 °C or more. Without additional subsurface data it is not possible to determine whether fluid flow and fluid temperatures were adequate to form gold-rich zones below any of the Kuskokwim epithermal systems. However, assuming similar ore fluid oxygen isotopic composition for all of these Kuskokwim deposits, the relatively light $\delta^{18}\text{O}$ value for quartz from Fisher Dome (Goldfarb and others, this volume) suggests that stibnite-rich quartz was deposited under higher temperature conditions than those of the other, more cinnabar-rich quartz veins within the Kuskokwim region. This interpretation is also supported by the slighter higher formation temperature of stibnite versus that of cinnabar reported in many hydrothermal ore deposits (Buchanan, 1981). Thus, the stibnite-rich Fisher Dome mineral occurrence could have formed closer to a gold-rich zone than many of the other deposits. The relatively large hydrothermal system at Red Devil could be representative, however, of the upper levels of a concealed gold system and may be a more viable target because of its size.

In other Hg-Sb-Au systems, antimony commonly occupies a position intermediate to that of mercury systems (above) and gold (below). In the Marlborough schists of New Zealand, vein systems are stibnite dominant in the near surface and gold bearing without stibnite at depths of 400 m (Pirajno, 1979). Similarly, quartz veins evolve from antimony rich to gold rich with increasing depth at Carbon Hill in the southern Yukon Territory (Craig Hart, Aurum Consultants, written commun., 1989). Economic concentrations of gold in the mercury-rich hot spring deposits at McLaughlin and Wilbur Springs in northern California suggest telescoping of mercury- and gold-rich parts of these deposit types. In many large antimony-bearing districts, such as those in the Iberian Peninsula of southern Europe (Gumiel and Arribas, 1987), stibnite is found in simple quartz veins, as well as in veins containing cinnabar or gold. At Red Devil, there is a transition from cinnabar without stibnite near the surface, to both phases at

intermediate depths, and to stibnite without cinnabar at deepest levels (about 200 m). Perhaps the Kuskokwim deposits represent surface expressions of deeper, more gold-rich deposits.

SUMMARY

Anomalous gold concentrations in several epithermal mercury-antimony deposits in the Kuskokwim River region of southwestern Alaska are the first reported for many of these deposits. These gold anomalies indicate the potential for byproduct gold in some of these deposits. Although many of the gold concentrations associated with these deposits in surface exposures are somewhat low, the gold anomalies may target more significant gold deposits below one or more of these mercury-antimony systems. Our results suggest that low-level gold analyses at the parts per billion level should be carried out during regional programs for gold exploration.

REFERENCES CITED

- Buchanan, L.J., 1981, Precious metal deposits associated with volcanic environments in the southwest, in Dickinson, W.R., and Payne, W.D., eds., Relations of tectonics to ore deposits in the Southern Cordillera: Arizona Geological Society Digest 14, p. 237-262.
- Cady, W.M., Wallace, R.E., Hoare, J.M., and Webber, E.J., 1955, The central Kuskokwim region, Alaska: U.S. Geological Survey Professional Paper 268, 132 p.
- Gray, J.E., Detra, D.E., Hill, R.H., Slaughter, K.E., and Sutley, S.J., 1990, Geochemical data and sample locality maps for stream-sediment and heavy-mineral-concentrate samples, and mineralogical data of nonmagnetic, heavy-mineral-concentrate samples, collected near five cinnabar-stibnite mineral occurrences in the Kuskokwim River region, southwestern Alaska: U.S. Geological Survey Open-File Report 90-299A.
- Gumiel, P., and Arribas, A., 1987, Antimony deposits in the Iberian Peninsula: Economic Geology, v. 82, p. 1453-1463.
- Hoare, J.M., and Coonrad, W.L., 1959, Geology of the Bethel quadrangle, Alaska: U.S. Geological Survey Miscellaneous Geological Investigations Series Map I-285, scale 1:250,000.
- McGimsey, R.G., Miller, M.L., and Arbogast, B.F., 1988, Paper version of analytical results, and sample locality map for rock samples from the Iditarod quadrangle, Alaska: U.S. Geological Survey Open-File Report 88-421-A, 110 p., 1 plate.
- Miller, M.L., Belkin, H.E., Blodgett, R.B., Bundtzen, T.K., Cady, J.W., Goldfarb, R.J., Gray, J.E., McGimsey, R.G., and Simpson, Shirley, 1989, Pre-field study and mineral

- resource assessment of the Sleetmute quadrangle, southwestern Alaska: U.S. Geological Survey Open-File Report 89-363, 115 p., 3 plates.
- Pirajno, Franco, 1979, Geology, geochemistry, and mineralization of the Endeavour Inlet antimony-gold prospect, Marlborough Sounds, New Zealand: *New Zealand Journal of Geology and Geophysics*, v. 22, p. 227-237.
- Roedder, Edwin, 1963, Studies of fluid inclusions II—Freezing data and their interpretation: *Economic Geology*, v. 58, p. 167-211.
- Rutledge, F.A., 1950, Investigation of mercury deposits, Cinnabar Creek area, Georgetown and Aniak districts, Kuskokwim region, southwestern Alaska: U.S. Bureau Mines Report of Investigation 4719, 9 p.
- Sainsbury, C.L., and MacKevett, E.M., Jr., 1960, Structural control in five quicksilver deposits in southwestern Alaska, in *Geological Survey Research 1960: U.S. Geological Survey Professional Paper 400-B*, p. B35-B38.
- _____, 1965, Quicksilver deposits of southwestern Alaska: *U.S. Geological Survey Bulletin 1187*, 89 p.
- Seward, T.M., 1984, The transport and deposition of gold in hydrothermal systems, in *Gold 82—The geology, geochemistry, and genesis of gold deposits: Geological Society of Zimbabwe Special Publication 1*, p. 165-181.
- Webber, B.S., Bjorklund, S.C., Rutledge, F.A., Thomas, B.I., and Wright, W.S., 1947, Mercury deposits of southwestern Alaska: U.S. Bureau of Mines Report of Investigation 4065, 57 p.

Chapter E

Stable Isotope Systematics of Epithermal Mercury-Antimony Mineralization, Southwestern Alaska

By RICHARD J. GOLDFARB, JOHN E. GRAY,
WILLIAM J. PICKTHORN, CAROL A. GENT,
and BARRETT A. CIEUTAT

U.S. GEOLOGICAL SURVEY BULLETIN 1950

GEOCHEMICAL STUDIES IN ALASKA BY THE U.S. GEOLOGICAL SURVEY, 1989

CONTENTS

Abstract	E1
Introduction	E1
Geological setting and character of the Kuskokwim mercury-antimony deposits	E2
Stable isotope studies	E3
Oxygen isotopes	E3
Hydrogen isotopes	E5
Sulfur isotopes	E5
Stable isotope implications for ore genesis	E6
Origin of the Kuskokwim deposits	E7
References cited	E8

FIGURES

1. Map showing location of cinnabar-and stibnite-bearing deposits, Kuskokwim Mountains, southwestern Alaska E1
2. Plot of δD versus $\delta^{18}O$ for ore fluids from the Kuskokwim region and for other studied hydrothermal systems E4

TABLE

1. Stable isotope data for ore-related minerals from mercury-antimony deposits, southwestern Alaska E3

Stable Isotope Systematics of Epithermal Mercury-Antimony Mineralization, Southwestern Alaska

By Richard J. Goldfarb, John E. Gray, William J. Pickthorn, Carol A. Gent, and Barrett A. Cieutat

Abstract

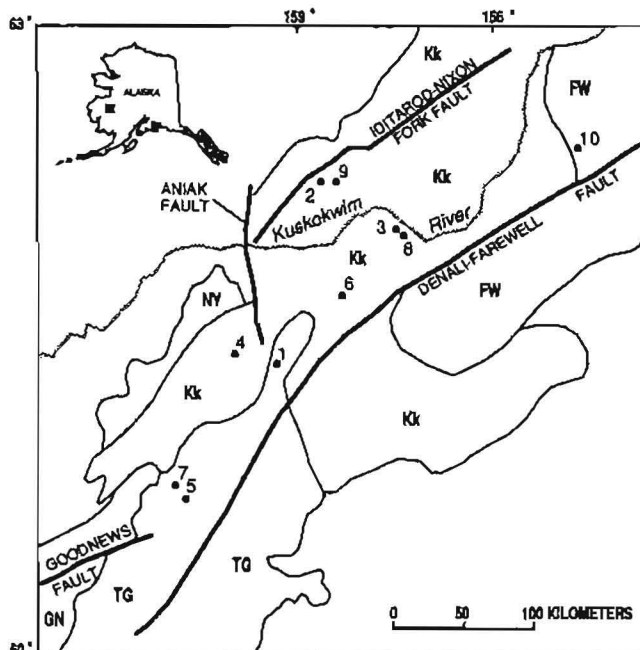
Epithermal mercury-antimony lode deposits and occurrences are in rocks of the Kuskokwim Group, Gemuk Group, and Holitna Group of southwestern Alaska. Vein quartz, probably coeval with much of the sulfide deposition, generally has $\delta^{18}\text{O}$ compositions of 23–30‰ (per mil) indicative of ore-forming fluids of 11–18‰. Hydrothermal dickite from the Red Devil deposit has a measured δD value of -127‰ , whereas fluid inclusion waters from host quartz are at least 23‰ lighter. The $\delta^{34}\text{S}$ values for cinnabar, stibnite, realgar, and orpiment for most of the deposits range from -3.0 to -6.7‰ .

Oxygen isotope data are most compatible with oxygen in the ore fluids being derived from dehydration of sedimentary rocks due to simple burial metamorphism or localized igneous activity. The relatively deuterium-depleted ore fluids suggest that much of the hydrogen was derived from breakdown of organic material. The sulfur in these deposits was generally derived from a similar organic source in the sedimentary rocks. Enrichment of sulfide minerals in ^{32}S at Mountain Top and Snow Gulch suggests that a more local sulfur reservoir may have contributed to these hydrothermal systems.

INTRODUCTION

Cinnabar- and stibnite-bearing quartz-filled fractures are present at many locations throughout the Kuskokwim Mountains region of southwestern Alaska (fig. 1). The veinlets are within the Cambrian to Devonian Holitna Group, the Triassic and Lower Cretaceous Gemuk Group, and the Cretaceous Kuskokwim Group. Many of the mineralized fractures are within or adjacent to silica-carbonate-altered mafic dikes that cut through these sedimentary rocks. Red Devil, the largest of these epithermal systems, has produced about 35,000 flasks of mercury since World War II (Miller and others, 1989). Detailed descriptions of the geology, mineralogy, and structural controls on mineralization for the more significant epithermal deposits and occurrences are given by Sainsbury and MacKevett (1965).

This paper presents the results of a stable isotope investigation of this group of mineral deposits and occurrences. These data provide new information that have



EXPLANATION		
DEPOSITS AND OCCURRENCES		GEOLOGY
1 Cinnabar Creek	6 Mountain Top	FW Farewell terrane
2 DeCourcy	7 Rainy Creek	TG Togiak terrane
3 Fairview	8 Red Devil	GN Goodnews terrane
4 Fisher Dome	9 Snow Gulch	NY Niyac terrane
5 Kagati Lake	10 White Mountain	Kk Kuskokwim Group

Figure 1. Cinnabar- and stibnite-bearing deposits in the Kuskokwim Mountains region, southwestern Alaska. Geology modified from Decker and others (Alaska Division of Geological and Geophysical Surveys, written commun., 1989).

significant implications for development of a genetic model. Hydrogen and oxygen isotope data constrain possible sources for the ore fluids and provide information regarding processes of mineral precipitation. Sulfur isotope data aid in defining physiochemical conditions of ore deposition and in

identifying sources for the sulfur within the hydrothermal systems. These new isotopic data, when applied to the conceptual ore deposit model for cinnabar- and stibnite-bearing mineral occurrences within southwestern Alaska, may improve our ability to predict favorable exploration target areas within the Kuskokwim Mountains region.

Acknowledgments.—This paper benefited from critical reviews by John Galloway, Albert Hofstra, Tom Nash, and Ian Ridley. Marti Miller kindly provided samples of mafic dikes, and Tom Frost contributed samples from Kagati Lake and Fisher Dome.

GEOLOGICAL SETTING AND CHARACTER OF THE KUSKOKWIM MERCURY-ANTIMONY DEPOSITS

Miller and others (1989) and Decker and others (Alaska Division of Geological and Geophysical Surveys, written commun., 1989) have provided the most recent detailed descriptions of the rocks of southwestern Alaska that host cinnabar and stibnite mineralization. The Cambrian to Devonian Holitna Group, forming part of what presently is referred to as the Farewell tectonostratigraphic terrane, consists dominantly of partly dolomitized limestone. The Triassic and Lower Cretaceous Gemuk Group, accreted to the Alaskan margin as part of the Togiak terrane in late Early Cretaceous time, is comprised of massive siltstone and lesser chert and volcanic rocks. Cretaceous marine turbidite, forming the Kuskokwim Group, filled an extensional basin between the above Farewell and Togiak accretionary terranes. Widespread igneous activity occurred during the Late Cretaceous and early Tertiary in southwestern Alaska, subsequent to terrane accretion. Volcano-plutonic complexes of varied composition; rhyolite sheets, dikes, and sills; and intermediate to mafic dikes and sills are scattered throughout much of the region.

The majority of the known cinnabar (\pm stibnite)-bearing deposits and occurrences are within rocks of the Kuskokwim Group. Ore-bearing veinlets at Red Devil, DeCourcy, and Mountain Top are spatially associated with altered mafic dikes. Cady and others (1955) and Sainsbury and MacKevett (1965) emphasized that mineralized rocks are concentrated at the intersection of the dikes and bedding-plane faults. Also within the Kuskokwim Group, mineralized rocks at Fairview and Rhyolite crosscut rhyolite porphyry dikes and sills. Stibnite-bearing quartz veins, lacking cinnabar, cut a granitic stock and rhyolite dikes at Fisher Dome and Snow Gulch, respectively. At the Rainy Creek occurrence, cinnabar- and realgar-bearing quartz veinlets fill fractures in a more competent graywacke unit within interbedded graywacke and shale of the Kuskokwim Group.

Mineralized rocks are also hosted by the Gemuk and Holitna Groups. Deposits at Red Top and Cinnabar Creek are hosted in siltstone-dominant sequences of the Gemuk and localized in the more competent graywacke. Quartz veins at Kagati Lake that contain cinnabar, stibnite, and realgar (Sainsbury and MacKevett, 1965) are hosted in quartz monzonite and granodiorite that intrude Gemuk sedimentary rocks. The White Mountain deposit is the only mercury-antimony epithermal system that is known to be hosted by carbonate units of the Holitna Group. It may be significant, however, that this deposit is only a few kilometers southeast of the clastic rocks of the Kuskokwim Group. In addition, clastic rocks of unknown affinity, but perhaps belonging to the Kuskokwim Group, crop out much closer to White Mountain (Tom Bundtzen, Alaska Division of Geological and Geophysical Surveys, oral commun., 1989).

Cinnabar-bearing quartz veinlets, disseminated cinnabar grains, and cinnabar-quartz cement of brecciated wall rock were found at all deposits and occurrences shown on figure 1 except Fisher Dome. Stibnite is closely associated with the cinnabar at about two-thirds of these. At Fisher Dome, quartz-bearing fractures contain stibnite but not cinnabar. Minor pyrite, realgar, orpiment, hematite, and limonite are in a few systems. Samples of high-grade mercury-antimony ore from some of the deposits and occurrences contain as much as 6.9 ppm Au (Gray and others, this volume). Free mercury is associated with much of the cinnabar-rich ore at the Cinnabar Creek deposit.

Quartz and dolomite are the main gangue minerals in all systems. Petrographic examination of polished thin sections from a number of the deposits and occurrences indicates that vein quartz and much of the cinnabar are paragenetically coeval. Hydrothermal dickite is also common at many of the occurrences. Sainsbury and MacKevett (1965) noted that dickite formed prior to the sulfide minerals at some occurrences and subsequent to the ore minerals at other occurrences. Most likely, the dickite represents an ore-stage alteration phase. Calcite veinlets are common in a number of the occurrences but probably postdate precipitation of sulfide minerals, quartz, dolomite, and dickite.

A limited amount of fluid inclusion data has been published for quartz and cinnabar samples from the Red Devil deposit. Roedder (1963) described primary three-phase CO₂-rich fluid inclusions in quartz from Red Devil. Melting of clathrate compounds at 11.1 °C in these inclusions suggests that hydrocarbons are present in the vein-forming fluids. Roedder described evidence for fluid immiscibility and was the first to point out that these high gas contents at Red Devil are uncharacteristic of shallow epithermal systems. Measurements by Belkin (*in* Miller and others, 1989) show homogenization temperatures of 158–164 °C for fluid inclusions in cinnabar and 169–210 °C for those in cinnabar-bearing quartz. Ice-melting data suggest

Table 1. Stable isotope data for ore-related minerals from epithermal mercury-antimony deposits, southwestern Alaska

[All isotope data in standard per mil notation. Abbreviations: c, cinnabar; d, dickite; fi, fluid inclusion waters; o, orpiment; r, realgar; s, stibnite]

Deposit	Regional host unit	Host lithology	$\delta^{18}\text{O}$ (quartz)	δD	$\delta^{34}\text{S}$
Red Devil	Kuskokwim Group	Clastic rocks, mafic dike	24.4-26.4 ¹	-152(fi) ¹	-3.7(c)
			26.2-27.4 ²	-191(fi) ²	-4.2(s)
			19.1	-127(d)	
Fairview	Kuskokwim Group	Rhyolite sill	24.6		-3.4(c) -3.7(s)
DeCourcy	Kuskokwim Group	Clastic rocks, mafic dike	29.3-29.5		-4.5(c) -4.0(s)
Mountain Top	Kuskokwim Group	Clastic rocks, mafic dike			-16.5(c)
Snow Gulch	Kuskokwim Group	Rhyolite dikes, clastic rocks	24.5		-23.2(s) -25.0(s)
Fisher Dome	Kuskokwim Group	Rhyolite	14.6		-6.2(s)
Rainy Creek	Kuskokwim Group	Clastic rocks	24.6		-6.7(x)
White Mountain	Holtna Group	Carbonate rocks			+6.0(c)
Cinnabar Creek	Gemuk Group	Clastic rocks	22.8		-5.2(c)
Kagati	Gemuk Group	Granitic stock	12.6		-3.0(c)

¹For cinnabar-rich quartz.

²For stibnite-rich quartz.

that inclusions within both minerals have a salinity of about 3.7 equivalent weight percent NaCl. Trapping pressures estimated by Belkin to be between 150 and 200 bars indicate depths of vein formation of at least 500–700 m.

STABLE ISOTOPE STUDIES

In this study we measured oxygen isotope compositions of quartz, dickite, and mafic dikes; hydrogen isotope compositions of dickite and fluid inclusion waters; and sulfur isotope compositions of sulfide minerals. Standard techniques for extraction and analysis were used as described by Clayton and Mayeda (1963), Craig (1961), Fritz and others (1974), Godfrey (1962), Grinenko (1962), Savin and Epstein (1970), and Taylor and Epstein (1962). Isotope data are reported in standard δ notation relative to the Vienna SMOW standard for oxygen and hydrogen and the Canyon Diablo troilite (CDT) standard for sulfur. The standard error of each analysis is approximately $\pm 0.2\text{‰}$ for sulfur and oxygen and $\pm 1.0\text{‰}$ for hydrogen. Results from analyses are summarized in table 1.

Oxygen Isotopes

The $\delta^{18}\text{O}$ values of cinnabar- and stibnite-bearing quartz are among the highest values measured from any mineralized system in western North America. All of the quartz values are between 23‰ and 29.5‰, except for a value of 14.6‰ for stibnite-bearing quartz from Fisher Dome and a value of 12.6‰ for realgar-orpiment-bearing quartz collected from Kagati (table 1). The quartz-water fractionation equation of Clayton and others (1972)

indicates a fractionation of 11.7‰ at 200°C. Fluid inclusion homogenization temperatures for quartz at Red Devil are about 200 °C, and CO₂ density data suggest that little, if any, correction for pressure is required for estimating fluid trapping temperatures (Miller and others, 1989). Therefore, in most of these systems the ore fluids are calculated to have had $\delta^{18}\text{O}$ values of about 11–18‰.

A $\delta^{18}\text{O}$ value of 19.1‰ for dickite from Red Devil indicates a fluid composition of approximately 14‰, assuming precipitation at 200 °C and using the kaolinite-water fractionation equation of Kulla and Anderson (1978). MacKevett and Berg (1963) pointed out, however, that the dickite at Red Devil most likely postdates sulfide deposition. If the dickite formed at 150 °C, a temperature just below that of 160 °C estimated for cinnabar deposition (Miller and others, 1989), it would have done so from a fluid having a $\delta^{18}\text{O}$ composition of 11.5‰. The $\delta^{18}\text{O}$ fluid values calculated for the dickite are similar to those calculated for cinnabar-bearing quartz; thus, both silicate phases probably were precipitated from an isotopically similar fluid.

The relative uniformity of the data from all systems, excluding Fisher Dome and Kagati Lake, hosted within Gemuk and Kuskokwim sedimentary rocks, rhyolite, monzonite, and mafic dikes suggests a fluid-dominated ore system. The isotopic composition of such a fluid is independent of local host rock control (Kerrick, 1987). The data are not compatible with a fluid derived from circulation of meteoric waters. Meteoric water in the Kuskokwim region has a $\delta^{18}\text{O}$ value of about -20‰ and a shift of more than 30‰ would be required to produce the estimated ore fluid range (fig. 2). A calculated meteoric water evolution path shows that for a fluid that has an initial $\delta^{18}\text{O}$ value of -20‰ at 200 °C and is migrating through pelitic rocks,

oxygen shifts under conditions of lowest water to rock ratios will result in final values of no greater than 8‰ (fig. 2). Temperatures of at least 400–500 °C are required, under conditions of very low water to rock ratios, to produce meteoric fluids that have shifted to the heavy $\delta^{18}\text{O}$ values (11–18‰) found in these deposits.

The oxygen isotope compositions of a silica-carbonate-altered dike and a relatively unaltered mafic dike collected near the DeCourcy deposit have $\delta^{18}\text{O}$ values of 14.6‰ and 11.5‰, respectively. Using the complete version of the equation of Criss and Taylor (1986) for water to rock ratios under closed system conditions, assuming the initial fluid near DeCourcy to have a $\delta^{18}\text{O}$ value of 17.7‰, and using a quartz-water fractionation of 11.7‰ at 200 °C, calculated water to rock values are approximately 0.1. Because the relatively unaltered dike does contain minor amounts of secondary quartz and calcite (Marti Miller, U.S. Geological Survey, written commun., 1989), the measured $\delta^{18}\text{O}$ value may be greater than the true magmatic value. If that is the case, then the water to rock ratio of 0.1 must be regarded as a minimum estimate. Examination of figure 2 indicates that even for a ratio as low as 0.1, oxygen isotope shifts from meteoric water values to calculated ore fluid values are unattainable.

Ore fluid $\delta^{18}\text{O}$ values are most compatible with the metamorphic water field, although host rocks are relatively unmetamorphosed (Marti Miller, oral commun., 1989). Therefore, a fluid produced during metamorphic dehydration would have been from deeper within the

Kuskokwim basin, where burial metamorphism was ongoing or where abnormal geothermal gradients correlate with increased igneous activity. Such a scenario is the most reasonable explanation for the oxygen data. Ore fluid values are significantly heavier than normal magmatic values, which commonly are 5.5–10‰. There also is no consistent spatial association between the epithermal systems and a specific igneous rock type. Thus, if ore-forming fluids were equilibrated with a specific magma, resulting igneous rocks must be unexposed below the different epithermal lodes and would be among some of the world's most ^{18}O -enriched igneous rocks.

The $\delta^{18}\text{O}$ values of 14.6‰ for stibnite-bearing quartz from Fisher Dome and 12.6‰ for realgar-orpiment-bearing quartz from Kagati Lake are distinctly different from those of the other vein systems. These values are more compatible with values from mesothermal gold-bearing vein systems (Kerrick, 1987) than with those of the other vein systems throughout the Kuskokwim region. The relatively light value for the Fisher Dome quartz could still reflect a fluid derived from a source similar in origin to the other sulfide-bearing veins in the Kuskokwim region. Vein formation at temperatures higher than those of the cinnabar-bearing epithermal vein systems would reduce $\Delta^{18}\text{O}_{\text{quartz-water}}$ and precipitate isotopically lighter quartz. Relatively high homogenization temperatures of fluid inclusions in Kagati Lake quartz, between 280 and 355 °C, and the fact that sulfide minerals were only found coating fractures in massive quartz suggest that sulfide mineralization is

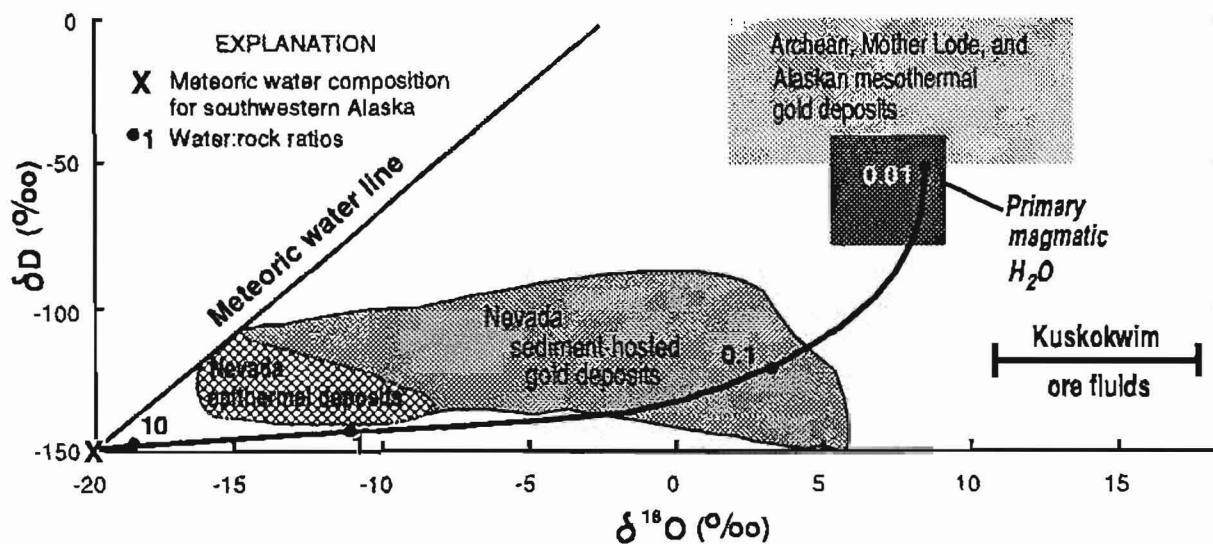


Figure 2. Plot of δD versus $\delta^{18}\text{O}$ for ore fluids from the Kuskokwim region and for other studied hydrothermal systems. A calculated fluid evolution path shows that a meteoric fluid, in southwestern Alaska, assumed to be at 200 °C and having an initial $\delta^{18}\text{O}$ composition of -20‰, cannot be shifted to values of more than about +8‰ even if water to rock ratios are as low as 0.01. (Calculations assume $\delta^{18}\text{O}_{\text{H}_2\text{O}} = 16\text{‰}$ and $\delta\text{D}_{\text{H}_2\text{O}} = -60\text{‰}$ and use plagioclase feldspar-H₂O and chlorite-H₂O fractionation factors for oxygen and hydrogen $\Delta_{\text{R-W}}$, respectively.) A crustal source is thus required for the ore fluids. The heavy oxygen and light hydrogen data for the Kuskokwim deposits are most compatible with fluid derivation from organic-rich sedimentary rocks containing an abundance of detrital chert grains.

younger than quartz deposition and that the quartz analyzed at Kagati Lake may be unrelated to mineralization. It is uncertain whether the sulfide minerals at Kagati Lake formed from different, perhaps magmatic, fluids or whether they precipitated from later circulating fluids similar to those that deposited the epithermal mineralization elsewhere in southwestern Alaska.

The ore-bearing quartz at the Red Devil deposit exhibits a vertical zonation in metal content: cinnabar-rich ore is nearest the surface and stibnite-rich ore is at a depth of 180 m (Miller and others, 1989). Our isotope data suggest that a simple decreasing temperature gradient was not the cause for the shift from an antimony-dominant zone to a shallower mercury-dominant zone at Red Devil. Compositions of $\delta^{18}\text{O}$ of 24.4–26.4‰ were determined for cinnabar-rich quartz and 26.6–27.4‰ for stibnite-rich quartz. Because the fractionation between quartz and water is inversely correlated with temperature, silica deposition simply by declining temperature would have resulted in isotopically heavier quartz hosting the mercury-rich ore nearer the surface.

Boiling or fluid immiscibility is a more plausible explanation for the observed zoning pattern at Red Devil. Roedder (1963) reported evidence from fluid inclusion studies for the occurrence of such immiscibility in cinnabar-bearing quartz from Red Devil. It is, therefore, reasonable to hypothesize that mercury separated from the antimony within the ore fluids and was transported to higher levels within the vapor phase. Due to differences in vapor pressures for the different isotopes, any H_2O within the vapor phase must be enriched in ^{16}O . This is in agreement with the relatively ^{18}O depleted, cinnabar-bearing quartz at the top of the system.

Hydrogen Isotopes

Hydrogen isotope data from dickite at the Red Devil deposit suggest the presence of organic water in the ore fluids. Dickite is closely associated with the ore minerals at Red Devil and has a δD value of -127‰ . The most recent H/D fractionation relationships for hydrous minerals and water (Kyser, 1987, p. 51) indicate no fractionation between dickite and water at 200 °C. At 160 °C, the approximate homogenization temperature of fluid inclusions in Red Devil cinnabar (Miller and others, 1989), fractionation data show that the clay would have formed from a fluid having a δD value of -120‰ . The dickite-forming fluid was, therefore, unquestionably isotopically much lighter than typical magmatic or metamorphic waters. Hydrogen isotope composition contours in Taylor (1979) suggest that meteoric surface waters should have δD values of about -150‰ across much of the Kuskokwim region, a composition 30‰ lighter than that of the calculated dickite-forming fluid. Because the previously described oxygen isotope data preclude the predominance of meteoric waters

within the ore fluids, the δD value is best interpreted as representative of a fluid having a strong organic water component. Such a deuterium-depleted water, as described by Sheppard (1986), is a likely product from dehydration of or exchange with organic material in rocks of the Kuskokwim Group.

Fluid inclusion waters extracted from cinnabar- and stibnite-bearing quartz collected at Red Devil are isotopically much lighter than the dickite-forming water. They have δD values of -152‰ and -191‰ , respectively, as compared with the -120‰ value estimated for the dickite. Inclusion waters from the cinnabar-hosted quartz are assumed to be dominantly meteoric in origin. The reason for the extremely negative value of the inclusion water from stibnite-bearing quartz is uncertain. If any fractionation of hydrogen isotopes had occurred during the previously described boiling at Red Devil, then the mercury-transporting vapor would contain the more reduced gases and the lighter hydrogen. In contrast to what was actually observed, heavier deuterium, if fractionated, would have remained behind in the antimony-bearing liquid. The assumption that the fluid inclusion waters accurately show ore fluid δD compositions is at best tenuous. Extracted fluid inclusion waters are likely to combine crustal fluids trapped in many different generations and may result in isotopic values that substantially differ from the true ore stage values (Pickthorn and others, 1987).

Sulfur Isotopes

The sulfur isotope compositions of sulfide mineral phases are extremely consistent for most epithermal systems from southwestern Alaska. Cinnabar, stibnite, realgar, and orpiment $\delta^{34}\text{S}$ values generally cluster between -3‰ and -7‰ (table 1), suggestive of a similar sulfur source for most deposits and occurrences. This source is likely to be either disseminated pyrite and (or) organic material throughout pelitic sedimentary rocks of the Kuskokwim region. Using known cinnabar- H_2S and stibnite- H_2S fractionation relationships (Field and Fifarek, 1985) and assuming sulfide precipitation at 200 °C, the $\delta^{34}\text{S}$ composition of the ore fluids was about 0‰ to -3‰ . This estimate assumes that reduced sulfur is equivalent to total sulfur within the ore fluids. This assumption may not be true for all deposits, however, because hematite probably was coeval with the sulfide minerals in some systems (Sainsbury and MacKevett, 1965), indicative of the presence of oxidized sulfur species.

Sulfur data from three of the deposits are noticeably anomalous. The $\delta^{34}\text{S}$ composition of ore fluids at White Mountain may originally have been equivalent to those from the other epithermal systems, but sulfur ratios likely shifted during changing physiochemical conditions. Cinnabar at the carbonate-hosted White Mountain deposit has a $\delta^{34}\text{S}$ value of $+6.0\text{‰}$. The presence of ore-related

dickite at White Mountain, as well as at many of the other deposits, suggests that the ore fluids were acidic and pH values were no greater than about 4.0. The interaction between such fluids, perhaps originating in nearby units of the Kuskokwim Group, and carbonate rocks of the Holitna Group would rapidly shift fluid pH to more alkaline values. As pointed out by Ohmoto (1972), the dissociation of H_2 and sulfur that accompanies the increase in pH would cause an increase in $\delta^{34}S$ of the sulfide minerals relative to the total sulfur in the system. It is, therefore, not surprising that the only deposit where Sainsbury and MacKevett (1965) described cinnabar replacing dickite was at White Mountain. The dickite was deposited from an originally acidic solution, and the isotopically heavy cinnabar could have been deposited following a subsequent shift in fluid pH.

Extremely light $\delta^{34}S$ values characterize cinnabar from the Mountain Top and stibnite from the Snow Gulch deposits. Such light values are commonly produced by fluid interaction with relatively oxidizing country rocks. Such interaction increases SO_4/H_2S ratios and the ^{32}S concentration of subsequently precipitated sulfide minerals because the lighter isotope preferentially is concentrated in the reduced sulfur species. But, both Mountain Top and Snow Gulch probably are within areas of rocks typical of the Kuskokwim Group, although rhyolite dikes hosting part of the latter occurrence are exceptionally silica rich (Cady and others, 1955). Mountain Top, however, is the one epithermal system within the Kuskokwim region known to contain both liquid and solid hydrocarbons (Sorg and Estlund, 1972). The sulfur at Mountain Top may therefore have been derived from a more local source, perhaps a relatively light petroleum reservoir, than the other Kuskokwim deposits. The $\delta^{34}S$ value of -23.2‰ for stibnite at Snow Gulch is much lighter than expected for sulfur contributed directly from a specific organic reservoir. The lack of cinnabar at Snow Gulch could indicate a preferential loss of mercury and H_2S during boiling off of a vapor phase. Such oxidation of the ore fluids is the most likely scenario for producing such ^{32}S -enriched stibnite.

Both cinnabar and stibnite grains from the Red Devil, Fairview, and DeCourcey deposits were analyzed for $\delta^{34}S$. Previously described fluid inclusion evidence from Roedder (1963) shows that boiling took place during ore deposition at Red Devil, and our sulfur data are in agreement with such a process. Oxidation of the liquid by loss of H_2 and H_2S from the ore fluid into the vapor phase during boiling would cause a ^{34}S depletion in any sulfide phases precipitated directly from the liquid. Therefore, the stibnite at Red Devil has a $\delta^{34}S$ value of -4.2‰ , whereas the cinnabar, mostly deposited from the vapor, has a value of -3.7‰ . A similar situation is possible for the Fairview deposit (table 1). At Decourcy, isotopically lighter cinnabar could be interpreted to indicate a simple temperature decrease rather than boiling as the dominant depositional mechanism. Precipitation of

stibnite at relatively higher temperatures would oxidize the ore fluids and precipitate isotopically lighter sulfur in subsequent cinnabar. Cady and others (1955) pointed out that much of the cinnabar within these epithermal systems was deposited subsequent to the stibnite.

STABLE ISOTOPE IMPLICATIONS FOR ORE GENESIS

The oxygen isotope data indicate that ore-forming fluids in the Kuskokwim region were different in origin from most other hydrothermal fluids responsible for Cenozoic epithermal mineralization in western North America. Although oxygen isotopic values of meteoric waters from the Basin and Range are similar to those of the Kuskokwim region, epithermal vein-forming fluids in the Kuskokwim are significantly enriched in ^{18}O (fig. 2). Volcanic-hosted epithermal deposits within the Basin and Range formed from fluids having $\delta^{18}O$ compositions between -15‰ and -6‰ , and sedimentary-hosted gold deposits formed from fluids having compositions between -16‰ and $+6\text{‰}$ (Field and Fifarek, 1985). These results have been interpreted by most workers as suggestive of vein formation from meteoric fluids under conditions of varied water to rock ratios. It is hard to envision how, if a similar ore-forming process occurred within the Kuskokwim region, all the ore fluids would be shifted by more than 30‰ from the meteoric water line. Rather, oxygen compositions should show a wide distribution of $\delta^{18}O$ compositions between about -20‰ and $+20\text{‰}$.

Heavy oxygen data for the mercury- and antimony-bearing quartz from southwestern Alaska are more like those described for mesothermal gold-bearing systems from the western Cordillera (Kerrich, 1989). The $\delta^{18}O$ values for vein-forming fluids for many of these deposits are similar to those from the Kuskokwim (fig. 2). The higher temperature of vein formation for the Cordilleran fluids is reflected in the lighter ratios of the precipitated quartz. Nesbitt and others (1987) showed that for the Canadian Cordillera the cooling of an ore fluid having a $\delta^{18}O$ value of $8\text{--}10\text{‰}$ could have precipitated gold-bearing quartz (17.5‰), then stibnite-bearing quartz (21‰), and lastly cinnabar-bearing quartz (29‰).

Calculated $\delta^{18}O$ values of $11\text{--}18\text{‰}$ for ore-forming fluids within the Kuskokwim region are only compatible with a fluid derived from dehydration of the sedimentary rocks. The ore fluids are slightly more enriched in ^{18}O than most other vein-forming fluids also believed to have been produced during sediment devolatilization (Kerrich, 1989); however, the abundance of chert fragments and lesser limestone fragments in Kuskokwim graywacke (Cady and others, 1955) and the clays within Kuskokwim shale favor such an ^{18}O -enriched fluid.

The origin of the δD composition of -120‰ , believed to be that of the dickite-forming fluid at Red Devil,

remains uncertain. The ratio is heavier than local meteoric water by about 30‰, yet it is also much lighter than that expected for a fluid of metamorphic origin. Fluid mixing between an isotopically lighter meteoric fluid and a heavier metamorphic fluid is one possibility for the dickite value; however, the consistently heavy oxygen data for all the Kuskokwim region systems do not support the fluid mixing hypothesis. Another possibility is that extensive post-ore, low-temperature hydrogen exchange occurred between the hydrothermal dickite and near-surface meteoric waters. Although there are differing opinions, some experimental data suggest that such hydrogen isotopic exchanges occurred without any accompanying shifts in the $\delta^{18}\text{O}$ composition of clay minerals (Longstaffe, 1989). The most likely explanation for the light value at Red Devil is that it reflects a strong hydrogen contribution to the ore fluids from the breakdown of organic material within the sedimentary rocks. Sheppard (1986) pointed out that such organic waters can be strongly depleted in deuterium relative to more typical metamorphic fluids.

The uniform sulfur composition of the epithermal deposits in such a large region (except at Mountain Top and Snow Gulch) suggests a common sedimentary rock source such as sulfur-bearing organic material within the shaley units of the Kuskokwim Group. Cady and others (1955) indicated that approximately one-third of the strata are very dark shales that contain relatively large concentrations of carbonaceous material. They described thin coaly seams and abundant plant remains within outcrops of the Kuskokwim Group at the mouth of the Holitna River, near Red Devil. Significant amounts of H_2S will be generated during late diagenesis of this organic material as burial temperatures approach 200 °C (Frey, 1987).

Occurrences at Rainy Creek and Kagati Lake both are within an area mostly underlain by the Gemuk Group, a sequence of rocks dominated by black siltstone. Sulfur derived from these rocks could have been added into the ore-forming fluids; however, sulfur values for orpiment at Kagati Lake and cinnabar at Cinnabar Creek are identical to those for most of the deposits hosted by rocks of the Kuskokwim Group. These two systems within the Gemuk Group are within a few kilometers of rocks of the Kuskokwim Group, and sulfur contributions from the latter cannot be ruled out. Also, as described above, the White Mountain deposit in the carbonate rocks of the Holitna Group is fairly close to outcrops of Kuskokwim clastic rocks. Therefore, we believe that organic material within the Kuskokwim Group, and perhaps within the Gemuk Group, was the source for the sulfur in all of the epithermal deposits and occurrences.

ORIGIN OF THE KUSKOKWIM DEPOSITS

Hot fluids were generated within the Kuskokwim basin during both diagenesis and subsequent burial meta-

morphism. The connate waters expelled from pore spaces during sediment compaction were unrelated to the epithermal mineralization. Such fluids would have had $\delta^{18}\text{O}$ values much closer to meteoric values than those observed for the epithermal systems. In addition, such fluids would have been relatively saline; fluid inclusion data from the Red Devil deposit suggest salinities of only about 3.7 weight percent NaCl equivalent (Miller and others, 1989). Very low grade metamorphic reactions, releasing H_2O -rich fluids, began at approximately 150–200 °C during burial metamorphism (Frey, 1987). Under a typical geothermal gradient of 30 °C/km, temperatures were in excess of 350 °C in the deeper parts of the Kuskokwim basin, where sediment thickness was probably greater than 12 km (Decker and others, written commun., 1989).

Much of the ore fluid responsible for the mineralized veins was derived from mineral dehydration reactions during very low grade metamorphism of rocks of the Kuskokwim Group; the sulfur and some of the hydrogen were derived from organic material, and mercury and antimony were likely mobilized from organic material and clays within shaley beds. If a 30 °C/km geothermal gradient is accurate for the Kuskokwim basin, very low grade metamorphism would have produced the ore-forming fluids at depths of about 5–6 km. Alternatively, the ore fluids could have been derived at shallower levels if anomalously high heat flow raised the normal gradient. Therefore, although ore fluids were derived by devolatilization at temperatures in excess of 200 °C, the epithermal systems still might show a spatial association with a specific igneous rock suite at depth.

The epigenetic mercury-antimony-bearing lodes in southwestern Alaska are most similar to a group of mineral deposits that have been termed hot-spring mercury, silica-carbonate mercury, and simple antimony deposits (Bliss and Orris, 1986; Rytuba, 1986a, b). These deposits commonly are within unmetamorphosed to very low grade metamorphic rocks in basins adjacent to areas of active orogenic activity. Like many of the mesothermal vein systems in adjacent orogenic belts, these epithermal systems exhibit strong carbonate alteration and formed from fluids enriched in ^{18}O relative to local meteoric water.

Three-phase, CO_2 -rich fluid inclusions and readily observable clathrate formation indicated to Roedder (1963) that the Red Devil deposit was atypical of many well-studied epithermal vein systems. The relatively high gas content for some of the fluid inclusions studied by Roedder are more suggestive of ore-fluid compositions commonly reported for mesothermal gold vein deposits. White and others (1973) have long suggested that many of the springs discharging within the relatively unmetamorphosed rocks along the western edge of North America represent the surface expression of the mercury-antimony ore-forming fluids. The anomalous CO_2 and H_2S within the springs, their

common spatial association with mercury deposits, and their heavy oxygen and hydrogen ratios led White and co-workers to suggest a metamorphic source for the spring waters.

REFERENCES CITED

- Bliss, J.D., and Orris, G.J., 1986, Descriptive model of simple Sb deposits, in Cox, D.P., and Singer, D.A., eds., Mineral deposit models: U.S. Geological Survey Bulletin 1693, p. 183-184.
- Cady, W.M., Wallace, R.E., Hoare, J.M., and Webber, E.J., 1955, The central Kuskokwim region, Alaska: U.S. Geological Survey Professional Paper 268, 132 p.
- Clayton, R.N., and Mayeda, T.K., 1963, The use of bromine pentafluoride in the extraction of oxygen from oxides and silicates for isotopic analyses: *Geochimica et Cosmochimica Acta*, v. 27, p. 43-52.
- Clayton, R.N., O'Neil, J.R., and Mayeda, T.K., 1972, Oxygen isotope exchange between quartz and water: *Journal of Geophysical Research*, v. 77, p. 3057-3067.
- Craig, Harmon, 1961, Isotopic variations in meteoric waters: *Science*, v. 133, p. 1702.
- Criss, R.E., and Taylor, H.P., Jr., 1986, Meteoric-hydrothermal systems, in Valley, J.W., Taylor, H.P., Jr., and O'Neil, J.R., eds., Stable isotopes in high temperature geological processes: *Mineralogical Society of America Reviews in Mineralogy*, v. 16, p. 373-424.
- Field, C.W., and Fifierek, R.H., 1985, Light stable-isotope systematics in the epithermal environment, in Berger, B.R., and Bethke, P.M., eds., *Geology and geochemistry of epithermal systems: Society of Economic Geologists, Reviews in Economic Geology*, v. 2, p. 99-128.
- Frey, M., 1987, Low temperature metamorphism: Glasgow and London, Blackie, 350 p.
- Fritz, P., Dřimánie, R.J., and Nowicki, V.K., 1974, Preparation of sulfur dioxide for mass spectrometer analyses by combustion of sulfides with copper oxide: *Analytical Chemistry*, v. 46, p. 164-166.
- Godfrey, J.D., 1962, The deuterium content of hydrous minerals from the east-central Sierra Nevada and Yosemite National Park: *Geochimica et Cosmochimica Acta*, v. 26, p. 1215-1245.
- Grinenko, V.A., 1962, Preparation of sulfur dioxide for isotope analysis: *Zeits. Neorgan. Khimii.*, v. 7, p. 2478-2483.
- Kerrick, R., 1987, The stable isotope geochemistry of Au-Ag vein deposits in metamorphic rocks, in Kyser, T.K., ed., Stable isotope geochemistry of low temperature fluids: *Mineralogical Association of Canada Short Course Handbook*, v. 13, p. 287-336.
- _____, 1989, Geochemical evidence on the source of fluids and solutes for shear zone hosted mesothermal Au deposits, in Bursnell, J.T., ed., *Mineralization and shear zones: Geological Association of Canada Short Course Notes*, v. 6, p. 129-197.
- Kulla, J.B., and Anderson, T.F., 1978, Experimental oxygen isotope fractionation between kaolinite and water, in Zartman, R.E., ed., *Short papers of the Fourth International Conference, Geochronology, Cosmochronology, Isotope Geology 1978: U.S. Geological Survey Open-File Report 78-701*, p. 234-235.
- Kyser, T.K., 1987, Equilibrium fractionation factors for stable isotopes, in Kyser, T.K., ed., *Stable isotope geochemistry of low temperature fluids: Mineralogical Association of Canada Short Course Handbook*, v. 13, p. 1-84.
- Longstaffe, F.J., 1989, Stable isotopes as tracers in clastic diagenesis, in Hutcheon, I.E., ed., *Short course in burial diagenesis: Mineralogical Association of Canada Short Course*, v. 15, p. 201-277.
- MacKevett, E.M., Jr., and Berg, H.C., 1963, Geology of the Red Devil quicksilver mine, Alaska: U.S. Geological Survey Bulletin 1142-G, p. G1-G16.
- Müller, M.L., Belkin, H.E., Blodgett, R.B., Bundtzen, T.K., Cady, J.W., Goldfarb, R.J., Gray, J.E., McGimsey, R.G., and Simpson, S.L., 1989, Pre-field study and mineral resource assessment of the Sleetmute quadrangle, southwestern Alaska: U.S. Geological Survey Open-File Report 89-363, 115 p.
- Nesbitt, B.E., Muehlenbachs, K., and Murowchick, J.B., 1987, Genesis of Au, Sb, and Hg deposits in accreted terranes of the Canadian Cordillera: *Geological Association of Canada, Programs with Abstracts*, v. 12, p. 76.
- Ohmoto, H., 1972, Systematics of sulfur and carbon isotopes in hydrothermal ore deposits: *Economic Geology*, v. 67, p. 551-579.
- Pickthorn, W.J., Goldfarb, R.J., and Leach, D.L., 1987, Comment on "Dual origins of lode gold deposits in the Canadian Cordillera": *Geology*, v. 15, no. 5, p. 471-472.
- Roedder, Edwin, 1963, Studies of fluid inclusions II—Freezing data and their interpretation: *Economic Geology*, v. 58, p. 167-211.
- Rytuba, J.J., 1986a, Descriptive model of hot spring Hg, in Cox, D.P., and Singer, D.A., eds., *Mineral deposit models: U.S. Geological Survey Bulletin 1693*, p. 178.
- _____, 1986b, Descriptive model of silica-carbonate Hg, in Cox, D.P., and Singer, D.A., eds., *Mineral deposit models: U.S. Geological Survey Bulletin 1693*, p. 181.
- Sainsbury, C.L., and MacKevett, E.M., Jr., 1965, Quicksilver deposits of southwestern Alaska: U.S. Geological Survey Bulletin 1187, 89 p.
- Savin, S.M., and Epstein, S., 1970, The oxygen and hydrogen isotope geochemistry of clay minerals: *Geochimica et Cosmochimica Acta*, v. 34, p. 25-42.
- Sheppard, S.M.F., 1986, Characterization and isotopic variations in natural waters, in Valley, J.W., Taylor, H.P., Jr., and O'Neil, J.R., eds., *Stable isotopes in high temperature geological processes: Mineralogical Society of America, Reviews in Mineralogy*, v. 16, p. 165-183.
- Sorg, D.H., and Estlund, M.B., 1972, Geologic map of the Mountain Top mercury deposit, southwestern Alaska: U.S. Geological Survey Miscellaneous Field Studies Map MF-449, scale 1:600.
- Taylor, H.P., Jr., 1979, Oxygen and hydrogen isotope relationships in hydrothermal mineral deposits, in Barnes, H.L., ed., *Geochemistry of hydrothermal ore deposits (2nd ed.)*: New York, John Wiley and Sons, p. 236-277.

Taylor, H.P., Jr., and Epstein, S., 1962, Relation between O^{18}/O^{16} ratios in coexisting minerals of igneous and metamorphic rocks—I. Principles and experimental results: Bulletin of the Geological Society of America, v. 73, p. 461–480.

White, D.E., Barnes, Ivan, and O'Neil, J.R., 1973, Thermal and mineral waters of non-meteoritic origin, California Coast Ranges: Geological Society of America Bulletin, v. 84, p. 547–560.

Chapter F

Gold Anomalies and Newly Identified Gold Occurrences in the Lime Hills Quadrangle, Alaska, and Their Association with the Hartman Sequence Plutons

By MICHAEL S. ALLEN

U.S. GEOLOGICAL SURVEY BULLETIN 1950

GEOCHEMICAL STUDIES IN ALASKA BY THE U.S. GEOLOGICAL SURVEY, 1989

CONTENTS

Abstract	F1
Introduction	F1
General geology	F2
Methods of study	F2
Drainage-sediment gold anomalies	F4
Fish Creek area	F5
Terra Cotta Mountains	F5
South Fork Kuskokwim River region	F5
Tired Pup pluton region	F9
Styx River region	F9
Identified lode gold occurrences	F9
Three Cub occurrence	F9
Terra Cotta Mountains	F12
Upper Swift River area	F12
Summary and discussion	F12
References cited	F15

FIGURES

1-7. Maps showing:

1. Location of study area and the Lime Hills quadrangle, Alaska F1
2. Geology of the eastern part of the Lime Hills quadrangle F4
3. Geochemical anomalies for gold in -80-mesh sediment samples, Lime Hills quadrangle F6
4. Geochemical anomalies for gold in nonmagnetic heavy-mineral concentrate samples, Lime Hills quadrangle F7
5. Mineralogically determined anomalies for gold in nonmagnetic heavy-mineral concentrate samples, Lime Hills quadrangle F8
6. Geology and localities of geochemical samples containing anomalous amounts of gold, Three Cub occurrence F10
7. Geology and localities of geochemical samples containing anomalous amounts of gold, Terra Cotta Mountains F14

TABLES

1. Whole-rock analyses of rock samples from the Hartman sequence, Lime Hills quadrangle, Alaska F3
2. Geochemical data for rock samples having anomalous metal contents from the Three Cub occurrence, Terra Cotta Mountains, and upper Swift River area, Lime Hills quadrangle, Alaska F11
3. Geochemical data for rock samples from the Kahiltna terrane, Lime Hills quadrangle, Alaska F13

Gold Anomalies and Newly Identified Gold Occurrences in the Lime Hills Quadrangle, Alaska, and Their Association with the Hartman Sequence Plutons

By Michael Steven Allen

Abstract

A drainage-sediment geochemical survey in the eastern part of the Lime Hills quadrangle has identified numerous areas containing anomalous gold concentrations. Heavy-mineral concentrates of drainage sediment from the Hartman River region also are anomalous in Ag, As, B, Ba, Bi, Co, Ni, Sb, and W. Most drainage basins containing anomalous samples are underlain by sedimentary rocks of the Kahiltna terrane and intrusive igneous rocks. The most significant geochemical anomalies for gold are associated with gabbroic to granodioritic plutons of the Hartman sequence, some of which are alkalic.

Lode sources for drainage-sediment gold anomalies were identified near the Hartman plutons, both southeast of Fish Creek and in the Terra Cotta Mountains. Rock samples from outcrop, moraine, and talus collected within and around Hartman plutons contain significant concentrations of gold (as much as 26 ppm). The highest gold values are in pyrite- and arsenopyrite-bearing quartz-carbonate veins that cut Kahiltna rocks adjacent to plutons. Alteration generally comprises thin selvages of silica and carbonate±sericite±chlorite±barite. Veins are generally less than 15 cm wide. In addition to gold, anomalous concentrations of As, Sb, and Cu and less consistently Ag, Pb, and Zn characterize vein samples. Locally, unveined Kahiltna strata contain as much as 50 percent disseminated and stratiform pyrite. Sulfide-bearing strata are enriched in Ag, Ba, Co, Cr, Cu, Fe, V, Sb, and Zn. Carbonaceous graywacke with disseminated pyrite contains 3.5 ppm Au. Samples of Hartman igneous rocks cut by thin aplite dikes and quartz veins also have anomalous gold contents (0.2–1.3 ppm). The rocks of the Kahiltna terrane and the Hartman sequence are considered both potential hosts and possible source rocks for gold occurrences.

INTRODUCTION

During the summers of 1987 and 1988, a geochemical survey was conducted in the eastern part of Lime Hills quadrangle, Alaska (fig. 1), as part of the Alaska Mineral Resource Appraisal Program (AMRAP). This geochemical survey covers an area of approximately 10,000 km² that includes part of the Alaska Range.

Previous work in the region includes reconnaissance geologic mapping, aeromagnetic, and stream-sediment geochemical surveys in the southern Alaska Range undertaken

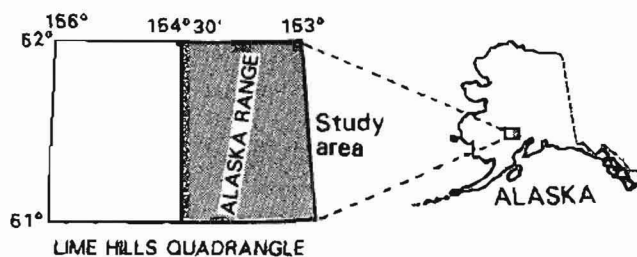


Figure 1. Location of study area (shaded) and the Lime Hills quadrangle, Alaska.

by the U.S. Geological Survey in the late 1960's (Reed and Elliott, 1970). Geologic maps, geochronology, and geochemical data on the Alaska–Aleutian Range batholith have been published by Reed and Lanphere (1969, 1972, 1973) and Lanphere and Reed (1985). Additional geochemical and geophysical surveys in the region were carried out as part of the National Uranium Resource Evaluation (NURE) program (Jacobsen and others, 1979; Hinderman, 1982). The present study was undertaken because of the limitations of sampling density, sample type, analytical methods, and numbers of elements determined for the previous geochemical surveys (Gamble and others, 1988).

This report shows the distribution of drainage basins containing anomalous gold contents and describes the geologic and geochemical character of newly identified bedrock gold sources. Anomalous concentrations of other metals, including Ag, Ba, Bi, Cu, Mo, Pb, Sn, Th, U, W, Zn, and rare-earth elements (REE), occur in many samples collected from the study area and indicate potential for the discovery of other mineral occurrences. Geochemical results are presented by Allen and others (1990), Allen and Slaughter (1990), Malcolm and others (1990), and Motooka and others (1990). Only data having implications for gold resources are discussed here.

Acknowledgments.—I acknowledge the following people for their assistance in this study: Elizabeth Bailey, Barrett Cieutat, Tracy Delaney, Karen Duttweiler, Richard

Goldfarb, John Gray, Alfred Hofstra, Gregory Lee, Elizabeth Leibold, Molly Malcolm, Jerry Motooka, Scott Rose, Karen Slaughter, and Steven Smith.

GENERAL GEOLOGY

The major geologic units in the study area include rocks of the Dillinger and Kahiltna lithotectonic terranes (Jones and others, 1984) and the Alaska Range batholith (fig. 2).

Rocks of the Dillinger terrane, exposed in the northwestern part of the study area, consist of Cambrian through Devonian graptolitic shale, basinal carbonate rocks, calcareous sandstone, and minor chert and conglomerate. These rocks comprise a shallowing-upward sequence deposited in basinal, turbidite-fan, and foreslope environments (Churkin, 1984; Bundtzen and others, 1987). The rocks of this terrane were isoclinally folded prior to the Jurassic (Reed and Nelson, 1980).

The Kahiltna terrane is an Upper Jurassic to Lower Cretaceous flysch sequence that consists of graywacke, phyllite, and shale and lesser conglomerate, limestone, radiolarian chert, ferruginous sandstone, and tuff. The present study indicates that some carbonaceous graywacke and graphitic schist within the Kahiltna terrane contain as much as 50 percent disseminated and stratiform pyrite. The rocks of this terrane were deformed and isoclinally folded after the Cenomanian (Lanphere and Reed, 1985).

The Alaska Range batholith includes rocks formed during three intervals of igneous activity (Reed and Lanphere, 1973): Middle to Late Jurassic, Late Cretaceous to early Tertiary, and middle Tertiary. Jurassic plutonic rocks have not been identified in the Lime Hills quadrangle.

Late Cretaceous to early Tertiary intrusive rocks consist of an older suite of gabbro to quartz monzonite plutons, which includes the Hartman and Crystal Creek sequences and the Mount Estelle pluton, and a younger suite of quartz monzonite to granite plutons, which includes the Merrill Pass and Tired Pup plutons (Reed and Lanphere, 1973). Results presented in this study indicate that some rocks of the older intrusive suite, particularly the Hartman sequence, are alkalic (table 1), ranging in composition from monzogabbro to syenite, and display foliation. The alkalic pyroxenite listed in table 1 is an oddity; it is present in outcrop with borderline subalkalic/alkalic gabbro along convoluted gradational contacts, a relationship suggestive of magma segregation or mixing.

Middle Tertiary igneous rocks include quartz monzonite to granite intrusions, such as the Windy Fork pluton. Intermediate to felsic volcanic rocks, including flows, breccias, and tuffs, in the quadrangle are of uncertain Tertiary age. Megabreccias and breccia dikes suggest the

presence of caldera structures near Snowcap Mountain (Gamble and others, 1988) and south of the divide separating the Styx and Chilligan Rivers (M.S. Allen, unpub. data).

There are no active mines or identified mineral resources in the Lime Hills quadrangle. Data for 67 mineral occurrences were compiled by Gamble and others (1988). Reed and Elliott (1970) identified several sites in the quadrangle at which float and outcrop samples contain detectable gold, including one site (H-10, fig. 6) northwest of the Hartman River. Results of the present study define areally extensive drainage-basin gold anomalies northwest of the Hartman River that are coincident with outcrops of Hartman plutons. Previously unreported gold-bearing veins are described in this region and near the headwaters of the Swift River.

METHODS OF STUDY

Drainage-sediment geochemical surveys are a rapid means to identify drainage basins that contain significant upstream mineralized bedrock, but the effectiveness of these surveys is dependent on many factors including the use of sample media appropriate for the dominant geochemical dispersion processes. In this part of Alaska, which is characterized by pronounced drainage development, steep drainage profiles, and active glaciation, mechanical dispersion is believed to be the dominant mechanism for transportation of eroded metals. Due to the resistate nature and high density of many ore minerals, especially gold, heavy-mineral fractions of drainage sediment are enriched in ore metals relative to bulk sediment. Therefore, this reconnaissance survey utilized both -80-mesh (<177 μ m) and heavy-mineral concentrate fractions of drainage sediment.

Both sample types were collected from approximately 920 sites. Samples were taken from active stream sediment where possible, but moraine and inactive alluvium were collected at some localities. The -80-mesh drainage-sediment samples were analyzed by a variety of methods for 36 elements (Motooka and others, 1990). Heavy-mineral concentrates were processed through heavy-liquid and magnetic separations to obtain a nonmagnetic heavy-mineral fraction for mineralogical and chemical analysis. Mineralogical analyses using stereoscopic microscopy, oil-immersion petrography, and X-ray diffraction were performed before chemical analyses (Allen and Slaughter, 1990). Heavy-mineral concentrates were analyzed for 38 elements by emission spectrography (Malcolm and others, 1990). Approximately 400 rock samples were also collected and analyzed for 36 elements (Allen and others, 1990).

Table 1. Whole-rock analyses of rock samples from the Hartman sequence, Lime Hills quadrangle, Alaska

[Samples are listed based on location from north to south in the plutonic belt. Latitude and longitude are in degrees, minutes, and seconds, north and west, respectively. Analytical values are in weight percent]

Sample	Rock type ¹	Affinity ²	Latitude	Longitude	SiO ₂	Al ₂ O ₃	Fe ₂ O ₃ ³	MgO	CaO	Na ₂ O	K ₂ O	TiO ₂	P ₂ O ₅	MnO	LOI ⁴
808R.....	Diorite	S61 56 14	153 30 20	56.8	17.1	8.23	2.99	5.58	2.93	2.75	1.52	0.40	0.18	1.06
869R.....	Granodiorite	S61 53 38	153 28 49	65.1	14.8	4.30	3.01	3.90	3.03	3.39	0.56	0.17	0.06	0.94
871R.....	Diorite	S61 50 36	153 24 14	58.1	16.4	6.91	3.95	6.69	3.24	1.59	0.90	0.24	0.11	1.56
821RA.....	Tonalite	S61 46 27	153 37 39	64.1	14.9	4.88	2.83	4.26	2.76	3.70	0.66	0.20	0.08	0.82
815RA.....	Granodiorite	S61 45 08	153 41 17	68.6	13.9	3.50	0.49	1.83	3.06	4.78	0.36	0.17	0.05	2.40
817RE.....	Tonalite	S61 45 06	153 40 31	63.7	14.7	4.58	3.47	4.48	3.08	3.22	0.60	0.14	0.07	1.28
867RA.....	Pyroxenite	A61 39 05	153 43 54	40.2	15.4	16.9	6.74	11.9	2.47	0.23	4.12	2.27	0.22	<.10
867RB.....	Gabbro	SA61 39 05	153 43 54	52.2	16.9	12.7	2.47	7.67	3.97	1.14	2.17	0.82	0.26	<.10
866RA.....	Syenite	A61 38 56	153 39 12	60.8	16.3	3.38	0.68	3.88	5.16	5.45	0.41	0.11	0.10	0.15
866RB.....	Monzogabbro	A61 38 56	153 39 12	52.9	19.1	7.85	2.18	8.64	4.00	3.14	0.74	0.43	0.21	0.75
865R.....	Monzonite	A61 31 12	153 41 36	60.5	16.3	6.00	1.72	3.82	3.47	5.94	0.68	0.34	0.12	0.53
872R.....	Monzodiorite	A61 34 17	153 20 45	57.5	15.8	6.60	4.47	4.82	3.04	4.86	0.87	0.45	0.11	0.69

¹Based on the chemical classification for plutonic rocks of De LaRoche and others (1980).

²Based on the total alkali versus silica discrimination of Irvine and Baragar (1971); S, subalkalic; A, alkalic, SA, borderline subalkalic/alkalic.

³Total iron expressed as Fe₂O₃.

⁴Loss on ignition.

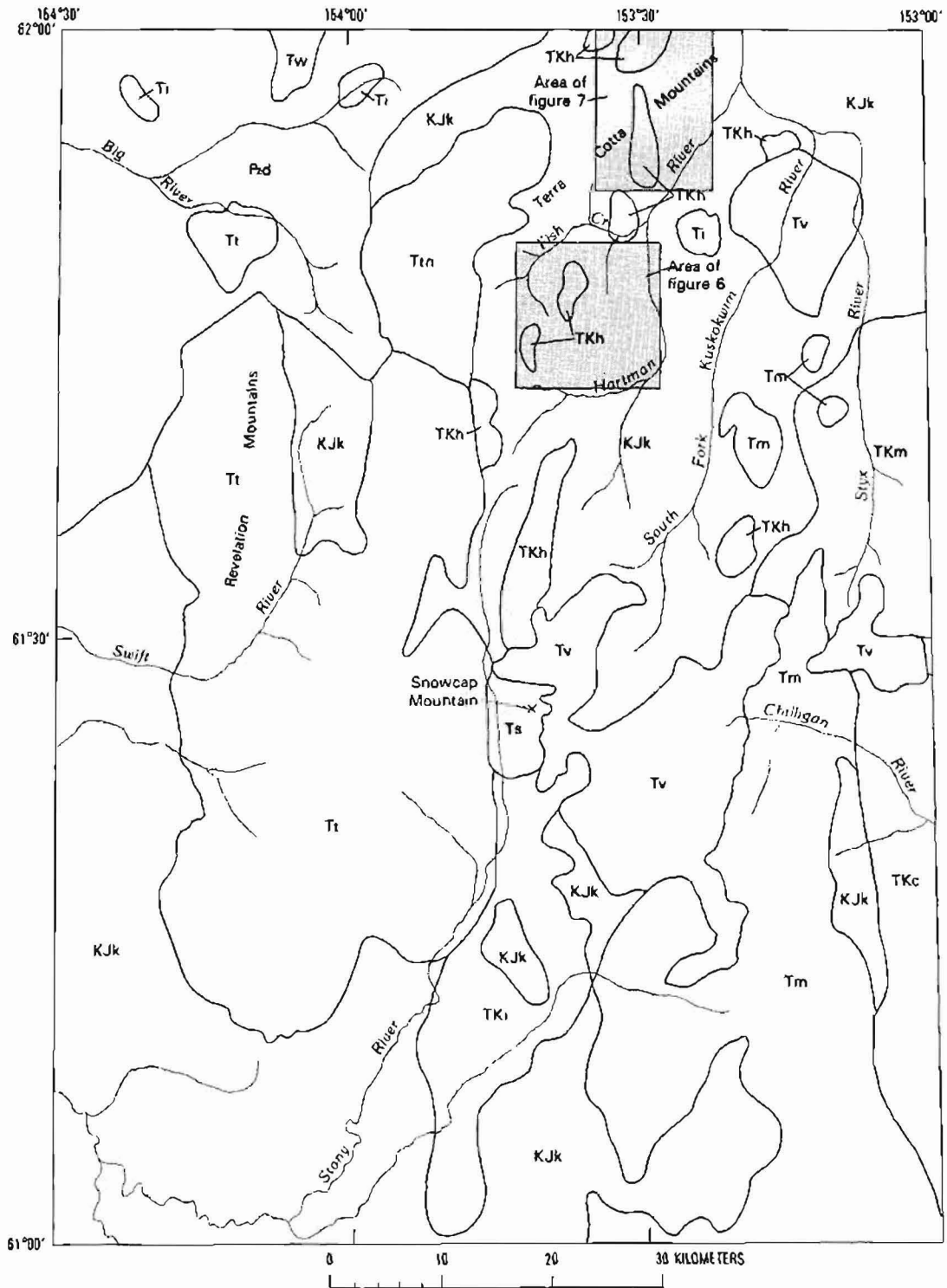


Figure 2 (above and facing page). Geology of the eastern part of the Lime Hills quadrangle, Alaska. Geology from Reed and Elliott (1970) and Reed and Lanphere (1973).

DRAINAGE-SEDIMENT GOLD ANOMALIES

Figures 3–5 show the distribution of drainage basins containing anomalous gold contents (>0.05 ppm in

–80-mesh sediments; ≥20 ppm in concentrates; ≥1 grain of gold detected microscopically). Only the more significant multisite anomalies are described here in detail. Of the three data sets, the most anomalies are defined

EXPLANATION

Tv	Volcanic rocks (Tertiary)
Ti	Intrusive rocks (Tertiary)
Tw	Windy Fork pluton (Tertiary)—Granite
Tt	Tired Pup pluton (Tertiary)—Quartz monzonite and granite.
Ttn	Northeast prong—Granite
Ts	Snowcap sequence (Tertiary)—Granodiorite to quartz monzonite
Tm	Merrill Pass sequence (Tertiary)—Quartz monzonite and granite
TKi	Intrusive rocks (Tertiary and Cretaceous)
TKm	Mount Estelle pluton (Tertiary and Cretaceous)—Quartz diorite to granodiorite
TKc	Crystal Creek sequence (Tertiary and Cretaceous)—Quartz monzonite
TKh	Hartman sequence (Tertiary and Cretaceous)—Gabbro to granodiorite
KJk	Kahiltna terrane (Cretaceous and Jurassic)—Graywacke, slate, and argillite
Pd	Dillinger terrane (Paleozoic)—Shale, limestone, and graywacke

by gold detected microscopically in heavy-mineral concentrate samples. Although the anomalies of greatest areal extent are revealed by all methods, each method defines some anomalies uniquely. It is therefore valuable to use a variety of sampling and analytical methods in gold exploration in the Alaska Range.

Most of the gold anomalies are in the northeastern part of the study area (figs. 3–5), which is underlain predominantly by sedimentary rocks of the Kahiltna terrane that are intruded by small plutons of the Hartman and Merrill Pass sequences. Several anomalies are also along the margin of the Tired Pup pluton where it intrudes rocks of the Kahiltna terrane. In addition, several anomalies are clustered near outcrops of Tertiary volcanic rocks in the lower and upper Styx River region and near Snowcap Mountain. Few gold anomalies are present within the main outcrop areas of the large Merrill Pass and Tired Pup plutons or in the region underlain by the carbonate rocks of the Dillinger terrane.

Many gold anomalies are spatially associated with areas in which rocks of the Kahiltna terrane were intruded by igneous rocks. The most significant of these anomalies, in terms of areal extent and gold concentrations, are associated with plutons of the Hartman sequence. The most significant of the drainage-sediment anomalies are discussed below.

Fish Creek Area

In the region between the Hartman River and Fish Creek, 12 sites have one or more drainage-sediment samples

containing anomalous gold content (figs. 3–5). One heavy-mineral concentrate sample (fig. 6, sample locality 29) contains 30 grains of gold. The anomalous samples define a combined drainage area of more than 60 km² that is underlain by carbonaceous graywacke and shale intruded by two large plutons of the Hartman sequence. Other elements anomalous in heavy-mineral concentrate samples from this area include Ag, As, B, Ba, Bi, Co, Mo, Ni, Sb, and W (Malcolm and others, 1990). Concentrate samples contain abundant arsenopyrite, barite, and scheelite and rare molybdenite (Allen and Slaughter, 1990). Followup of the drainage-sediment anomalies led to discovery of gold-bearing quartz-carbonate veins between the exposure of the two plutons, informally referred to as the Three Cub occurrence. Glacial cover in this area obscures much of the anomalous area such that significant mineralized rocks may be unexposed. Gold in rock from a basal moraine (table 2, sample 819) indicates that mineralized rock may also be present beneath the glacier in section 8 (T. 19 S., R. 24 W.).

Terra Cotta Mountains

In the Terra Cotta Mountains, drainage-sediment samples from 14 sites have anomalous gold contents (figs. 3–5). The combined drainage area, in excess of 70 km², is underlain by graywacke of the Kahiltna terrane and intruded by the Hartman sequence. Heavy-mineral concentrate samples containing anomalous gold contents also contain anomalous values for Ag, As, B, Ba, Bi, Co, Ni, Sb, Sn, and W. Pyrite, arsenopyrite, barite, and scheelite and lesser chalcopyrite, cinnabar, stibnite, and tourmaline were also observed in the concentrate samples. Gold-bearing veins and breccias were discovered in the northern part of the area in rocks of the Kahiltna terrane and Hartman sequence.

South Fork Kuskokwim River Region

Drainage-sediment samples containing anomalous gold contents occur in a broad arcuate area near the headwaters of the South Fork of the Kuskokwim River. Gold was visible microscopically in almost all heavy-mineral concentrate samples (fig. 5). In this region, graywacke of the Kahiltna terrane is intruded by two large plutons of the Hartman sequence, one on the east side of the area and one on the west side. Volcanic rocks crop out in the southern part of the area. The source of the gold is not known. Additional elements that are anomalous in heavy-mineral concentrates include Ag, As, B, Ba, Bi, Co, Ni, Pb, Sb, and W. These samples contain barite, pyrite, arsenopyrite, chalcopyrite, fluorite, molybdenite, scheelite, and stibnite.



EXPLANATION



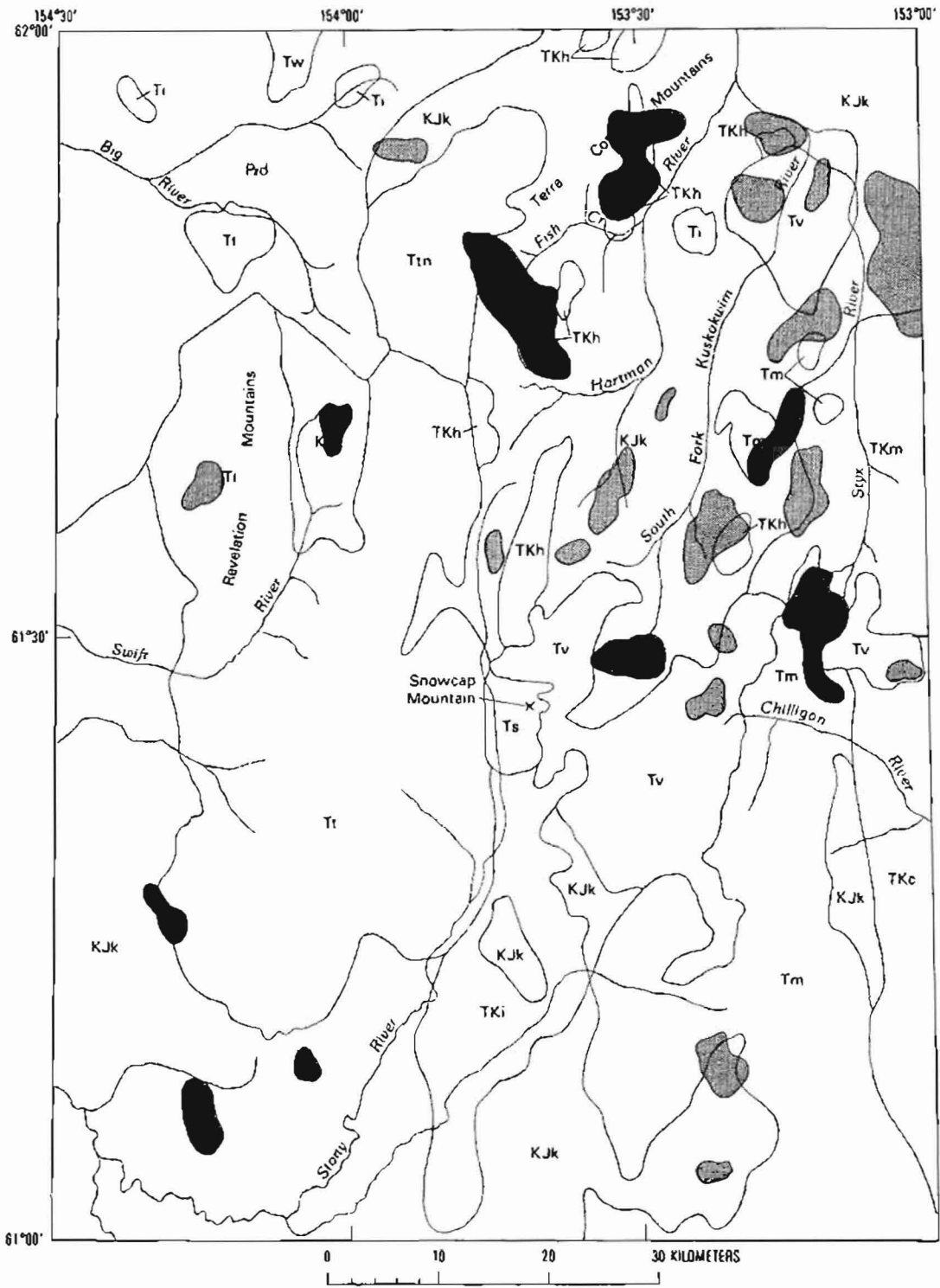
-  Drainage-basin anomaly for samples containing 0.05–0.5 ppm Au
-  Drainage basin anomaly for samples containing more than 0.5 ppm Au

Figure 3. Geochemical anomalies for gold in -80-mesh sediment samples, Lime Hills quadrangle, Alaska. Geology as in figure 2.



EXPLANATION



-  Drainage-basin anomaly for samples containing 10–100 ppm of Au
-  Drainage basin anomaly for samples containing 100 ppm of Au or more

Figure 4. Geochemical anomalies for gold in nonmagnetic heavy-mineral concentrate samples, Lime Hills quadrangle, Alaska. Geology as in figure 2.



EXPLANATION



-  Drainage-basin anomaly for samples containing 1-4 grains of gold
-  Drainage basin anomaly for samples containing 5 grains or more of gold

Figure 5. Mineralogically determined anomalies for gold in nonmagnetic heavy-mineral concentrate samples, Lime Hills quadrangle, Alaska. Geology as in figure 2.

Tired Pup Pluton Region

Some drainages around the margin of the Tired Pup pluton are anomalous in gold (figs. 3–5). Few isolated anomalous drainages are within the outcrop area of the pluton. The anomalous basins along the southwestern part of the pluton and near the headwaters of the Swift River, east of the Revelation Mountains, are underlain by rocks of the Kahiltna terrane. Heavy-mineral concentrates from drainages along the southwestern part of the pluton contain anomalous concentrations of Ag, As, Ba, Cu, Pb, Sb, Sn, and W. The bedrock source for the metals is not known. Heavy-mineral concentrates from the headwaters of the Swift River contain anomalous contents of Ag, As, Ba, Co, Cu, Ni, Pb, Sb, and W. In this area, gold- and arsenopyrite-bearing quartz veins occupy low-angle fault zones that cut graphitic schist of the Kahiltna terrane.

Styx River Region

On the east side of the Styx River, samples containing anomalous gold contents were collected from basins that are underlain by graywacke of the Kahiltna terrane that is intruded by the Mount Estelle pluton (figs. 3–5). This pluton is similar in age and composition to the Hartman sequence. Heavy-mineral concentrates also contain anomalous contents of Ag, As, B, Ba, Cu, Pb, Sb, and Zn (Malcolm and others, 1990). Gold-bearing quartz veins and shear zones occur within the granodiorite of Mount Estelle, just east of the Lime Hills quadrangle (Reed and Elliott, 1970). A vein gold deposit within and adjacent to the pluton has also recently been discovered (Northern Miner, 1987).

Near the headwaters of the Styx River, an anomalous area defined by gold in heavy-mineral concentrates coincides with exposed volcanic rocks (figs. 4, 5). Thick units of ash-flow tuff and agglomerate and megabreccias and breccia dikes may be related to a caldera in this area. Large zones of pyritic, sericitic, and argillic alteration are also present. Anomalous concentrations of Cu, Pb, and Zn also occur in heavy-mineral concentrate samples from this area. The geologic setting and the primarily base-metal geochemical signature distinguish this anomaly from those described previously. Polymetallic base-metal veins in faults and fractures cut volcanic and intrusive rocks in this region (Resource Associates of Alaska, 1976).

IDENTIFIED LODGE GOLD OCCURRENCES

Field investigations and rock sampling in this study identified two lode sources for the drainage-sediment gold anomalies spatially coincident with the Hartman plutons. One is the Three Cub occurrence southeast of Fish Creek, and the second is in the Terra Cotta Mountains. Gold-

bearing veins also were observed near the headwaters of the Swift River, adjacent to the exposure of the Tired Pup pluton. These discoveries, resulting from limited followup of the reconnaissance geochemical data, suggest that further exploration may lead to additional discoveries in other anomalous areas.

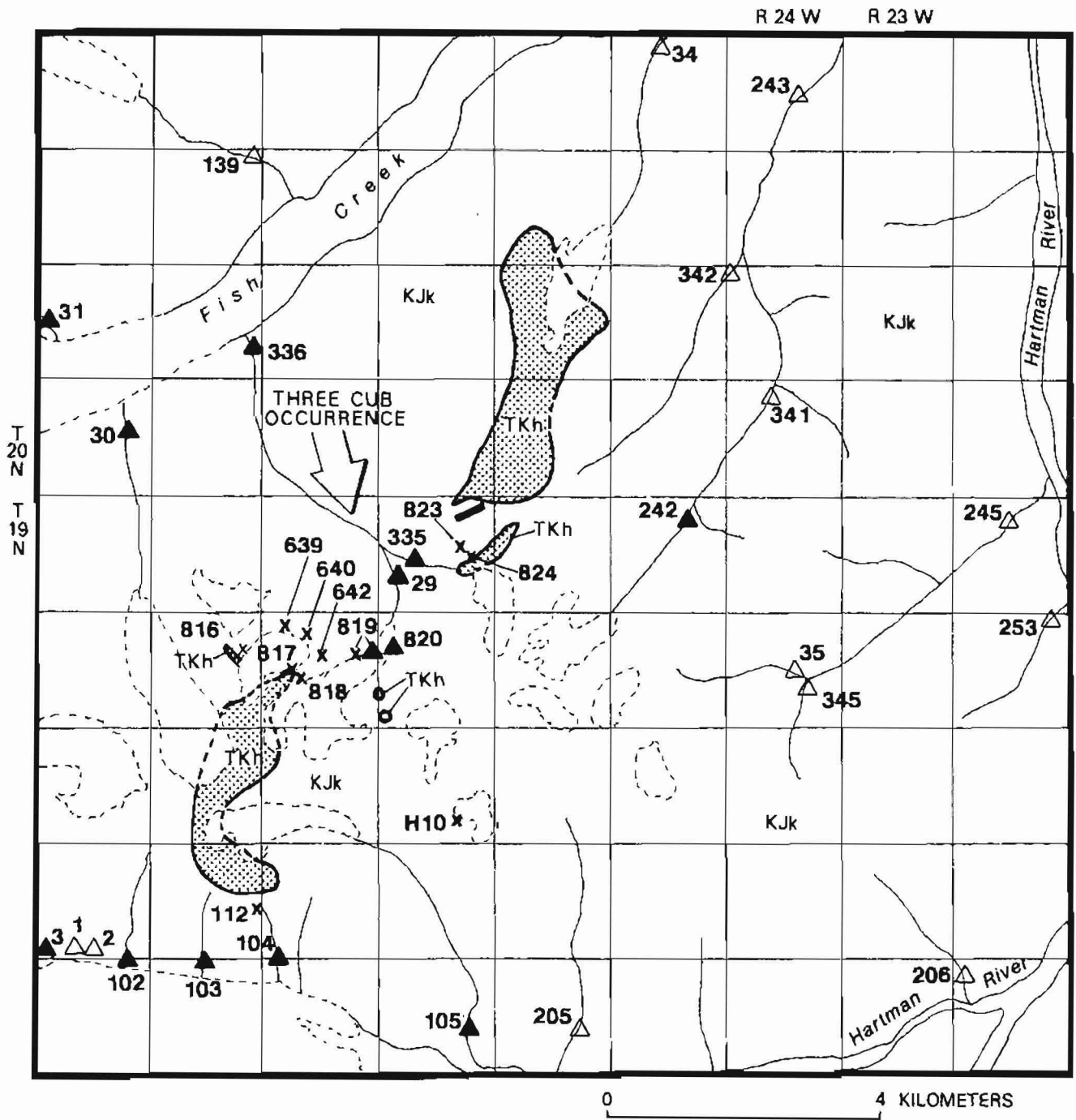
Three Cub Occurrence

In the region between Fish Creek and the Hartman River, gold-bearing veins were discovered along the margins and within plutons of the Hartman sequence (fig. 6). Gold-bearing quartz-carbonate veins cut both sedimentary and igneous rocks but are most prevalent in carbonaceous graywacke of the Kahiltna terrane and contain as much as 26 ppm Au (table 2). The veins are generally less than 15 cm wide and are spaced a few meters apart. Although most veins are simple and have sharp regular contacts, a few within the sedimentary rocks are brecciated and contain fragments of graywacke. Alteration adjacent to the veins is limited to thin selvages of silica and carbonate and less commonly chlorite, sericite, and barite. Locally, some calc-silicate skarn is developed along the margin of the pluton (table 2, samples 817RA and 818).

The veins contain dominantly quartz, carbonate, pyrite, and arsenopyrite and less commonly barite, chalcopryrite, stibnite, galena, and sphalerite. Vein samples taken at or near the contact of the northern pluton also contain anomalous contents of silver (as much as 170 ppm). Some aplite dikes (fig. 6, sample locality 817), quartz veins, and pyrite-bearing fracture surfaces in the igneous rocks contain scheelite and arsenopyrite. Scheelite is rarely present in veins within the sedimentary rocks except where calc-silicate skarn is developed (table 2, sample 817RA).

The presence of gold (0.2 ppm) and arsenic (> 5,000 ppm) in an unaltered, granophyric, quartz-albite aplite dike (table 2, sample 817RC) suggests that Hartman plutons could be gold sources. In places (fig. 6, sample localities 817 and 824), however, abundant xenoliths of mica-rich mafic rocks and sedimentary rocks within the Hartman sequence indicate possible contamination and assimilation of metals and volatiles into Hartman magmas. Samples of unaltered rocks of the Hartman sequence contain no detectable gold (< 0.05 ppm).

Some strata within the Kahiltna terrane in this and other parts of the study area weather conspicuously reddish brown rather than more typical greyish black and locally contain as much as 50 percent pyrite, which is disseminated or in conformable lenses. Carbonaceous and pyritiferous graywacke units of the Kahiltna terrane are enriched in Fe, Ba, Co, Cr, V, Ag, As, Sb, Cu, and Zn relative to average shale (table 3). A sample of carbonaceous graywacke with disseminated pyrite contains 3.5 ppm Au (table 2, sample 104RA). Anomalous gold and other metals within the sulfide-rich rocks suggest that these units might be source



EXPLANATION

- Geologic contact (dashed where inferred)
- Dike
- - - Glacier
- △ Drainage sample site
- ▲ Drainage sample site with anomalous gold content
- x Rock sample site (see table 2)

Figure 6. Geology and localities of geochemical samples containing anomalous amounts of gold, Three Cub occurrence. Location of map area shown on figure 2. Geologic units: TKh, Hartman sequence (gabbro to granodiorite); KJk, Kahiltna terrane (graywacke, slate, and argillite). Sample H-10 from Reed and Elliott (1970).

Table 2. Geochemical data for rock samples having anomalous metal contents from the Three Cub occurrence, Terra Cotta Mountains, and upper Swift River area, Lime Hills quadrangle, Alaska

[All values are in parts per million (micrograms/gram). Analytical methods: A, atomic absorption analysis; I, inductively coupled plasma emission spectroscopy. <, element detected but concentration below limit of determination listed; N, element not detected at limit listed; >, element concentration greater than limit listed]

Sample	Source	Terrane or unit	Rock type	Alteration or vein type ¹	Au-A	Au-I	Ag-I	As-I	Sb-I	Cu-I	Pb-I	Zn-I
THREE CUB OCCURRENCE												
29RB	Float	Kahiltna	Graywacke	Quartz vein	<0.05	0.15N	0.19	560	3.1	36	4.8	32
34R	Float	Kahiltna	Graywacke	Quartz veins	0.20	0.15N	0.63	230	1.5	320	3.2	74
102RE	Float	Hartman	Monzonite	Quartz veins	0.15	0.15N	13	11	1.8	16	55	13
104RA	Float	Kahiltna	Graywacke	Disseminated pyrite	3.5	1.9	1.4	>3,000	15	140	11	70
112RB	Outcrop	Hartman	Monzonite	Carbonate veins	1.05	0.15N	0.082	28	4.3	23	7.2	56
112RC	Outcrop	Hartman	Monzonite	Quartz-carbonate vein	1.9	0.15N	0.095	380	1.8	88.	6.6	27
639RB	Outcrop	Kahiltna	Graywacke	Quartz vein	0.25	0.15N	0.11	1700	9.5	5.7	1.8	13
639RE	Outcrop	Kahiltna	Graywacke	Quartz vein	<0.05	0.15N	0.07	300	8.9	54	0.6N	7.9
640R	Outcrop	Kahiltna	Graywacke	Quartz vein	0.10	0.15N	0.045N	52	0.6N	32	0.6N	12
642R	Outcrop	Kahiltna	Graywacke	Quartz-carbonate vein	<0.05	0.15N	0.14	99	15	17	2.1	17
816RA	Talus	Kahiltna	Graywacke	Quartz vein	0.10	0.50	1.4	250	1.9	610	1.0N	24
817RA	Outcrop	Kahiltna	Hornfels	Calc-silicate vein	0.25	1.8	1.4	90	8.4	440	1.3	66
817RC	Outcrop	Hartman	Aplite		0.20	0.25N	0.67	>5,000	3.9	0.22	8.2	7.9
817RD	Outcrop	Kahiltna	Graywacke	Quartz-carbonate veins	0.30	0.40	0.76	980	44	54	4.0	75
818RA	Outcrop	Kahiltna	Graywacke	Calc-silicate vein	2	5.9	2.3	1,800	10	870	1.0N	>800
819RA	Moraine	Kahiltna	Graywacke	Quartz-chlorite vein	0.15	0.58	0.15	140	6.5	28	1.0N	43
819RB	Moraine	Kahiltna	Graywacke	Quartz vein	19	26	3.1	>5,000	35	71	34	68
823RB	Outcrop	Kahiltna	Graywacke	Quartz vein	1.3	6.1	110	910	9.6	>2,000	1.0N	150
824RB	Outcrop	Hartman	Vein at contact	Quartz-carbonate-pyrite	1.9	7.8	170	1,500	670	270	1,600	>800
TERRA COTTA MOUNTAINS												
346RA	Float	Kahiltna	Breccia	Silicified	0.40	0.46	0.33	>3,000	41	1.3	2.3	3.9
346RB	Float	Kahiltna	Breccia	Quartz-sericite-pyrite	0.55	0.65	5.6	570	86	2.4	14	0.77
809RA	Outcrop	Kahiltna	Breccia vein	Quartz pyrite	1.0	2.5	130	>5,000	1,300	>2,000	2,100	180
810RA	Outcrop	Kahiltna	Graywacke	Pyrite veins	0.05	0.26	2.5	1,600	77	520	7.9	57
811RA	Talus	Kahiltna	Graywacke	Carbonate vein	0.05N	1.1	8.6	22	960	7.3	14,000	93
813RA	Outcrop	Hartman	Monzonite	Quartz vein	<0.05	0.25N	3.2	1,500	17	240	9.3	18
814RA	Outcrop	Hartman	Monzonite	Quartz vein	0.70	1.3	41	63	13	>2,000	1.0N	96
UPPER SWIFT RIVER AREA												
1019RA ¹	Float	Kahiltna	Hornfels	Quartz vein	3	5.6	15	1,900	12	370	1.0N	>800
1027RA ²	Float	Kahiltna	Graphitic schist	Quartz vein	0.30	0.25N	1.4	69	1.0N	59	1.1	22
1027RB ²	Outcrop	Kahiltna	Graphitic schist	Quartz vein	1.0	2.3	8.1	>5,000	31	66	6.4	380

¹Lat 61°40'28"N., long 154°04'13"W.

²Lat 61°40'25"N., long 154°04'58"W.

materials from which metals in the veins were derived and could be hosts to disseminated gold deposits.

Terra Cotta Mountains

Mineralization in the Terra Cotta Mountains is similar to that at the Three Cub occurrence in that gold-bearing quartz-carbonate veins occur in rocks of both the Kahiltna terrane and Hartman sequence (fig. 7). Iron staining and argillic alteration are more prevalent, however, in the Terra Cotta Mountains and are concentrated in east-northeast-trending zones cutting graywacke. Silicified and pyritized dikes also occur in these zones. Altered zones are 1–3 m wide and are spaced about 20 m apart. Gold-bearing quartz-carbonate breccia veins (table 2, sample 809) 10–15 cm wide within these altered zones contain pyrite and arsenopyrite and lesser stibnite and chalcopyrite. Veins and breccias also contain anomalous concentrations of silver (as much as 130 ppm). Large zones of iron-stained, silicified sedimentary rocks cut by numerous veinlets of pyrite and arsenopyrite contain lesser amounts of Au, As, and Cu.

Quartz veins (table 2, samples 813 and 814) containing anomalous amounts of gold (as much as 1.3 ppm) occur within a Hartman pluton in the area. The veins, similar to those hosted in the sedimentary rocks, contain pyrite and arsenopyrite and less commonly chalcopyrite. Argillic and sericitic alteration restricted to thin selvages immediately adjacent to the veins has resulted in complete destruction of mafic minerals and feldspar. Although the total extent of veining is unknown, much of the Terra Cotta Mountains is indicated to be favorable for gold occurrences by gold anomalies in the drainage-sediment survey (fig. 7). The newly discovered occurrences described here suggest pluton margins may be good targets for exploration.

Upper Swift River Area

Another lode source of gold was identified near the headwaters of the Swift River, east of the Revelation Mountains (fig. 4). Gold-bearing quartz-arsenopyrite veins cut graphitic schist and hornfels of the Kahiltna terrane adjacent to the Tired Pup pluton. In this area, the sedimentary rocks are pyritiferous and weather reddish brown. The veins occupy low-angle faults that dip westward. No mineralized veins were identified in the igneous rocks. The veins are generally less than 15 cm wide and are concentrated in zones which are themselves widely spaced (tens of meters). The veins contain as much as 5.6 ppm Au and 50 percent arsenopyrite and traces of chalcopyrite and sphalerite.

SUMMARY AND DISCUSSION

Reconnaissance geochemical investigations in the eastern part of the Lime Hills quadrangle utilizing chemical and mineralogical analysis of heavy-mineral concentrate

and –80-mesh fractions of drainage sediments have identified numerous basins containing anomalous gold contents. Basins containing the most highly anomalous samples are underlain by sedimentary rocks of the Kahiltna terrane that have been intruded by plutons of the Hartman sequence. Gold-bearing quartz-carbonate veins cut Kahiltna and Hartman rocks near Fish Creek and in the Terra Cotta Mountains. Gold-bearing quartz-arsenopyrite veins also occupy low-angle fault zones cutting Kahiltna rocks near the margin of the Tired Pup pluton. Followup work of reconnaissance data was limited, and exploration within other anomalous drainage basins may locate additional lode gold occurrences.

Mineralized veins associated with the Hartman sequence are thin and generally widely spaced but locally may be extensively brecciated and altered. Vein samples contain anomalous contents of As, Cu, and Sb and less commonly Ag, Pb, and Zn. Quartz-carbonate veins contain pyrite, arsenopyrite, chalcopyrite, stibnite, barite, galena, and sphalerite, in decreasing order of abundance. Most alteration is restricted to thin selvages of quartz and carbonate and less consistently chlorite, sericite, and barite.

The origin of these vein deposits is unknown, but the metalliferous nature of the Kahiltna terrane and the alkalic affinity of the Hartman sequence may be important factors in the genesis of these occurrences. These rocks may have been sources of gold or influenced the nature and action of hydrothermal fluids.

The metalliferous nature of some strata within the Kahiltna terrane suggests that these rocks are a potential source of gold that was leached by vein-forming hydrothermal fluids. Veins hosted within sedimentary rocks also have the highest gold contents; thus, the carbonaceous and sulfide-rich sedimentary units may have influenced precipitation of metals from hydrothermal fluids through reduction. In addition, gold-bearing graywacke containing disseminated pyrite may indicate potential for disseminated gold deposits. Stratigraphic and geochemical studies of the Kahiltna terrane in this region are needed and should focus on the identification of metal-rich strata and depositional environments favorable for the concentration and preservation of sulfides (for example, restricted basins).

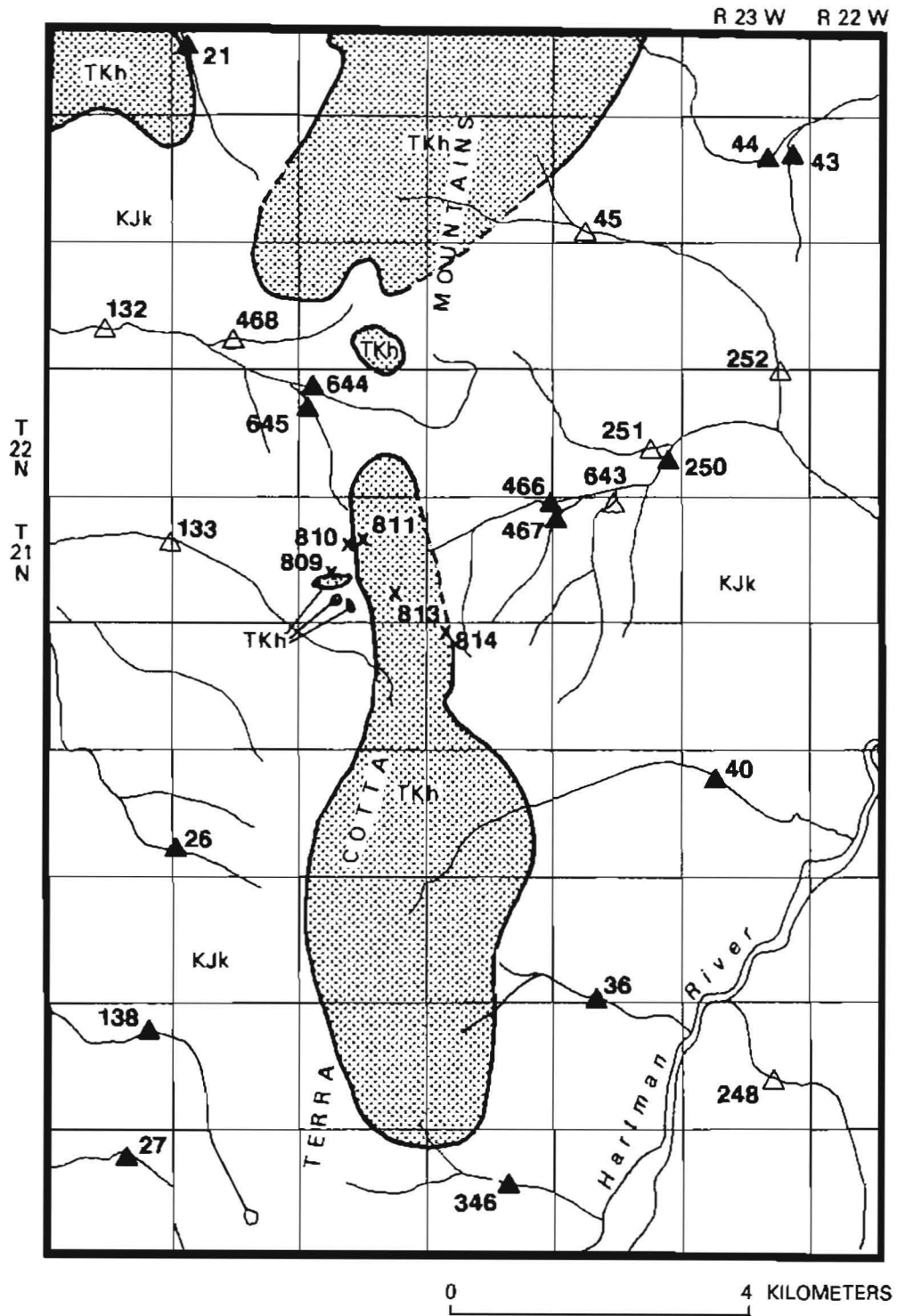
The association between gold-bearing veins and the Hartman sequence may indicate a relationship between gold mineralization and the petrogenesis of the intrusive rocks. The spatial and probable genetic association of certain mineral-deposit types to igneous rocks of particular chemical affinity is well established in Alaska and elsewhere; hence, the petrochemical classification of igneous rocks in the Alaska Range batholith can provide a guide to favorable environments for ore deposits. Some mafic alkalic rocks are notably enriched in gold and may be gold sources (Wedepohl, 1978; Boyle, 1979; Rock and others, 1987). Additionally, significant precious-metal deposits are known

Table 3. Geochemical data for rock samples from the Kahiltna terrane, Lime Hills quadrangle, Alaska

[Latitude and longitude in degrees, minutes, and seconds, north and west, respectively. All analytical values are in parts per million, except for Fe which is in weight percent. Analytical methods: S, emission spectrography; I, inductively coupled plasma emission spectroscopy. <, element detected but concentration below limit of determination listed; N, element not detected at limit listed]

Sample	Source	Rock type	Alteration ¹	Latitude	Longitude	Fe-S	B-S	Ba-S	Co-S	Cr-S	Ni-S	V-S	Ag-I	As-I	Sb-I	Cu-I	Pb-I	Zn-I	
137RC	Outcrop	Graywacke	Fresh	61 52 02	153 40 40	3	10	500	15	150	50	150	0.068	14	0.6	73	1.2	52	
310R	Outcrop	Graphitic schist	Fresh	61 38 41	153 31 54	7	70	1,500	30	200	100	200	0.053	0.6N	0.6	12	3.6	130	
639RD	Outcrop	Graywacke	Fresh	61 45 24	153 40 33	5	20	2,000	20	200	70	200	0.15	16	0.74	39	3.9	81	
703R	Float	Graywacke	Fresh	61 49 02	153 02 47	3	50	700	15	100	30	100	0.35	0.6N	1.7	20	4.7	75	
805RD	Outcrop	Graywacke	Fresh	61 56 03	153 29 53	7	300	1,000	30	200	70	300	0.075N	1.0N	2.1	27	13	140	
822RA	Outcrop	Graywacke	Fresh	61 45 60	153 37 55	5	50	700	15	150	70	150	0.12	17	1.7	41	10	62	
857RA	Outcrop	Slate	Fresh	61 05 39	154 10 24	7	100	1,000	15	200	70	300	0.075N	16	1.0	26	17	120	
26R	Float	Graywacke	Diss. Py.	61 54 23	153 32 37	3	10	2,000	15	30	20	70	0.24	5.2	6.6	22	8.4	75	
282RA	Float	Sandstone	Diss. Py.	61 15 31	153 17 32	5	10	1,000	15	10	<5	30	0.66	0.6N	0.6	140	1.7	21	
886RA	Float	Graywacke	Diss. Py.	61 12 37	153 40 09	10	70	700	15	150	50	300	0.25	1	3.0	98	3.1	140	
888RA	Float	Graywacke	Diss. Py.	61 16 02	153 34 37	10	10	150	30	70	100	200	0.49	26	3.6	210	8.3	130	
906RA	Moraine	Slate	Diss. Py.	61 43 42	153 59 58	7	70	700	70	150	150	300	0.48	26	3.7	69	13	110	
1004RA	Outcrop	Graywacke	Diss. Py.	61 44 49	153 57 26	7	100	1,000	30	300	100	300	0.27	15	10	80	1.6	94	
1107R	Outcrop	Graphitic schist	Diss. Py.	61 40 58	154 02 25	3	30	300	15	70	30	70	0.11	3.9	1.9	71	19	140	
1108RB	Float	Graywacke	Diss. Py.	61 48 41	154 13 28	7	20	1,000	20	70	50	300	0.30	37	1.5	64	8.3	44	
1109R	Float	Graywacke	Diss. Py.	61 48 32	154 11 51	3	70	2,000	10	30	150	300	0.20	4.1	1.9	30	22	110	
1110R	Float	Graywacke	Diss. Py.	61 46 28	154 12 58	7	150	1,000	20	150	70	300	0.065	3.6	1.1	45	11	110	
1112RA	Moraine	Graywacke	Diss. Py.	61 45 11	154 10 15	7	70	3,000	50	200	150	700	1.40	30	3.9	120	5.3	290	
1115RB	Float	Graywacke	Diss. Py.	61 38 39	154 04 55	5	100	500	30	150	70	300	0.51	68	2.6	48	4.5	130	
1117RC	Float	Graywacke	Diss. Py.	61 36 30	154 03 00	10	100	500	30	300	70	300	0.075N	38	1.0	68	2.7	120	
1118R	Float	Graywacke	Diss. Py.	61 35 41	154 03 56	3	100	500	15	150	50	200	0.14	1.0N	1.0	34	1.4	160	
1154R	Float	Graywacke	Diss. Py.	61 46 48	154 19 21	7	100	1,500	30	150	70	300	0.11	1.0N	1.0	61	9.7	99	
1187RA	Float	Graywacke	Diss. Py.	61 02 26	153 44 42	5	10	1,000	15	70	20	300	0.47	7.6	1.3	64	11	83	
1191RA	Float	Graywacke	Diss. Py.	61 07 45	153 40 08	5	50	700	20	70	30	300	0.075N	34	1.0	23	1.1	73	
1198RA	Float	Graywacke	Diss. Py.	61 04 59	153 40 32	2	50	3,000	10	30	20	200	0.33	20	3.8	33	5.3	110	
1217RA	Float	Graywacke	Diss. Py.	61 03 35	153 34 09	7	10N	1,000	15	10	<5	150	0.10	1.9	1.0	19	1.1	64	
826RA	Moraine	Graphitic shale	Strat. Py.	61 45 39	153 38 40	15	10N	70	15	100	70	100	0.20	16	5.3	70	9.3	120	
883RA	Float	Graphitic schist	Strat. Py.	61 14 39	153 43 55	7	20	700	20	150	50	300	0.075N	17	4.0	60	7.9	87	
883RB	Float	Graywacke	Strat. Py.	61 14 39	153 43 55	10	10N	150	10	30	30	150	0.16	4.5	3.6	78	1.2	110	
903RD	Float	Graphitic shale	Strat. Py.	61 48 04	153 58 01	7	70	1,500	50	150	100	700	1.40	41	3.2	120	5.2	350	
1075RA	Outcrop	Graphitic schist	Strat. Py.	61 40 20	154 04 34	7	100	1,500	20	300	70	300	0.19	7.1	1.0	55	2.5	160	
1114RA	Moraine	Graywacke	Strat. Py.	61 42 53	154 07 37	5	70	1,500	10	70	30	150	0.24	1.4	1.0	58	1.0	120	
1201RA	Outcrop	Slate	Strat. Py.	61 05 44	153 40 13	1.5	50	3,000	10N	20	7	150	0.26	13	2.0	18	6.8	100	
						Mean	6.1	62	1,100	22	130	61	250	0.29	15	2.4	60	6.8	116
						Turekian and Wedepohl (1961) average shale	4.7	100	580	19	90	68	130	0.07	13	1.5	45	20	95

¹Abbreviations: Diss., disseminated; Py, pyrite; Strat., stratiform.



- EXPLANATION**
- Geologic contact (dashed where inferred)
 - △ Drainage sample site
 - ▲ Drainage sample site with anomalous gold content
 - × Rock sample site (see table 1)

Figure 7. Geology and localities of geochemical samples containing anomalous amounts of gold, Terra Cotta Mountains. Location of map area shown on figure 2. Geologic units: TKh, Hartman sequence (gabbro to granodiorite); KJk, Kahiltna terrane (graywacke, slate, and argillite).

to be related to alkalic rocks within the North American Cordillera (Giles, 1983; Mutschler and others, 1985; Thompson and others, 1985; Rock and Groves, 1988; Nikic, 1989; Rebagliati, 1989).

The recognition of alkalic rocks within early phases of the Alaska Range batholith also needs to be addressed in the understanding of the genesis and tectonic development of the batholiths. Alkalic rocks form under substantially different physicochemical conditions (that is, pressure, volatile composition) than coeval subalkalic rocks (Sorensen, 1979). Reed and Lanphere (1973) suggested that, based on AFM trends, the older Cretaceous to Tertiary rocks of the Hartman, Crystal Creek, and Mount Estelle plutons originated from a different parent than the younger igneous rocks, though the character of the source was not identified. The alkalic and subalkalic affinities of the Hartman sequence (table 1) possibly indicate a need for redefinition of the members of the sequence or that the sequence is a result of contamination or mixing of alkalic and subalkalic magmas.

REFERENCES CITED

- Allen, M.S., Malcolm, M.J., Motooka, J.M., and Slaughter, K.M., 1990, Geologic description, chemical analyses and sample locality map for rock samples collected from the eastern portion of the Lime Hills quadrangle, Alaska: U.S. Geological Survey Open-File Report 90-69, 51 p.
- Allen, M.S., and Slaughter, K.E., 1990, Mineralogical data and sample locality map for nonmagnetic, heavy-mineral-concentrate samples collected from the eastern portion of the Lime Hills quadrangle, Alaska: U.S. Geological Survey Open-File Report 90-67, 64 p.
- Boyle, R.W., 1979, The geochemistry of gold and its deposits: Geological Survey of Canada Bulletin 280, 584 p.
- Bundtzen, T.K., Kline, J.T., Smith, T.E., and Albanese, M.D., 1987, Geologic map of the McGrath A-2 quadrangle, Alaska: Alaska Division of Geological and Geophysical Surveys Professional Report 91, scale 1:63,360.
- Churkin, Michael, Jr., 1984, Nixon Fork-Dillinger terranes—A dismembered Paleozoic craton margin in Alaska displaced from Yukon Territory: Geological Society of America Abstracts with Programs, v. 16, no. 5, p. 275.
- De LaRoche, H., Leterrier, J., Grandclaude, P., and Marchal, M., 1980, A classification of volcanic and plutonic rocks using R1R2-diagram and major-element analyses—Its relationship with current nomenclature: Chemical Geology, v. 29, p. 183-210.
- Gamble, B.M., Allen, M.S., McCammon, R.B., Root, D.H., Scott, W.A., Griscom, A., Krohn, M.D., Ehmman, W.J., and Southworth, S.C., 1988, Lime Hills Quadrangle, Alaska—An AMRAP planning document: U.S. Geological Survey Administrative Report, 167 p.
- Giles, David L., 1983, Gold mineralization in the laccolithic complexes of central Montana, in Proceedings of the Denver Region Exploration Geologists Society Symposium—The genesis of Rocky Mountain ore deposits; changes with time and tectonics: Denver Region Exploration Geologists Society, p. 157-162.
- Hinderman, T.K., 1982, National Uranium Resource Evaluation, Lime Hills quadrangle, Alaska [National Uranium Resource Evaluation program, PGJ/F-057(82)]: Grand Junction, Colo., U.S. Department of Energy, 18 p., 14 plates, scale 1:500,000.
- Irvine, T.N., and Baragar, W.R.A., 1971, A guide to the chemical classification of the common volcanic rocks: Canadian Journal of Earth Sciences, no. 8, p. 523-548.
- Jacobsen, S.I., Aamodt, P.L., and Sharp, R.R., 1979, Uranium hydrogeochemical and stream sediment reconnaissance of the Lime Hills and Tyonek NTMS quadrangles, Alaska, including concentrations of forty-three additional elements: Los Alamos Scientific Laboratory Informal Report LA-7348-MS, 224 p.
- Jones, D.L., Silberling, N.J., Coney, P.J., and Plafker, George, 1984, Lithotectonic terrane map of Alaska west of the 141st meridian, in Silberling, N.J., and Jones, D.L., eds., Lithotectonic terrane maps of the North America Cordillera: U.S. Geological Survey Open-File Report 84-523, p. A1-A12.
- Lanphere, M.A., and Reed, B.L., 1985, The McKinley sequence of granitic rocks—A key element in the accretionary history of southern Alaska: Journal of Geophysical Research, v. 90, no. B13, p. 11413-11430.
- Malcolm, M.J., Allen, M.S., and Slaughter, K.E., 1990, Analytical results and sample locality map of the nonmagnetic, heavy-mineral-concentrate samples collected from the eastern portion of the Lime Hills quadrangle, Alaska: U.S. Geological Survey Open-File Report 90-68, 85 p.
- Motooka, J.M., Allen, M.S., Malcolm, M.J., and Slaughter, K.E., 1990, Analytical results and sample locality map for stream-sediment samples collected from the eastern portion of the Lime Hills quadrangle, Alaska: U.S. Geological Survey Open-File Report 90-70, 105 p.
- Mutschler, F.E., Griffin, M.E., Stevens, D.S., and Shannon, S.S., Jr., 1985, Precious metal deposits related to alkaline rocks in the North American Cordillera—An interpretive review: Transactions of the Geological Society of South Africa, no. 88, p. 355-377.
- Nikic, Z.T., 1989, Mount Polley alkalic porphyry copper-gold deposit: Northwest Mining Association, Annual Convention, 95th, Spokane, Abstracts, p. 3.
- Northern Miner, 1987, Platinoval/Cominco in south Alaska venture: Northern Miner, v. 73, no. 40, p. 7.
- Rebagliati, Mark, 1989, Mt Milligan—An alkaline intrusive related porphyry Au-Cu deposit: Northwest Mining Association, Annual Convention, 95th, Spokane, Abstracts, p. 3.
- Reed, B.L., and Elliott, R.L., 1970, Reconnaissance geologic map, analyses of bedrock and stream sediment samples, and an aeromagnetic map of parts of the southern Alaska Range: U.S. Geological Survey Open-File Report 70-271 (413), 24 p., 3 sheets, scale 1:250,000.
- Reed, B.L., and Lanphere, M.A., 1969, Age and chemistry of Mesozoic and Tertiary plutonic rocks in south-central Alaska: Geological Society of America Bulletin v. 80, p. 23-44.

- _____ 1972, Generalized geologic map of the Alaska-Aleutian Range batholith showing potassium-argon ages of plutonic rocks: U.S. Geological Survey Miscellaneous Field Studies Map MF-372, 2 sheets, scale 1:100,000.
- _____ 1973, Alaska-Aleutian Range batholith—Geochronology, chemistry, and relation to circum-Pacific plutonism: Geological Society of America Bulletin, v. 84, p. 2583-2610.
- Reed, B.L., and Nelson, S.W., 1980, Geologic map of the Talkeetna quadrangle, Alaska: U.S. Geological Survey Investigations Map I-1174, scale 1:250,000.
- Resource Associates of Alaska, 1976, Geology and geochemistry of certain lands within the proposed Lake Clark National Park: Contract report (RDF) J0166108 prepared for the U.S. Bureau of Mines, 109 p., 6 vols. of analytical data, 13 sheets, various scales.
- Rock, N.M.S., Duller, P., Haszeldine, R.S., and Groves, D.I., 1987, Lamprophyres as potential gold exploration targets—Some preliminary observations and speculations, in Ho, S.E., and Groves, D.I., eds., Recent advances in understanding Precambrian gold deposits: Perth, University of Western Australia Publication, p. 271-286.
- Rock, N.M.S., and Groves, D.I., 1988, Can lamprophyres resolve the genetic controversy over mesothermal gold deposits: Geology, v. 16, p. 538-541.
- Sorensen, H., 1979, The alkaline rocks: New York, John Wiley and Sons, 622 p.
- Thompson, T.B., Trippel, A.D., and Dwelley, P.C., 1985, Mineralized veins and breccias of the Cripple Creek district, Colorado: Economic Geology, v. 80, p. 1669-1688.
- Turekian, K.K., and Wedepohl, K.H., 1961, Distribution of the element some major units of the Earth's crust: Geological Society of America Bulletin, v. 72, p. 175-192.